University of Genoa

Doctorate Course in Science and Technology

of Chemistry and Materials

XXXVIII Cycle

Curriculum: Pharmaceutical, Food and Cosmetic Science

PhD Thesis

Study, preparation and evaluation of eco-sustainable bioactive ingredients for potential applications in the dermocosmetic field

Dr. Debora Caviglia

Advisor: Prof. Carla Villa

Co-Advisor: Prof. Anna Maria Schito

Ai miei genitori

Table of contents

PROJECT BACKGROUND AND OBJECTIVES

The cosmetics industry is a dynamic sector of chemistry that is subject to constant change. It is currently defined by a perpetual and increasing demand for novel eco-friendly solutions and products, in accordance with environmental and sustainability issues, which are pivotal factors in determining competitiveness and awareness. In accordance with contemporary trends in the field of chemistry, research in the domain of cosmetics has consequently given rise to an approach that is designated as Green Cosmetic Chemistry.

While in the early years this philosophy mainly represented a tendency to seek only new 'natural' raw materials through the use of botanical derivatives, today it has taken on a broader meaning, which includes respect for the environment and the protection of biodiversity through the study, design, and development of new sustainable ingredients, formulas, and processes, reducing energy consumption (including through the use of alternative sources), and exploiting raw materials from renewable natural resources (preferably locally sourced) according to the principles of Green Chemistry and Green Extraction. The formulation of products based on this philosophy, which favours the use of new plant-derived ingredients and respects biodiversity, requires greater commitment to studying ingredient compatibility, performance, and stability. This, in turn, results in increased time and costs in the development of the finished cosmetic product. It is therefore essential to find a balance between the desire for maximum naturalness and the need to provide consumers with a stable, safe, and pleasant product that guarantees its effectiveness over time at a competitive price. This transition necessitates a multidisciplinary scientific approach, wherein the integration of diverse cross-disciplinary competencies is essential for the development of processes and products that are both safe for humans and environmentally sustainable.

The development of this doctoral project was informed by the considerations outlined above, with the aim being the acquisition and/or deepening of a variety of skills that would then facilitate the study of innovative strategies and products from both a technological and functional perspective. For this reason, my research project was carried out both at the Department of Pharmacy, Section of Medicinal and Cosmetic Chemistry, and at the Department of Surgical, Microbiological and Organ Transplantation Sciences (DISCMIT) of the University of Genoa.

In the first laboratory (Green Cosmetic Lab), the most technological aspects of the research were developed. In particular, it was possible to design, study, and apply eco-friendly extraction procedures to obtain innovative ingredients, and to carry out several characterisation studies using different analytical methods. The main objective was the study of multifunctional natural ingredients, focusing on the valorization of natural renewable sources, including botanical matrices (*Paeonia lactiflora* Pall., *Laurus nobilis*, Manna), ethnobotanical matrices (fermented plant food - *Tocosh* flour), agri-food waste (beetroot stalks) and agricultural by-products (olive mill wastewater). In the second laboratory I focused primarily on biological studies, with a particular emphasis on microbiology-related experiments. The valuable cosmetic potential of the ingredients obtained was assessed by means of specific *in vitro* biological assays, particularly evaluating antimicrobial properties.

INTRODUCTION

Green Chemistry, Green Extraction and Circular Economy

In recent years, a combination of regulatory initiatives, strategic approaches, and heightened awareness of environmental and human health concerns has positioned sustainability as a core objective across any industrial chemical sector. Environmental protection and sustainable development have become central to corporate strategies, driving companies to explore new ideas for growth and enhance their competitiveness. The cosmetics industry is playing a key role in this extraordinary shift towards sustainability, with manufacturers committed to improving their environmental profile. In order to stay ahead in a highly competitive market where safety, sustainability and ever greater efficacy are expected by the consumer, a company's green growth goals should focus on creating innovative sustainable products and ingredients. Real sustainability today requires an honest and careful evaluation of all impact factors throughout the entire life cycle (LCA - *Life Cycle Assessment*) of each constituent, the final product, or the packaging thereof [1].

In the context of an innovative cosmetic project, it is imperative to consider a range of significant factors, including but not limited to sourcing, processing, functionality, efficiency, safety, ecotoxicity, biodegradability, and waste. In addition, the cosmetic market is ruled today, as many others, by the 6R principles of a "circular economy": a model of production and consumption which pay attention to sharing, leasing, reusing, repairing, refurbishing and recycling existing materials as long as possible thus extending the life cycle of the products [2].

The term was first introduced in 1991 by the economists David W. Pearce and R. Kerry Turner [3], to explain a concept that reflects a growing awareness that the planet's resources are limited and highlights the urgent need to limit waste and give priority to renewable resources and ensure long-term environmental sustainability [4]. Since that time, research into the recovery and

recycling of organic waste has expanded significantly, supported by both academic studies and industrial innovation, with many initiatives promoted through European-funded projects [5].

In the cosmetics field, this transition has manifested in the emergence of *upcycling*, a sustainable approach that aims to minimise waste and optimise resource efficiency. The process of *upcycling* involves the transformation of by-products and residual materials into high-value added cosmetic ingredients, thereby facilitating the closed-loop recycling process in product development.

The development of a new cosmetic ingredient must consider a wide range of critical factors to ensure the creation of a truly sustainable and effective product. These include the origin of raw materials, the environmental impact of the manufacturing process, ecotoxicity, biodegradability, and waste management. This comprehensive perspective on sustainability is consistent with the overarching framework of the *6Rs of Sustainability*, a set of principles first proposed by Joshi et al. [6] which are highly associated with the concept of the circular economy (**Figures 1a and 1b**). This model strategically emphasizes the sharing, reuse, repair, refurbishment, and recycling of existing materials. These practices are fundamental mechanisms designed to extend product life cycles and achieve a substantial reduction in environmental impact [2].

Figure 1a. *6R Principles for Sustainability* [7]. **Figure 1b**. Concept of circular economy based on the 6 principles (Source: European Parliament Research Service).

This green transition toward more sustainable practices is supported by the scientific concept of Green Chemistry, which aims to minimize or eliminate the use and generation of hazardous substances right from the design cycle of products. The concept of Green Chemistry was first introduced by Paul Anastas and John Warner in the 1990s [8]. This approach is guided by twelve foundational principles that serve as a practical guideline for the development of processes and ingredients that are safer, more efficient, and environmentally friendly.

Green Chemistry is defined as a multidisciplinary approach, encompassing principles and methods from different scientific fields such as chemistry, chemical engineering, toxicology and environmental science. Within this context, chemists are developing innovative catalytic systems with the aim of reducing reagent consumption and minimising the generation of waste. Concurrently, chemical engineers formulate production processes that facilitate the recovery and reuse of materials, while optimising energy efficiency. Research in green chemistry also explores sustainable process innovations, including the use of alternative solvents, renewable energy sources, and micro-scale continuous flow technologies.

It is evident in these studies that these developments hold significant potential for application within the chemical industry, particularly in sectors such as pharmaceuticals and cosmetics.

To support this multidisciplinary and systemic approach, Green Chemistry is structured through 12 Principles, formulated to guide the development of processes and products that are more respectful of both the environment and human health:

1. **Prevention**: it is better to prevent waste than to treat or clean up waste after it is formed.
2. **Atom Economy**: synthetic methods should be designed to maximize the incorporation of all materials used in the process into the final product.
3. **Less Hazardous Chemical Syntheses**: wherever practicable, synthetic methods should be used and generate substances that possess little or no toxicity to human health and the environment.
4. **Designing Safer Chemicals**: chemical products should be designed to be effective while minimizing their toxicity.

5. **Safer Solvents and Auxiliaries**: the use of auxiliary substances (e.g., solvents, separation agents) should be made unnecessary whenever possible and innocuous when used.
6. **Design for Energy Efficiency**: energy requirements should be minimized. Synthetic methods should be conducted at ambient temperature and pressure whenever possible.
7. **Use of Renewable Feedstocks**: a raw material or feedstock should be renewable rather than depleting whenever technically and economically practicable.
8. **Reduce Derivatives**: necessary derivatization (e.g., use of blocking or protecting groups) should be avoided whenever possible.
9. **Catalysis**: catalytic reagents (as selective as possible) are superior to stoichiometric reagents.
10. **Design for Degradation**: chemical products should be designed so that they break down into innocuous substances after use and do not persist in the environment.
11. **Real-Time Analysis for Pollution Prevention**: analytical methodologies should allow for real-time monitoring and control during synthesis to prevent the formation of hazardous substances.
12. **Inherently Safer Chemistry for Accident Prevention**: substances and the form of a substance used in a chemical process should be chosen to minimize the potential for chemical accidents, including releases, explosions, and fires.

Contextualizing the 12 green chemistry principles in the extractive sector, in 2012 Prof. Chemat *et al.* [9] introduced the concept of **Green Extraction** to the scientific community, proposing a series of guiding principles for achieving sustainable extraction processes.

"Green Extraction is based on the discovery and design of extraction processes capable of reducing energy consumption, using alternative solvents and renewable natural products, ensuring a safe and high-quality extract/product" [9].

This concept meets the challenges of the 21st century, with the aim of protecting both environment and consumers, driving innovation and setting new standards for academic and industrial research [9].

- **Principle 1**: innovation by selection of varieties and use of renewable plant resource.
- **Principle 2**: use of alternative solvents and principally water or agro-solvents.
- **Principle 3**: reduction of energy consumption by energy recovery and using innovative technologies.

- **Principle 4**: production of co-products instead of waste towards bio-refinery concepts.
- **Principle 5**: reduction of unit operations number and development of safe, robust and controlled processes.
- **Principle 6**: aim for green extract with green values and non-denatured and biodegradable extract without contaminants.

Having established the importance of Green Chemistry and Green Extraction as leading paradigms for sustainable chemical innovation, the research project tried to follow several principles common to these philosophies, with the aim of creating truly ecologically sustainable processes and products and directly contributing to the Circular Economy model.

1) RENEWABLE SOURCES

Plants and Agrifood by-products Residues as Renewable Natural Sources

The need for a sustainable industrial system requires the management and transformation of plant-based by-products, which are emerging as a crucial and globally abundant resource. Plant-based food production generates considerable volumes of residues. The process of converting waste into renewable and recyclable, high-value raw materials directly contribute to mitigating ecological impacts.

A wide range of plant-based wastes and by-products are generated during primary production and subsequent processing and distribution, from diverse sources, including fruits, vegetables, cereals, oilseed crops, roots, and tubers [10,11]. The most used matrices for biorefining include crop residues: these derive from the processing of fruits and vegetables and include peels, stems, leaves, seeds, and stones. Due to their composition, they represent a significant source of high-value compounds, being particularly rich in fiber, alkaloids, and vitamins [12]. Similarly, residues from cereals and oilseeds, such as bran, germ, pomace, and cake, are known for their high content of proteins, fiber, polyphenols, and residual oil [13,14].

Scientific interest focuses on the possibility of valorizing these wastes through the extraction of bioactive molecules. Numerous studies have demonstrated the effective recovery of essential components, including both macronutrients (proteins, amino acids, essential fatty acids, and dietary fiber [15,16] and micronutrients and bioactive compounds (vitamins, flavonoids, carotenoids such as lycopene and beta-carotene, phenolic acids, and tannins; [17,18]. These extracted bioactive compounds possess significant health benefits, exhibiting potent antioxidant and antimicrobial activity essential for combating chronic conditions such as diabetes, cancer, and neurodegenerative and cardiovascular diseases [19,20].

Large volumes of by-products with high concentrations of functional compounds originate from specific industrial sectors, providing clear targets for circular strategies. The citrus industry, for example, generates approximately 50-60% of global by-products (over 60 million tonnes), including peels, pulp, seeds, and leaves. Orange peels are a rich source of carotenoids, polyphenols, pectins, and essential oils [21]. Similarly, the cereal industry produces waste that constitutes a rich reserve of essential vitamins and micronutrients, mainly concentrated in the bran and germ fractions. These processing wastes are particularly rich in both macrominerals (e.g., calcium, magnesium) and essential trace elements (e.g., zinc, iron) [22]. Furthermore, cereal by-products contain significant amounts of B vitamins, including niacin, pantothenic acid, and thiamine [23]. Finally, the olive oil industry produces significant quantities of by-products, the valorization of which provides a valuable source of phenolic compounds distributed among the leaves (rich in secoiridoids and flavonoids), the pomace (containing phenols and essential amino acids) and the vegetation wastewater, which presents a high concentration of phenolic compounds and pectic polysaccharides [24,25].

In line with the above considerations, the natural resources employed in this study encompass botanical matrices, agricultural by-products, and agro-food waste. They can have a high

environmental impact and often are difficult to dispose of, but they are very interesting for the cosmetic and pharmaceutical fields because still rich in bioactive ingredients [26,10,11].

These were carefully selected based on their specific chemical-physical characteristics, their availability, and their high potential for valorisation within a circular economy perspective. The main properties of each matrix used in this research will be described below.

Cosmetic valorization of botanical matrices

Laurus Nobilis L. (Laurel leaves)

Bay laurel (*Laurus nobilis* L.) is a historically and economically significant evergreen species of the Lauraceae family, indigenous to the Mediterranean Basin. The plant's utility extends beyond its ornamental function, positioning it as plant cultivated for its high-value spice attributes and as a primary resource for the flavouring and fragrance industries. The plant's Essential Oil (EO) is widely featured in traditional remedies, with extensive literature documenting its therapeutic efficacy, which stems from its antioxidant, antimicrobial, and anti-inflammatory characteristics [27]. A comprehensive literature review confirms that extracts obtained via essential oil, methanol, ethanol, seed oil, and supercritical fluid exhibit a broad spectrum of bioactivities, including significant antioxidant, antimicrobial, antiproliferative, antitoxigenic, anti-diabetic, antiacetylcholinesterase, and cytotoxic effects [28]. Furthermore, aqueous extracts derived from laurel fruits and foliage have historically been applied in traditional medicine for treating gastrointestinal, neurological, and urological ailments, as well as serving as astringent agents in topical dermatological preparations [29]. This confirmed spectrum of bioactivities positions laurel derivatives as highly relevant for contemporary integration into cosmetic formulations and complementary medical therapies [30], having demonstrated success in applications such as dandruff control and psoriasis management. The biological properties of Laurus are attributed to a broad spectrum of biologically active

compounds including terpenoids, norisoprenoids, alkaloids, tannins, carotenoids, antotocopherols, and a vast number of phenols and polyphenols such as phenolic acids, flavonoids, and lignans [31] **Figures 2** and **3**.

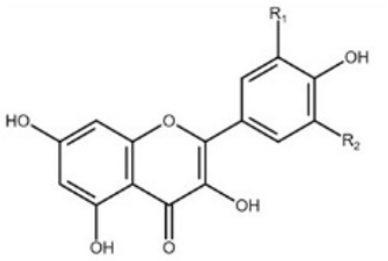

Flavonol	R1	R2
Kaempferol	H	H
Quercitin	OH	H
Isorhamnetin	OMe	H

Figure 2. Chemical structure of the main flavonols found in *L. nobilis* L. leaves (adapted from Li et al. [32]).

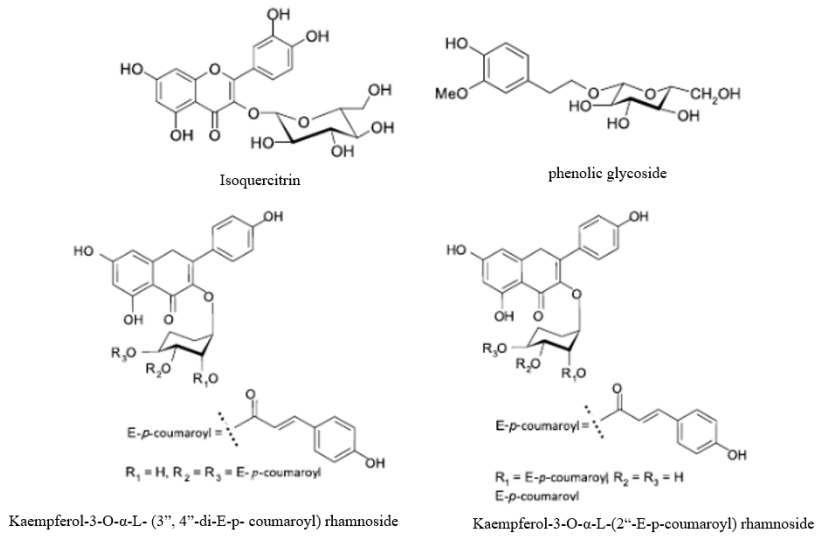

Figure 3. Chemical structure of the main phenolic found in *L. nobilis* L. leaves [33].

This phytochemical complexity encompasses various terpenoids and norisoprenoids with 1,8-cineole (Eucalyptol) being a principal volatile component linked to therapeutic value [30] due to its well-known mucolytic and antiseptic action. Similarly, the monoterpenoids Linalool and Eugenol **Figure 4** are recognized for their strong antimicrobial action, while the presence of Sesquiterpene Lactones, such as Costunolide, contributes significantly to the plant's anti-inflammatory profile, although attention is required due to its allergenic potential [28].

Conventionally, the isolation of these valuable compounds is achieved through established methods such as steam distillation (for EO) or classic extractive procedures utilizing organic or hydroalcoholic solvents. Alternative approaches have been recently used to improve the release of these components from the plant matrix [34].

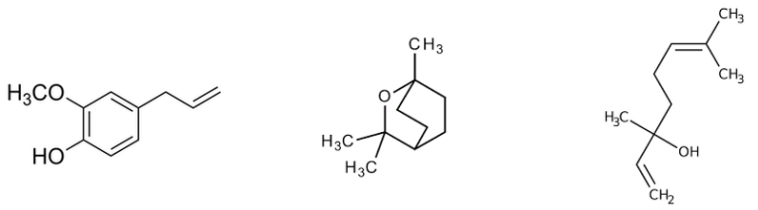

Eugenol 1-8 Cineole Linalool

Figure 4. Chemical structure of the Eugenol, 1-8 Cineole and Linalool in *L. nobilis* L. leaves.

Paeonia Lactiflora Pall. (Peony Flowers)

Paeonia lactiflora Pall. has a long and deep-rooted history of therapeutic applications throughout the Asian continent, particularly in Traditional Chinese Medicine, where preparations derived from its roots are used to manage numerous pathological conditions, including dysmenorrhea, amenorrhea, pain, infections, neurological diseases and inflammatory conditions [35]. This tradition is validated by modern scientific research, which confirms that the species possesses significant anti-inflammatory, antioxidant, antibacterial, antidepressant and antitumor activities [36]. The pharmaceutical importance of the plant is confirmed by its inclusion in various official pharmacopoeias, and its extracts are recognized by the European Commission's CosIng database [37], specifically for use as antioxidant and skin-protective ingredients in cosmetic formulations. The genus Paeonia, the sole member of the Paeoniaceae family, is recognized worldwide for both its ornamental beauty and medicinal utility, native to China, which remains the epicenter of its biodiversity and primary use [38]. The medicinal use of peony in China dates back to at least the 3rd century BC, giving rise to well-established traditional remedies such as Mudanpi (from the bark of Paeonia suffruticosa) and Chi Shao and

Bai Shao (from the root of *P. lactiflora*) [39]. Chi Shao (Paeoniae Radix Rubra) and Bai Shao (Paeoniae Radix Alba) are prepared through differential processing - Rubra from the dried whole root, Alba from the root after boiling and peeling - which results in quantitatively distinct phytochemical profiles [36,40]. The oldest preparation method involves decoction of the root, producing water-soluble compounds used for spasms and fever [41], while the most widespread modern method is hydroalcoholic extraction to obtain total peony glucosides (TGP), a standardized extract rich in monoterpene glucosides [41-44]. Due to impurities, crude TGP usually requires post-extraction purification by filtration or chromatography [45] Morphologically, *Paeonia lactiflora* Pall. is a perennial herbaceous plant, generally 40-70 cm tall, characterized by a thick root and a temperate distribution [36]. The most characteristic and critical active components of the plant are the monoterpene glucosides with their characteristic "cage" structure (**Figures 5** and **6**), especially paeoniflorin, which serves as a quality standard for medicinal use [45], along with albiflorin and oxypaeoniflorin [36].

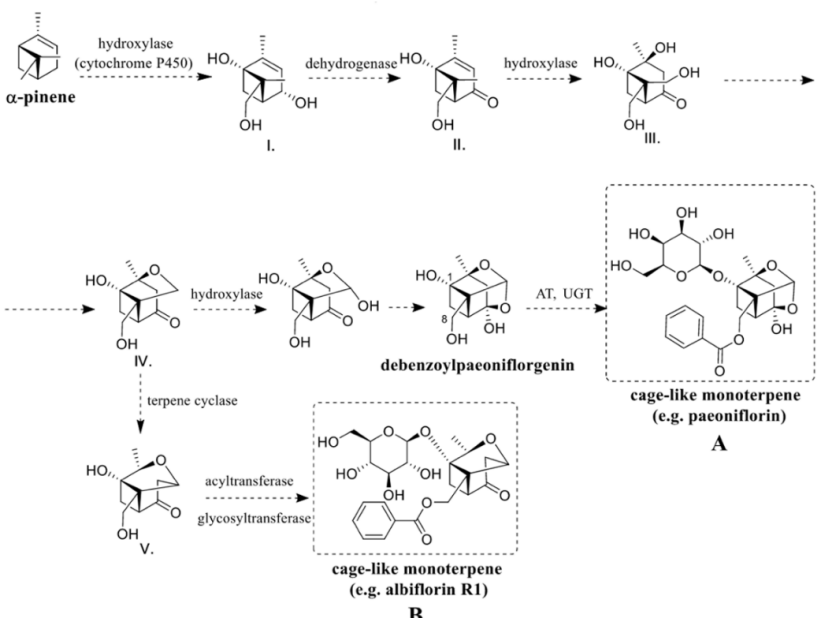

Figure 5. Possible biosynthetic pathways of monoterpenoids with a "cage" structure [36].

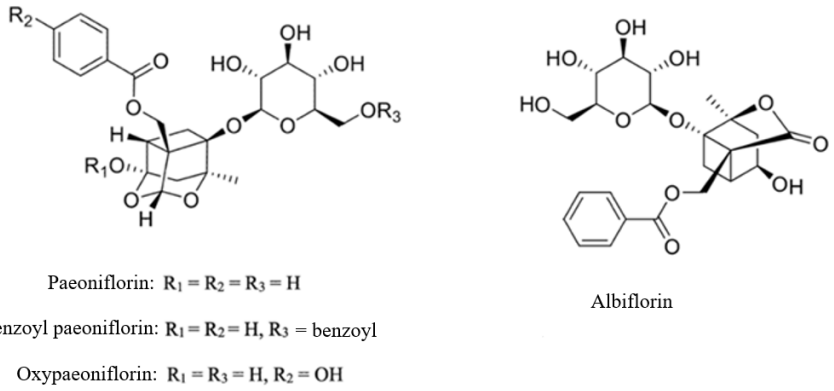

Figure 6. Structures of the main monoterpene glucosides present in *P. lactiflora.*

The second major class of compounds comprises phenols and polyphenols (**Figure 7**), including paeonol, gallic acid derivatives, stilbenes (such as resveratrol), and numerous flavonoids (**Figure 8**), along with various organic acids [36,46].

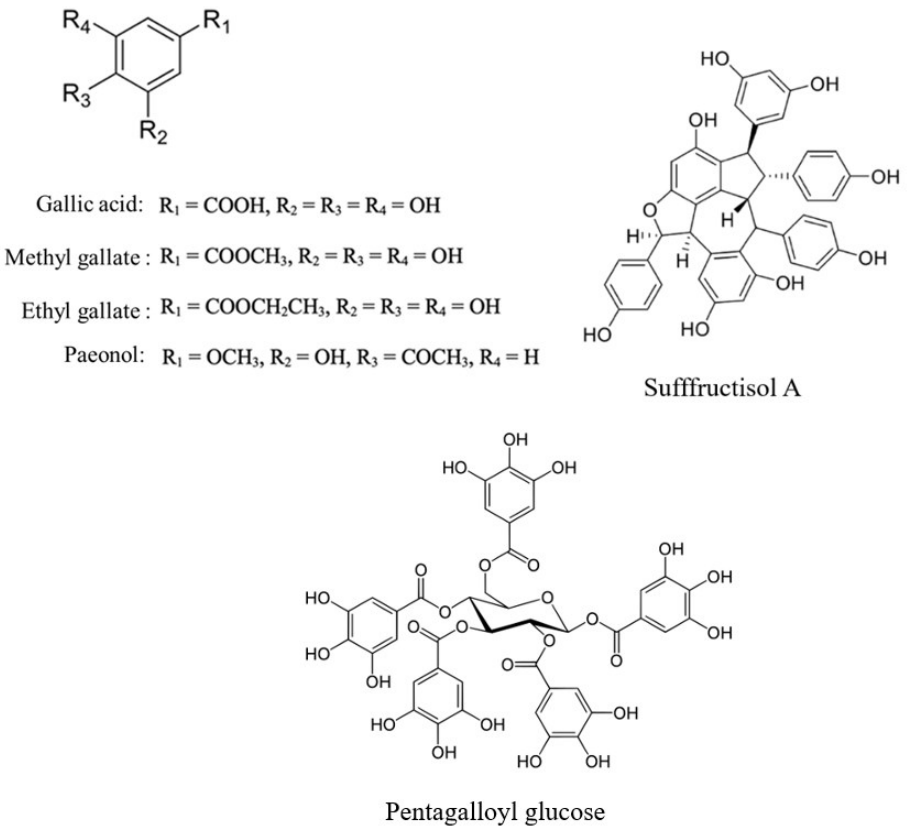

Figure 7. Structures of the main polyphenols present in *P. lactiflora.*

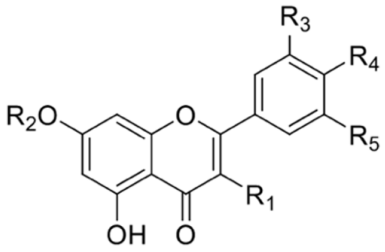

Chrysin: $R_1 = R_2 = R_3 = R_4 = R_5 = H$

Quercetin: $R_1 = R_3 = R_4 = OH$, $R_2 = R_5 = H$

Kaempferol: $R_1 = R_4 = OH$, $R_2 = R_3 = R_5 = H$

Figure 8. Structure of the most represented flavonoids in *P. lactiflora.*

These diverse compounds collectively drive the wide range of pharmacological activities (**Figure 9**), including the potent anti-inflammatory effects demonstrated by the ability of paeoniflorin and albiflorin to inhibit COX-2 and reduce pro-inflammatory cytokines such as TNF-alpha and IL-6 [47].

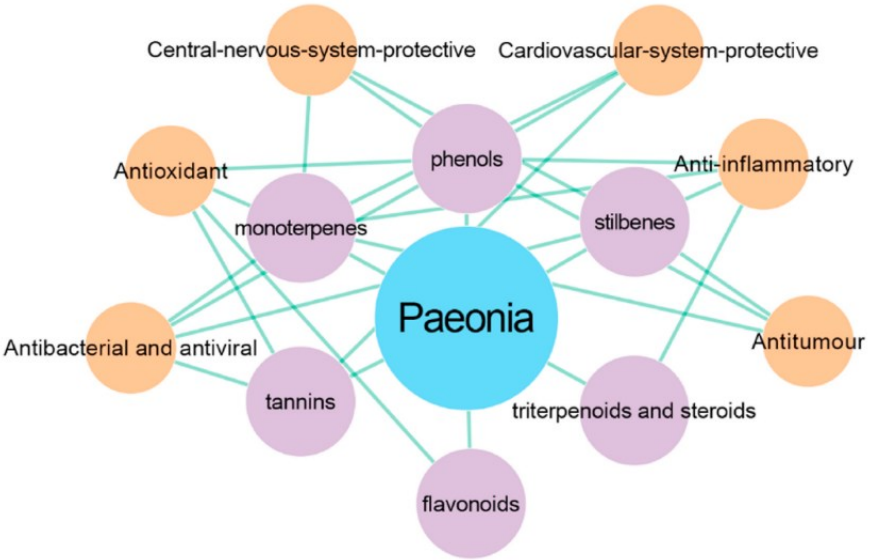

Figure 9. Main biological activities of the compounds present in the genus Paeonia [38].

The antioxidant activity is mainly attributed to the phenolic and flavonoid moieties, which act as radical scavengers and enhance endogenous antioxidant enzymes [38,48-50]. Of particular

interest is its robust antibacterial and anti-biofilm activity; extracts have shown efficacy against oral bacteria [51] and clinical pathogens, including methicillin-resistant *Staphylococcus aureus* (MRSA), where compounds such as methyl gallate and gallic acid exhibit synergistic effects with antibiotics [52,53]. Furthermore, paeonol and paeoniflorin interfere with the integrity of the bacterial cell membrane and inhibit biofilm formation [36,39]. In addition, plant constituents, such as PGG and paeoniflorin, are linked to significant antiviral activities against viruses such as influenza A and hepatitis B [54,38] and exhibit cardiovascular protective (e.g., antithrombotic and anti-atherosclerotic effects) and neuroprotective actions against depression and Parkinson's disease, often mediated by paeoniflorin and paeonol [35,38,46,55]. This broad-spectrum functionality positions *P. lactiflora* as a highly relevant and multifunctional resource for modern pharmaceutical and cosmetic development.

Fraxinus ornus L. (Manna Exudate)

Manna is a unique saccharine exudate obtained via incision from the bark of *Fraxinus ornus* L., its production now being geographically restricted to the municipalities of Castelbuono and Pollina within the Madonie Park in Sicily. The feasibility of cultivating these ash trees for manna extraction is contingent upon specific local climatic conditions, characterized by elevated temperatures, low diurnal temperature variations, and minimal atmospheric humidity, typically realized between the last decade of June and mid-September. The ash trees can subsist across diverse soil types, including loose, stony, arid, clay, and calcareous terrains [56]. Optimal manna yield requires a southeast exposure, as this orientation maximizes sun exposure and minimizes thermal fluctuations [57]. The exudate emerges as a bitter liquid which quickly condenses and crystallizes into a sweet substance upon exposure to air. The chemical composition of manna is dominated by mannitol (a polyol), alongside sugars such as glucose and fructose, water, minerals, mucilages, and resin. Its properties were leveraged in antiquity

for various applications, including decoctions and tisanes. The most recognized therapeutic effect is its laxative and prebiotic property, favored in pediatric use due to the absence of intestinal mucosal irritation. Manna was also historically employed against gout, rheumatism, and respiratory and ocular ailments. Its low glucose and fructose content renders manna suitable as a natural sweetener for diabetic individuals [58]. Recent evidence also highlights manna's potential as a mineral supplement, particularly potassium, which is of interest in sports nutrition [56]. Furthermore, traditional practices in Castelbuono involved applying a creamy manna derivative topically as an emollient. This traditional use is supported by modern research suggesting that ash manna extract may improve epidermal barrier function, reduce inflammation, and stimulate 5 α reductase activity [59]. Overall, manna exhibits antioxidant, depurative, diuretic, emollient, expectorant, and laxative properties.

The production cycle of manna typically begins after the ash tree reaches 8–10 years of age, though the initiation of sap flow is highly variable. Since the tree does not naturally produce manna without damage (e.g., from the Rodilegno insect), human intervention is essential. The mannicoltore incises the trunk, specifically severing the cortical zone to intercept the descending phloem sap, which is rich in elaborated sugars and vital for manna formation [58]. The incision process is carried out during summer, the period of maximum manna yield, when the experienced mannicoltore recognizes specific maturity symptoms. Hydric stress from summer heat is considered crucial for optimal production. The cuts are performed using a specialized, sharp tool called the mannaloro (**Figure 10**), ensuring a clean incision that passes through the bark and phloem but does not penetrate the wood.

Figure 10. The incision made with a Mannaloro.

The process begins with lightly stripping the superficial bark, followed by a series of daily cuts starting from the base upwards (**Figure 11**). Farmers observe that the presence of red ants at the incision site indicates near-maturity, while black or brown ants suggest full maturity (**Figure 12**). After a two-day rest period, the second incision confirms the tree's readiness.

Figure 11. Daily cuts starting from the base upwards.

Figure 12. Black ants on the incision.

The characteristic cerulean liquid begins to exude only after the third incision, subsequently solidifying into the crystalline whitish manna upon contact with the air (**Figure 13**). The daily incision process continues for approximately one month, provided the tree shows no signs of stress or exhaustion, such as frothy discharge after heavy rain or leaf closure.

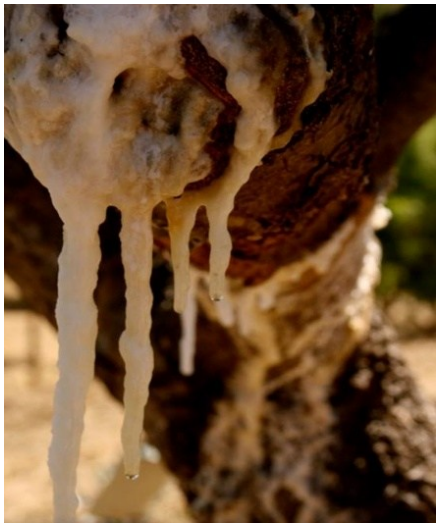

Figure 13. Manna flow from incision [58].

For collection, manna that does not dry directly on the trunk is gathered using "tabare," or dried prickly pear pads (**Figure 14a**). These pads dehydrate into a cup shape, serving as natural receptacles. The use of these pads provides a sustainable advantage: they are cost-free and decompose on the soil after the harvest period, contributing organic matter to the ash grove [58]. Historically, manna quality was classified into three categories: Manna cannolo (pure) Manna rottame (with slight impurities) **figure 14b** and **c** and Manna industria (highly impure, designated for industrial processing). Once collected, manna was spread on a wooden or cork drying rack called a "stinnituri" and left to thicken in the shade for a day before being exposed to the sun in thin layers. The manna was deemed fully preserved when it emitted a sharp, dry sound upon movement [58].

a **b** **c**

Figure 14.a) Manna flow; **b)** Manna Cannolo; **c)** Manna Rottame [58].

The most abundant active compound in Manna is the hexavalent alcohol D-mannitol, also known as 'Manna sugar' [60], which is an osmotically active and cell-compatible polyol [61]. This compound is responsible for Manna's well-established use as a natural remedy for constipation and as a sweetener. Its activity and safety profile are well understood in medicine and pharmacology, but mannitol is also widely used in the food and skincare industries. Its moisturising and antioxidant properties make it an ideal ingredient for cosmetic and dermatological formulations. Mannitol has potent free radical scavenging activity, protecting dermal cell membranes and extracellular matrix components from reactive oxygen species and UV radiation products [62]. The other constituents of Manna are simple sugars (glucose and fructose) (2-3%), complex carbohydrates (mannotriose and mannotetraose) (8–10%), lactic acid (1%), succinic acid (0.2%) and malic acid (0.07%), as well as water (10%) and ash (4%). Small percentages of inorganic compounds, such as potassium (0.5%), magnesium (0.06%) and calcium (0.09%), are also present. Fatty acids represent 0.2% of the substance, with high levels of oleic and palmitic acids [63,64]. Due to its emollient properties, Manna can be used as a valuable ingredient in cosmetics such as creams and soaps [57,65].

Solanum tuberosum (Tocosh Fermented Flour)

The Peruvian Andean region constitutes a primary global center for the cultivation and diversification of domesticated plants. The resulting high genetic variation in local species is a direct consequence of evolutionary processes influenced by the vast environmental diversity of the mountain ecosystems, coupled with ancient domestication practices conducted by native cultures. These populations have continuously shaped their cultures over time, informed by evolving worldviews and indigenous knowledge [66]. This intense human-environment interaction has fostered the development of varieties highly adapted to the extreme climatic conditions of the Andean region, yielding a crucial agricultural biodiversity heritage. Peru, in particular, exhibits the world’s greatest potato diversity, harboring eight native species and

2,301 varieties, in addition to 91 of the 200 known wild potato species, many of which are non-edible but play a crucial role in scientific research and the genetic improvement of cultivated varieties [67]. One representative staple food of the Andean tradition is Tocosh, often colloquially termed the “Natural Penicillin of Peru” due to its noted nutritional and pharmacological properties [68]. The preparation of Tocosh relies on an ancient food preservation technique involving the anaerobic fermentation of the potato tuber. This designation is reflected in its Quechua origin, “togosh,” meaning wrinkled and fermented [69]. Practiced since Inca times, this production process consists of the fermentation of potatoes immersed within natural water pools for a variable duration. This traditional method achieves both food preservation and the enrichment of bioactive compounds beneficial to human health [70]. Tocosh represents a primary nutritional source for Andean populations, providing essential energy and nutrients [71], and its consumption remains widespread despite its characteristic pungent odor. The traditional production method involves a highly localized practice, such as that observed in Palca, Huancavelica, at an average elevation of approximately 3,500 meters above sea level [72]. The site selection is critical, requiring an area near a constantly flowing water source to optimize the fermentation process. A pit is excavated to a depth of approximately 1.5-2 meters (**Figure 15 A**), allowing progressive infiltration of groundwater to fill the cavity (**Figure 15 B and C**). Subsequently, a layer of straw (*paja* or *Ichu*) is positioned over the water and around the basin walls (**Figure 15 D**), then secured with large stones to apply mechanical pressure and prevent displacement (**Figure 15 E-F**). The potatoes are then placed into the pit, layered and interspersed with additional straw to ensure homogeneous anaerobic fermentation. The pit is finally sealed by covering it with the excavated soil, protecting the contents from light and air. A lateral channel is constructed to facilitate the continuous flow of subterranean water, maintaining the ideal humidity conditions. This fermentation requires a variable period, typically spanning six to eight months [73], after which the tubers are extracted.

The resulting Tocosh is a soft product characterized by its pungent odor (**Figure 16 H)**, confirming the successful anaerobic transformation.

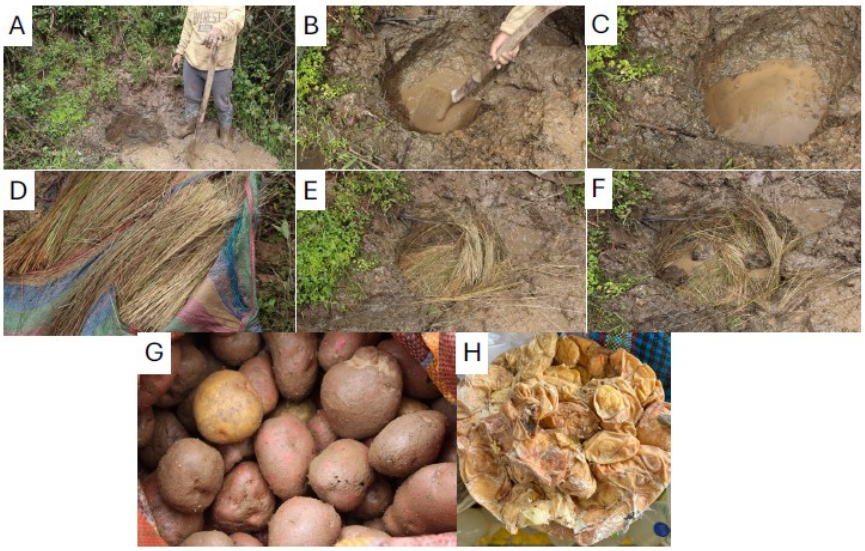

Figure 15. Traditional method of producing Tocosh (A-F). Panels G and H show photos of the potatoes before and after the fermentation process.

The chemical composition of potato Tocosh, derived from potato fermentation, disclosing the presence of carbohydrates (mainly starch 80%), proteins (3.92g%) and small amounts of fatty acids, alkaloids, free amino acids, minerals and thiamine and riboflavin, among other vitamins [74]. From a microbiological point of view, Tocosh results from microbial fermentation, mainly by Lactobacilli spp., that seems to be the responsible for its large diversity of medical properties. It is considered an effective and low-cost antibiotic, energizer, and probiotic useful for gastrointestinal, respiratory and urinary diseases, loss of hair and skin care. For its antibacterial properties it is known as such as the “natural penicillin of the Andes”.

Despite its long-standing cultural use and interesting functional potential, Tocosh remains underexplored in scientific literature, with only a limited number of studies addressing its chemical composition, microbiological profile, and possible pharmaceutical and cosmetic

applications. This lack of research highlights the necessity for further research to elucidate its bioactive properties and potential for innovative development of bioactive ingredients.

Beta vulgaris var. *rubra* (Red beetroot stalks)

The red beetroot (*Beta vulgaris* var. *rubra*) is a flowering plant, typically biennial or rarely perennial, belonging to the Chenopodiaceae family. Native to the Mediterranean scrubland, it is now cultivated extensively across America, India, and Europe [75]. The edible component is the root, which exhibits a characteristic elongated, tapered, and robust shape with colours spanning from deep red-violet to yellow-golden or white, depending on the specific cultivar [76]. Among the various species and subspecies, *B. vulgaris* is the most vital and commercially recognized, notably as common beetroot or sugar beet, with global production approximating 42 million tonnes. The edible root is highly valuable due to its richness in carbohydrates, fats, proteins, micronutrients, and numerous functional constituents, including polyphenols and flavonoids, which impart significant health benefits such as antioxidant, antimicrobial, and anti-inflammatory properties. Furthermore, the root contains a substantial quantity of betalains, [77] which are water-soluble pigments divided into betacyanins (e.g., betanin and isobetanin, providing intense red-violet colours) and betaxanthins (e.g., indicaxanthin and vulgaxanthin, yielding yellow-orange hues). These pigments are frequently employed in food colouring (E162, betalain) owing to their high tinting strength. Betalains themselves offer positive health effects, having demonstrated considerable antioxidant and anti-inflammatory activity [78,79]. Bioactive compounds and their relative structures are detailed in **Figure 16**.

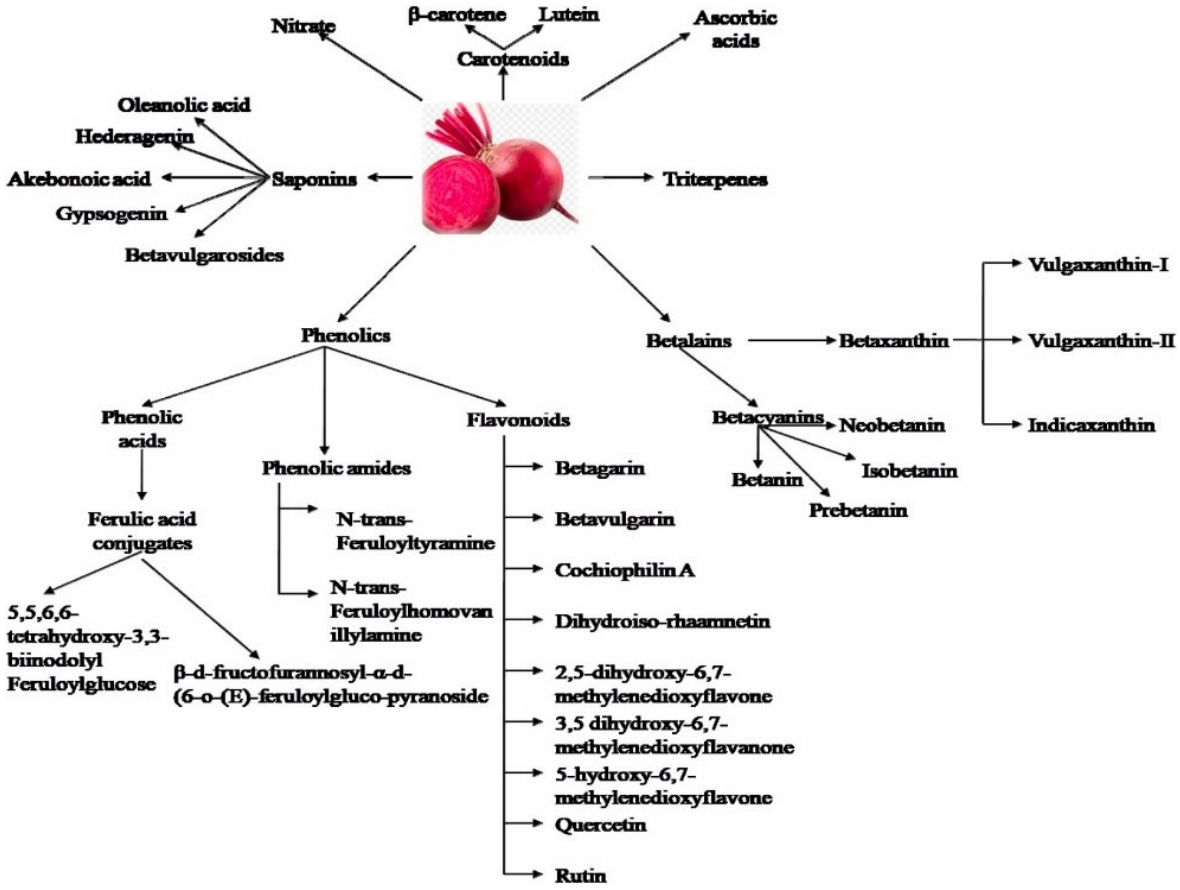

Figure 16. Main components of *Beta vulgaris* var. *rubra* [75].

The processing and consumption of beetroot are continually increasing, driven by its recognition as an essential source of natural antioxidants. Critically, the inedible stems constitute approximately 35% of the total weight, resulting in a disposal challenge of around 14 million tonnes of agricultural waste post-processing. Various studies have highlighted the high potential of these stems, as they remain rich in valuable bioactive molecules, including phenolic compounds such as rutin, kaempferol, quercetin, catechin, vanillic, syringic, and ellagic acids, in addition to a significant content of betalains **Figure 17**. Consequently, beetroot stems represent a massive, underutilized agricultural waste stream that can be transformed into a valuable renewable and recyclable natural resource for the cosmetic and pharmaceutical sectors. This beetroot residue contains a functional blend of compounds associated with

antianemic, antihypertensive, anti-inflammatory, antioxidant, antitumor, antipyretic, antimicrobial, detoxifying, and diuretic properties [76].

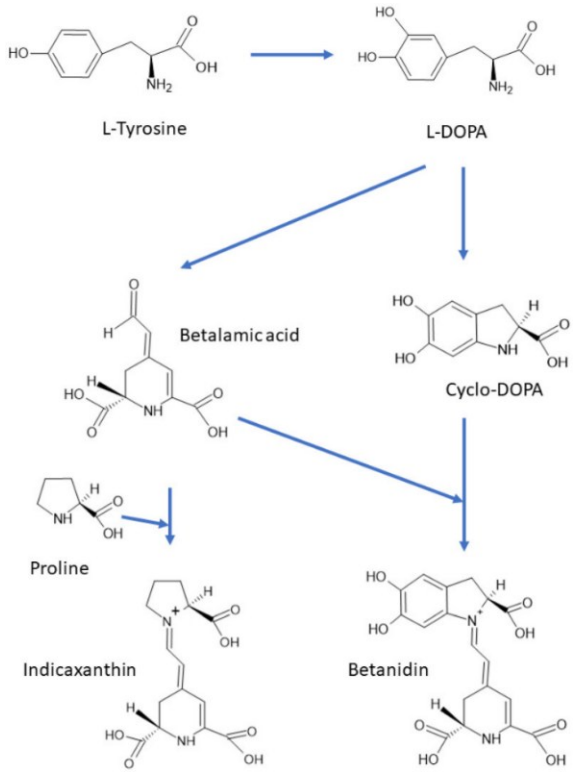

Figure 17. Biosynthesis of betalains [80].

Betalamic acid, due to its conjugated double bonds, serves as the main chromophore of all betalains, which exhibit two absorption maxima: one in the UV range (270-280 nm), and a second in the visible range (535-540 nm, dependent on the solvent). The position and nature of substituents determine the effective colour. The maximum peak at 540 nm is specifically due to the condensation of betalamic acid with cyclo-DOPA, inducing a bathochromic shift compared to betaxanthins, which typically show a maximum at 480 nm. Betalains display a wide colour gamut (from yellow to red and violet) strongly correlated to their structure and influenced by external factors such as temperature, solar radiation, and pH. They are generally stable within a pH range of 3 to 7, showing no spectral change; however, lowering the pH below 3 results in a hypochromic effect in the 535-540 nm absorption band, accompanied by a slight

hyperchromic effect in the 575-650 nm range and a corresponding colour shift from red toward violet as the pH increases. Conversely, values above pH 7 lead to shifts in the maximum absorption wavelength and a hypochromic effect. Betalains are also sensitive to heat; temperatures exceeding 50°C can cause the colour of the solutions to fade. For example, at 100°C, the red colour of an aqueous betanin solution gradually fades, turning yellowish-brown due to the formation of new degradation products, including neobetacyanins, betalamic acid, and newly formed betaxanthins (**Figure 18**).

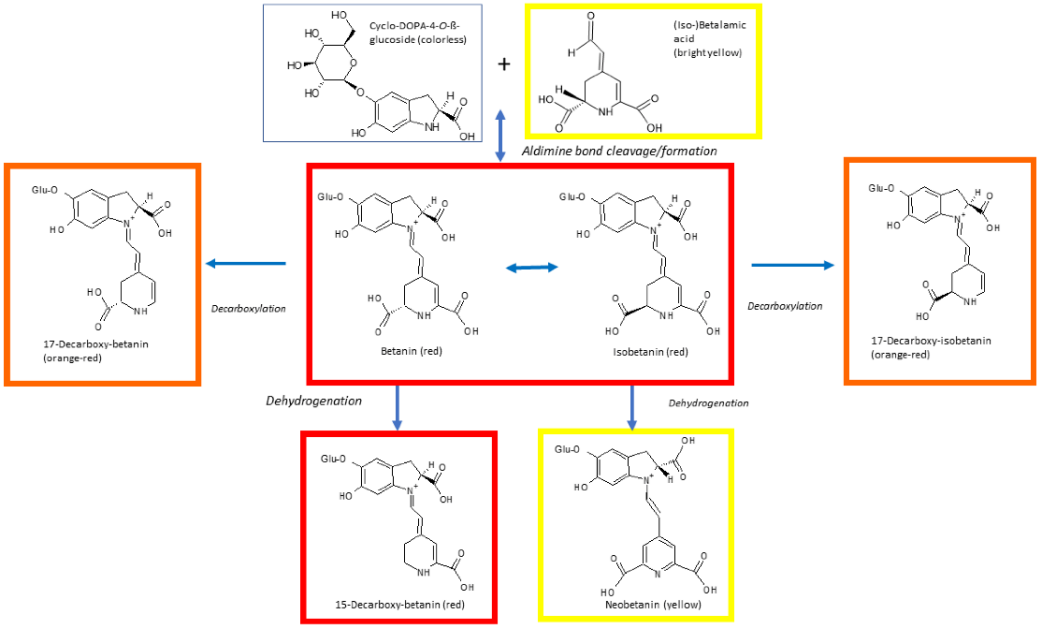

Figure 18. Degradation pathways of some betalains [80].

Various studies consistently indicate that betacyanins are more stable than betaxanthins, both at ambient temperature and upon heat exposure. For instance, the half-life of heat-treated betanin has been reported to be 11 times greater than that of vulgaxanthin I [81]. Among instability factors, the presence of a high water content is a key in controlling betalain degradation, which accelerates when stored in dilute aqueous solutions. Betalain stability is also significantly influenced by water activity during processing.

Moreover, red beetroot stalks are one of the best sources of phenolic compounds, including phenolic acids and flavonoids. These secondary metabolites, essential for plant growth and development, protect the plant from pathogens and predators. These molecules, in synergy with other constituents, can exert protective effects against cardiovascular disease by reducing the oxidative effect of free radicals on lipids and lowering blood pressure. They are associated with antioxidant, antimicrobial, anti-inflammatory, antiallergic, and antithrombotic properties [82].

Olea europaea (olive mill wastewater)

Olive oil is the primary source of lipids in the Mediterranean diet, with globally recognized nutritional benefits [83]. While triglycerides constitute the majority (98-99%) of olive oil [84], the oil also contains over 200 minor components, including sterols, waxes, tocopherols, carotenes, chlorophylls, and volatile and phenolic compounds [85]. The multi-stage production process, which involves defoliation, washing, crushing (using stone mills or hammer/blade crushers), malaxation, and solid-liquid extraction (**Figure 19**), generates significant quantities of industrial waste.

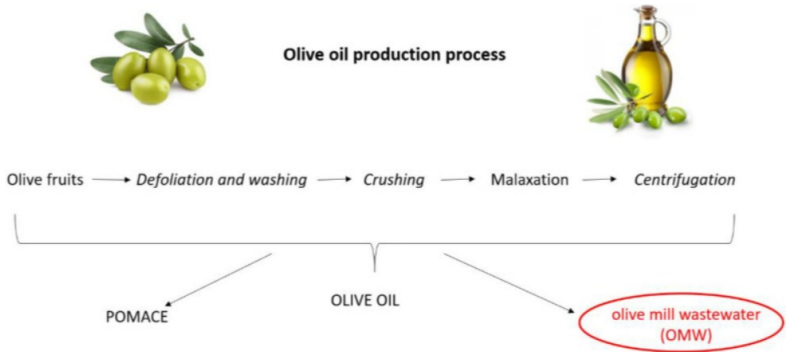

Figure 19. Stages of the olive oil production process.

The modern extraction method relies on a horizontal centrifuge, the "decanter," which separates materials-namely the olive pomace (solid residue), olive oil, and Olive Mill Wastewater (OMW)-based on density differences. A conventional milling procedure typically yields 20%

oil, 30% solid residue, and approximately 50% OMW [86]. Depending on the extraction system used (three, two, or two-and-a-half phase decanters), the volume of OMW can range dramatically, from 40 to 120 L per quintal of processed olives [87]. OMW is characterized by a dark brown-to-black color and an intense, typical olive odour. It consists of an aqueous phase containing dissolved organic (e.g., reduced sugars, organic acids, polyalcohols) and inorganic substances (e.g., potassium, phosphorus, calcium), alongside a suspended phase of unfiltered solid plant material. OMW poses a significant environmental challenge and is considered a major industrial pollutant [88]. The direct discharge of OMW into soil or rivers can cause damage to flora and lead to the depletion of potable water basins, largely due to its high content of (phyto)toxic compounds, particularly phenols [89]. To mitigate this environmental impact, various physico-chemical, biological, and combined processes have been investigated. One promising treatment strategy for concentrating phenols is membrane filtration. While most studies focus on pressure-driven processes (e.g., microfiltration, ultrafiltration, reverse osmosis, and nanofiltration), innovative membrane processes like membrane distillation are also being actively explored [90,91]. Recent research, including work conducted at the University of Genoa by the research group that hosted this thesis, focused on an innovative membrane process for OMW purification, commencing with microfiltration (MF) followed by reverse osmosis (RO) [92]. This work included the chemo-physical characterization (conductivity and IR spectroscopy), total polyphenol quantification (Folin-Ciocalteu assay), and antioxidant activity assessment (DPPH assay) of the purified OMW fractions (**Figure 20**).

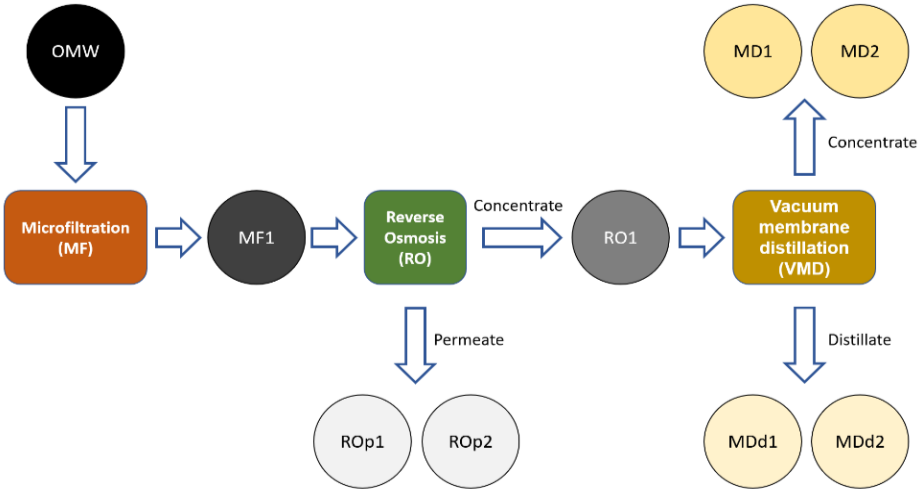

Figure 20. Schematic representation of the OMW purification process.

Attention has increasingly focused on the possibility of fractionating and recovering the phenolic compounds present in OMW as a valorization strategy aligned with circular economy principles [93,94]. The olive fruit contains diverse phenols, whose content varies by cultivar, including tyrosol and its derivatives, phenolic acids, secoiridoids, flavonoids, and lignans. However, since many of these substances are water-soluble, they largely remain in the aqueous residue, with only a small fraction moving into the oil. This is notably the case for hydroxytyrosol, a polar phenol sparingly soluble in oil, which exists either as a simple phenol or esterified with elenolic acid to form oleuropein aglycone, and which is naturally present in significant concentrations in the aqueous fraction [95]. Consequently, OMW, derived from the pressing of olives, is rich in these bioactive compounds, particularly polar phenols, and typically retains up to 98% of the total phenols originally present in the olive fruit [96]. The known health benefits of olive phenols are substantial; specifically, hydroxytyrosol exhibits considerable antioxidant and anti-inflammatory potential [97]. Oleuropein belongs to the secoiridoids, a specific group of coumarin-like compounds abundant in the Oleaceae family (including *Olea europaea* L.) and characterized by the presence of elenolic acid. These secoiridoids are formed by a phenylethyl alcohol (hydroxytyrosol or tyrosol), elenolic acid, and potentially a glycosidic

residue [98]. The aglyconic forms of secoiridoids found in olive oil are derived from the olive glycosides via hydrolysis by endogenous during crushing and malaxation. This hydrolysis process liberates simple phenols, such as hydroxytyrosol and tyrosol. These newly formed substances, due to their amphiphilic nature, partition between the oil layer and the OMW, but are more concentrated in the latter fraction due to their polar groups.

The most abundant secoiridoids in olive oil are the dialdehydic form of elenolic acid linked to hydroxytyrosol or tyrosol (p-HPEA), respectively termed 3,4-DHPEA-EDA and p-HPEA-EDA, and an isomer of oleuropein aglycone (3,4-DHPEA-AC) has also been identified in extra virgin olive oil [99-101]. Phenolic acids, which are aromatic secondary metabolites widely distributed throughout the plant kingdom [102,103], contain two distinct constitutive carbon skeletons: hydroxycinnamic and hydroxybenzoic. These acids contribute to the colour and sensory qualities of foods, as well as their health and antioxidant properties [104,105].

Flavonoids are another ubiquitous class of plant secondary metabolites. Their structural variation arises partly from modifications such as hydroxylation, methylation, prenylation, or glycosylation. Flavonoid aglycones are classified into flavones, flavonols, flavanones, and flavanols based on structural features like the presence of a carbonyl group at C-4, an OH group at C-3, and the saturation state of the C-2/C-3 bond. Luteolin and apigenin, for instance, may originate from their respective glucosides.

Consequently, OMW is a potential source rich in a vast array of phenols exhibiting numerous biological activities [96]. Notably, hydroxytyrosol, being the most abundant compound, possesses both strong antioxidant and antimicrobial activity. This dual functionality suggests that OMW extracts could be an excellent ingredient for use in wound dressings to promote healing.

The rationale for including these antioxidant compounds in wound care relates to the inflammatory phase of healing. While oxygen stimulates bactericidal action against pathogens through the formation of Reactive Oxygen Species (ROS) via the NADPH oxidase system in leukocytes [106], excessive ROS production leads to oxidative stress and cytotoxic effects that can significantly delay chronic wound healing [107]. Therefore, the neutralization of excess ROS is a critical strategy to improve healing outcomes, justifying the incorporation of OMW's polyphenols into wound dressings. The antioxidant action of polyphenols is exerted via three principal mechanisms: hydrogen Atom Transfer (HAT), Single Electron Transfer (SET), and Transition Metals Chelation (TMC).

Furthermore, the significant antimicrobial action of OMW is another crucial feature for wound care applications. Once the skin barrier is compromised, saprophytic flora can access underlying tissues. Contamination and subsequent infection pose serious complications, with sepsis being a major cause of morbidity or mortality in patients with deep wounds [108]. Infection in the compromised area triggers a systemic response and inhibits the evolution of the normal healing process. Since wounds are inherently prone to bacterial and/or fungal contamination, which damages tissue and impairs healing [109], the antimicrobial properties of OMW extracts driven by their phenolic content could effectively prevent microbial proliferation and subsequent infection when incorporated into cutaneous dressings.

2) ALTERNATIVE SOLVENTS

Green alternative solvents are environmentally friendly substitutes for traditional solvents in chemical and extractive procedures; they are designed to reduce toxicity, improve biodegradability, and minimize environmental impact and health risks. According to Gu and Jérôme [110], green solvents should fulfil 12 criteria relating to availability, price, recyclability, grade, synthesis, toxicity, biodegradability, performance, stability, flammability, storage and

renewability. In most of the cases not all requested parameters can be fulfilled by one solvent; therefore, the best solvent is always a compromise between these different requirements.

In the green extraction domain, the choice of a green solvent depends heavily on the specific application. Different key categories can be represented:

- Bio-based solvents (from renewable agricultural feedstocks or wood waste), which offer high performance with a lower carbon footprint.
- Supercritical Fluids (Supercritical Carbon Dioxide, and Supercritical Water), where these substances are heated and compressed beyond their critical points, exhibiting properties of both gases and liquids.
- Alternative Solvent Systems (such as water, ionic liquids and Deep eutectic solvents) represent the latest frontier in the study of solvents for sustainable extraction. My research focused on this last promising class of solvents.

Solvent-free Processes

Sometimes the best solvent is no solvent. In line with the fifth principle of green chemistry and extraction, in different processes, especially under microwave activation, solvents can be entirely eliminated. Of course, if the absence of a solvent leads to dangerous overheating or a higher energy demand, the advantages of a solvent-free process would be outweighed by these disadvantages.

Water

One of the most significant challenges in the field of chemistry pertains to the endeavor to substitute the use of organic solvents with water in chemical processes. The advantages offered by water include a low hazard potential, high availability and low cost. Furthermore, it discloses interesting aspects concerning reactivity, uncommon selectivity, the influence of hydrogen-bond networks on reaction behaviour, adjustable pH values, and the application of biphasic

reaction systems. In the extraction processes, subcritical water extraction (SWE) is a widespread green technique that uses hot, pressurized liquid water (between 100 and 374° C) as a solvent to extract bioactive compounds from natural sources like plants, microorganisms, and waste. Physical and chemical properties of subcritical water show a significant dependence on temperature and pressure, so that solvent properties are strongly influenced and adjustable. Altering the temperature, this method exploits the change in water's polarity, allowing it to dissolve both polar and non-polar compounds efficiently. It is cost-effective, environmentally friendly, and tunable. Despite this, it is crucial to recognise the inherent limitations since these processes are highly energy intensive [111].

Natural Deep Eutectic Solvents (NaDES)

NaDES are a new class of green, non-flammable solvent that offers an efficient, sustainable alternative to conventional ionic liquids. NaDES are easily prepared by combining naturally derived components and exhibit remarkable solubilising capabilities, particularly for lipophilic substances. Thanks to their distinctive physicochemical properties, these solvents are being increasingly explored in cosmetic and pharmaceutical contexts, including in eco-friendly extraction processes, the formulation of ready-to-use active ingredients and the design of biocompatible drug delivery systems. In the biomedical sector, NaDES can also act as biopolymer modifiers and therapeutic carriers. They can enhance the solubility and stability of a wide range of chemical compounds and galenic preparations. This contributes to the development of next-generation formulations [112].

The choice of solvent is a crucial point in any extraction, conventional organic solvents are widely employed for the extraction of active compounds such as fragrances, flavors, pharmaceuticals, and pigments from plant materials. However, their use raises significant environmental and safety concerns due to their toxicity, flammability, and adverse ecological

impact [113]. In response to these limitations, recent research efforts in the field of green extraction have increasingly focused on the development and application of environmentally friendly, non-toxic, and biodegradable solvent systems [114].

Among the most promising alternatives are ionic liquids (ILs) and deep eutectic solvents (DES), which offer viable substitutes for traditional hazardous organic solvents [113]. Ionic liquids consist of salts composed of an organic cation and a corresponding anion, typically exhibiting melting points below 100 °C and remaining in the liquid state under ambient conditions [115]. Deep eutectic solvents, on the other hand, are homogeneous liquid systems formed by combining two or more pure components, either ionic or neutral acting respectively as hydrogen bond donors (HBDs) and acceptors (HBAs) [116]. Both ILs and DES are valued for their high thermal stability, negligible vapor pressure, and tunable viscosity and polarity profiles [117,118].

Ionic liquids are characterized by their low melting points and extremely low volatility, and their chemical structure can be modified to tailor properties such as polarity and selectivity for specific applications, including chemical and enzymatic reactions [119,120]. Nevertheless, their practical use remains limited due to high toxicity, elevated production costs, and complex processes required for synthesis, purification, and disposal [121]. These drawbacks have paved the way for the increased use of DES, which often offer comparable or superior physicochemical properties with the added advantages of simpler synthesis and lower environmental impact [122].

Originally described by Abbott and collaborators [123], DES have gained attention for their simple preparation, reduced costs, and generally lower toxicity [124]. The preparation of a DES typically involves the combination of a quaternary ammonium salt (as HBA) and a suitable HBD in a defined molar ratio [125]. The interaction between these components results in the

formation of a stable supramolecular complex with unique chemical characteristics, including a significant depression of the melting point of the mixture compared to the individual constituents, which often between room temperature and 70°C. [118,126,127]. However, one challenge in using DES as green solvents is that some exhibit melting points that are still too high for practical use under ambient conditions [128].

To address this limitation, a new class of solvents known as natural deep eutectic solvents (NaDES) has emerged. It has been hypothesized that, in nature, plants can form eutectic mixtures from primary metabolites such as sugars, amino acids, organic acids, and alcohols, that serve diverse physiological functions. These mixtures may act as natural alternatives to water or lipids, facilitating the intracellular transport of hydrophobic compounds, which may explain the co-occurrence of hydrophilic and lipophilic molecules in plant tissues. When such metabolites are used to formulate DES, the resulting systems are termed “Natural Deep Eutectic Solvents” [129]. The concept and green potential of NaDES were first formally described by Choi et al. in 2011 [128-130].

NaDES aim to replicate this natural behavior and are now recognized as promising green solvents across various sectors, including cosmetics, pharmaceuticals, and food science. These solvents have been successfully employed for the extraction of phenolic compounds from botanical sources [131-133].

Furthermore, NaDES have demonstrated the ability to stabilize sensitive biomolecules such as enzymes (e.g., lysozyme, amylase) and nucleic acids, supporting their potential use in biomedical and biotechnological applications [129,133,134]. This has led to increased exploration of NaDES as innovative drug delivery systems for poorly soluble active pharmaceutical ingredients [135-137]. Thanks to their wide polarity range and high solubilization efficiency, NaDES outperform many traditional solvents, ILs, and even

conventional DES in terms of biocompatibility, biodegradability, cost-effectiveness, and ease of preparation [133].

Despite these advantages, some concerns remain regarding the ecological footprint of NaDES, particularly their potential contribution to eutrophication, although their overall toxicity are considered low [138]. When applied as alternative solvents in extraction processes, NaDES have shown high extraction efficiency and, in many cases, enhanced the stability and shelf life of target compounds such as phenols, β-carotene, and α-tocopherol [133,134,139-143].

After outlining the general advantages and applications of NaDES, the following section focuses on their preparation strategies and physicochemical properties, which support their practical use in cosmetic and pharmaceutical contexts.

Strategies for the preparation of NaDES

Many NaDES exhibit excellent environmental compatibility, characterized by high biodegradability and relatively low toxicity [144-146]. This is largely attributable to their composition based on naturally occurring and biocompatible metabolites such as organic acids, sugars, alcohols, polyols, amino acids, and quaternary ammonium salts, many of which are already widely utilized in pharmaceutical and cosmetic formulations due to their intrinsic biological activity.

From the perspective of cosmetic science, these characteristics confer significant formulation advantages. NaDES enable the development of compositions with a higher proportion of bioactive substances while reducing or eliminating the need for synthetic preservatives. This contributes to enhanced product stability, supports synergistic biological effects, and aligns with current trends favoring "clean label" and minimal-ingredient products. The ability to formulate using fewer components while maintaining efficacy represents a key innovation in natural product development.

NaDES synthesis is typically straightforward and does not generate waste, resulting in highly pure mixtures in accordance with the principles of green chemistry [147,148].

As previously discussed, NaDES are produced through the combination of a hydrogen bond acceptor (HBA) such as choline chloride, choline acetate, or betaine with a hydrogen bond donor (HBD) like glycerol, urea, glucose, sorbitol, or fructose. This process may or may not include the presence of water [128] and is commonly achieved through one of the following methodologies (**Figure 21**).

- Thermal stirring method: this conventional approach involves heating the component mixture (typically at 50 °C) under magnetic stirring until a homogeneous viscous liquid is obtained, usually within 30 to 90 minutes [128,133,149,150]. Alternatively, as proposed by Abbott et al. [123], mixing may be conducted at elevated temperatures (up to 80 °C) under continuous agitation [149,151,152].
- Freeze-drying technique: although less frequently applied, this method utilizes sublimation to eliminate water from a NaDES solution, resulting in a highly purified product [153].
- Evaporation approach: in this method, the mixture is dissolved in water and subjected to rotary evaporation at approximately 50 °C. The resulting liquid is subsequently placed in a desiccator with silica gel until constant mass is achieved [128].
- Manual grinding: a solvent-free and low-energy technique whereby the constituents are physically ground together using a mortar and pestle at room temperature until a uniform liquid phase is formed [154].
- Ultrasound-assisted preparation: this method employs ultrasonic waves to facilitate and accelerate the formation of the NaDES mixture, enhancing mixing efficiency [155].
- Microwave-assisted synthesis: the components are exposed to low-power microwave radiation for a short duration, promoting rapid and uniform formation of the eutectic mixture [156].

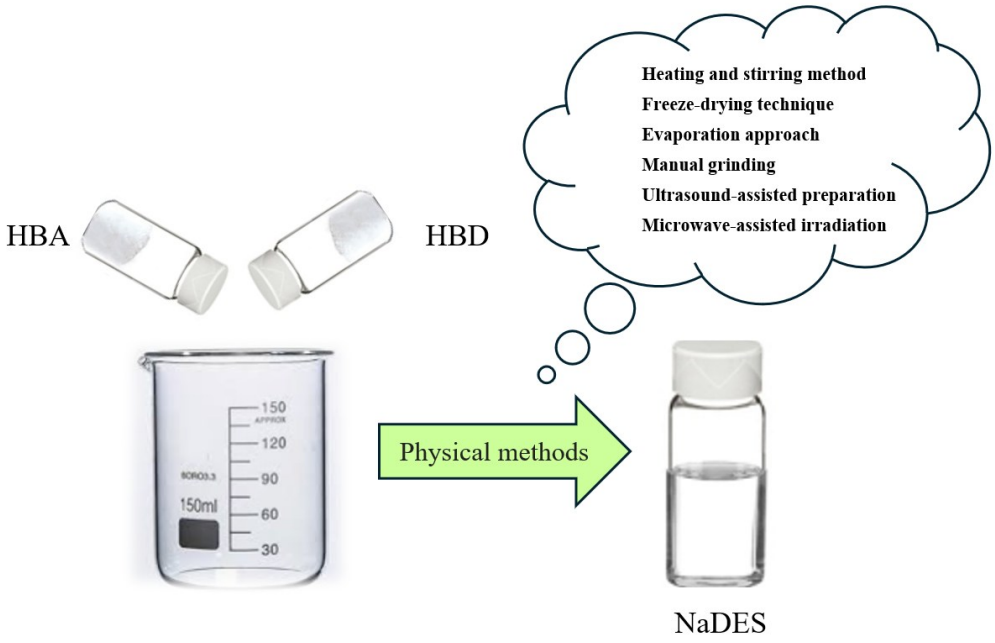

Figure 21. Different methodologies used in the preparation of the NaDES: these methods offer a sustainable and innovative approach, characterized by advantages such as improved yields, reduced energy consumption, and significantly shorter reaction times [112].

Structural features and physicochemical behavior of NaDES

The structural characteristics and functional properties of NaDES depend primarily on the type and molar ratio of their constituents and on the network of hydrogen bonds (HB) that form between them [128,157,158]. These HB interactions play a central role in defining the thermodynamic stability, phase transition behavior, and solvent capabilities of the eutectic mixtures [153]. Their influence is closely related to both their number and specific spatial arrangement within the supramolecular system [128].

A distinctive feature of NaDES is their significantly lower melting point compared to that of the individual components. This phenomenon results from the delocalization of charges between hydrogen bond donors (HBDs) and acceptors (HBAs), supported by van der Waals interactions, which inhibit crystallization of the mixture [139]. In general, a stronger affinity between HBA and HBD corresponds to a lower freezing point of the eutectic system [159].

The supramolecular structure of NaDES has been elucidated through various spectroscopic and analytical methods, including nuclear magnetic resonance (NMR), fast atom bombardment-mass spectrometry (FAB-MS), Fourier-transform infrared spectroscopy (FT-IR), and crystallography [128,149,160]. Nuclear Overhauser effect spectroscopy (NOESY) has confirmed the presence of extensive HB networks responsible for the liquid structure of NaDES [128]. However, this supramolecular organization is sensitive to water. Upon progressive dilution, especially beyond 50% v/v, the hydrogen bond network is disrupted, ultimately leading to the breakdown of the eutectic system [148]. It has also been observed that more concentrated NaDES exhibit greater chemical stability over time compared to their diluted counterparts [161].

The water tolerance threshold varies across different NaDES systems and must be determined empirically for each formulation. Furthermore, physicochemical properties such as viscosity, polarity, density and electrical conductivity, are strongly influenced by the chemical nature of the selected components [149]. As demonstrated by Craveiro et al., increasing water content can enhance the polarity of NaDES, thereby improving the solubility of certain compounds [162]. Concurrently, water addition can reduce viscosity, which is one of the major practical limitations of these solvents [128].

High viscosity can limit molecular diffusion and negatively impact extraction efficiency. This challenge can be mitigated either by increasing the temperature, which promotes molecular motion and weakens intermolecular forces [163], or by controlling water dilution, which lowers viscosity by disrupting hydrogen bonding [149].

Numerous studies in recent literature have reported the successful application of NaDES for the extraction of bioactive compounds from natural matrices, intended for use in cosmetic and pharmaceutical products. A key advantage is the potential to directly incorporate NaDES-based

extracts into topical formulations without substantially altering their rheological or sensory characteristics [164]. Nonetheless, despite their promising performance, only a limited number of NaDES systems are currently considered suitable for cosmetic use, primarily due to safety and regulatory restrictions [163].

3) ALTERNATIVE ENERGY SOURCES

Microwave Technology

Microwaves 5are non-ionizing electromagnetic radiation, positioned between infrared and radiofrequency bands, with wavelengths ranging from 0.01 to 1 m and frequencies between 30 and 0.3 [165] GHz **Figure 22**. To minimize potential interference with telecommunication and mobile communication systems, international standards have designated specific frequency bands for thermal applications. Among these, the frequency of 2.45 GHz (±0.05 GHz), corresponding to a wavelength of approximately 12.2 cm in vacuum, is the most widely adopted across industrial, scientific, medical, and domestic fields.

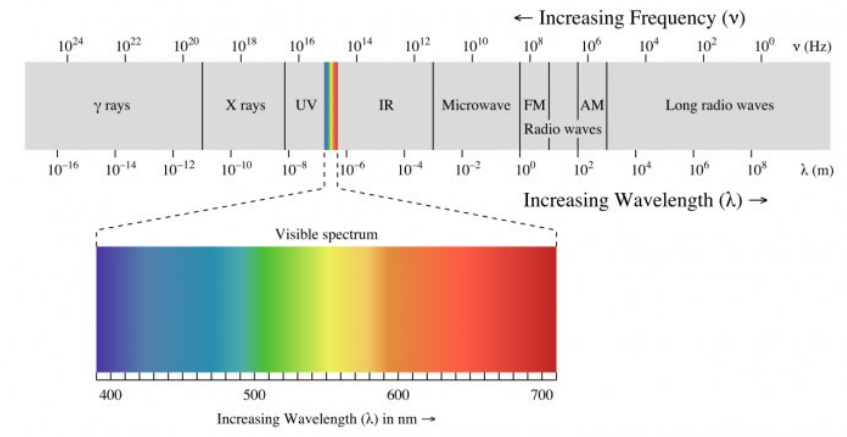

Figure 22. electromagnetic spectrum [166].

Microwave irradiation induces heating through a dipolar polarization **Figure 23a-c**; whereby polar molecules align with the oscillating electric field. This continuous reorientation generates

molecular agitation and friction, which is dissipated as homogeneous internal heating (**Figure 24**) [165].

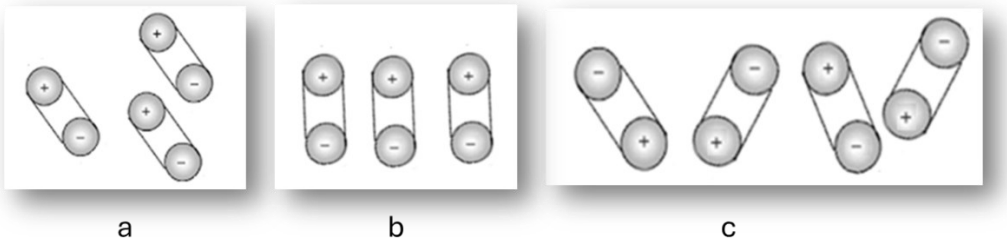

Figure 23a: Dipolar polarisation in absence of external electric field; **b**: without external electric field; **c**: with high frequency alternating electric field [167].

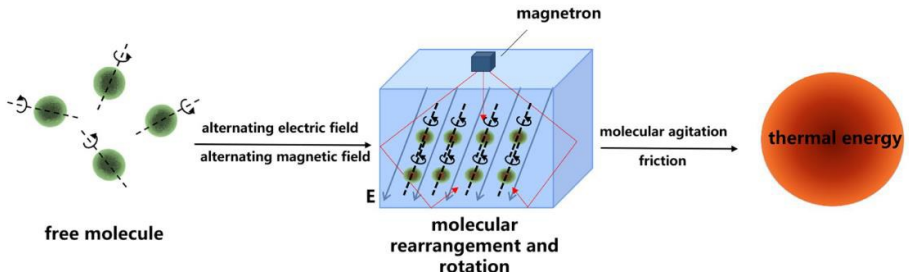

Figure 24. Heating mechanism by exposure to microwave radiation [168].

Microwave radiation is an important source of unconventional energy that is useful both for academic research and industrial production [169]. This technology offers significant advantages in organic synthesis and extraction processes, providing uniform, selective heating characterized by the absence of inertia due to rapid energy transfer throughout the entire mass of the material. In general, but with particular reference to its use for extraction purposes, the benefits of microwaves can be summarized as follows:

- **Temperature**: the rate of temperature increase is very high under microwave activation (up to 10 °C per second) compared to traditional heating. This results in a significant reduction in reaction times, with a consequent reduction in the possible degradation of the material being heated. The development of heat is defined as “core” because it proceeds from the

inside out, avoiding the risk of surface overheating of the matrix, which is easily encountered with traditional heating methods. The heating of the sample is therefore homogeneous.

- **Energy efficiency**: energy is used exclusively for heating the material without heat dispersion to the outside (air, furnace walls), resulting in significant energy savings and economic benefits.
- **Solvents**: in many cases, water can be used as an extractant because, thanks to its dielectric constant, it has unique extraction properties.
- **Consistency and reproducibility**: the reproducibility of the method is ensured by fine control of all process parameters throughout the extraction time, thanks to dedicated software and controllers interfaced with the microwave devices.

Microwave Apparatus

A microwave applicator is a device that has been specifically designed to transfer electromagnetic energy from the source directly to the material being processed. The configuration of such applicators is subject to variations depending on the type of substance to treat (e.g. powders, liquids, or pellets)., its dielectric properties, and volumes

In laboratory practice, different types of microwave applicators have been developed. Early experiments often relied on domestic multimode ovens, which, despite their accessibility, presented several limitations such as safety, temperature control and reproducibility.

In contrast to multimode systems, which generate multiple standing wave patterns resulting in non-uniform energy distribution, single-mode systems produce a well-defined electromagnetic field. This allows for more consistent irradiation, as energy is concentrated in a localised region, improving both heating, uniformity and reproducibility. Within the microwave cavity, the electromagnetic wave propagates continuously, alternating in polarity. This movement gives rise to a field that is characterised by regions of constructive and destructive interference,

corresponding to high and low energy, and nodes points where the net electromagnetic energy is effectively zero **Figure 25**.

Scientific single-mode and monomode reactors [170], with different configurations (**Figures 26** and **27**) have later overcome these drawbacks providing different safety tools with real-time monitoring of the process parameters, uniform energy distribution, integrated stirring, temperature and power control.

Subsequent advancements included the introduction of pressurised vessels, thereby expanding the range of applications even in different industrial fields.

Moreover, multimode prototypes can be modified to adapt domestic devices for chemical applications, incorporating optical fiber thermometers and feedback control units for power and temperature modulation.

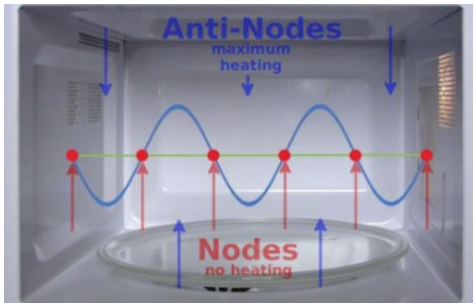

Figure 25. Mode, Anti-node and Nodes in the microwave cavity [171].

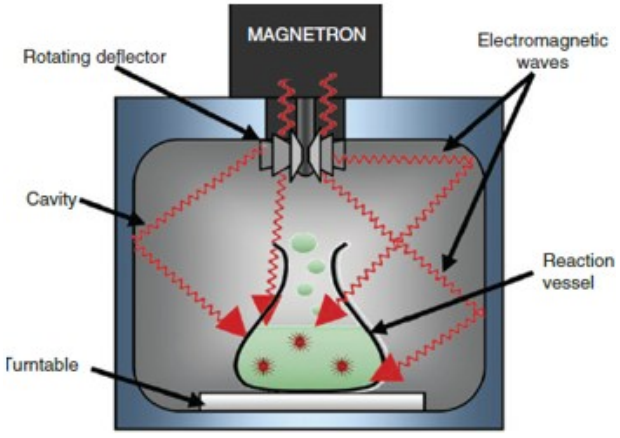

Figure 26. Multimode cavity [172].

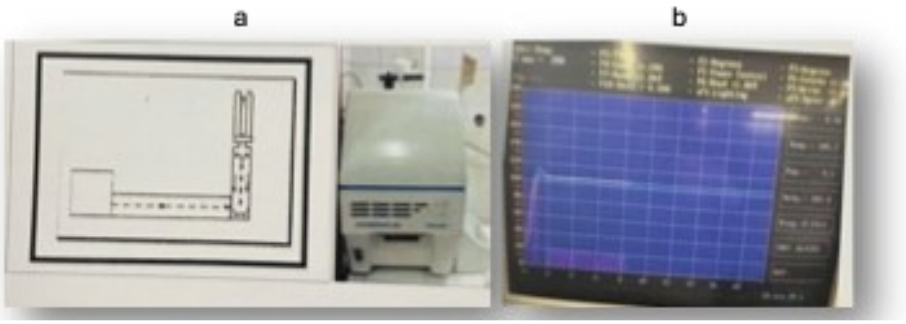

Figure 27. monomode microwave applicator.

Multimode Scientific Oven Prototype used in the research

In consideration of the previous statements, Professor Carla Villa, in collaboration with the Department of Engineering at the University of Modena and Reggio Emilia, designed and developed a multimode microwave oven prototype, structurally modifying a domestic microwave oven to adapt it to the requirements of chemical applications on a laboratory scale (**Figure 28**).

The microwave applicator consists of a multimode cavity equipped with a specially designed Pyrex reactor, a magnetron operating at 2.45 GHz, two optical fiber cables for temperature measurement and a feedback control unit which allows to manage and modulate different parameters of the process such as emitted power and temperature. Moreover, the furnace presents two holes on the walls of the cavity, which allows exploiting the prototype applicator for several applications, under different configurations such as mw synthesis, continuous flow reactions., and mw extraction with and without solvents.

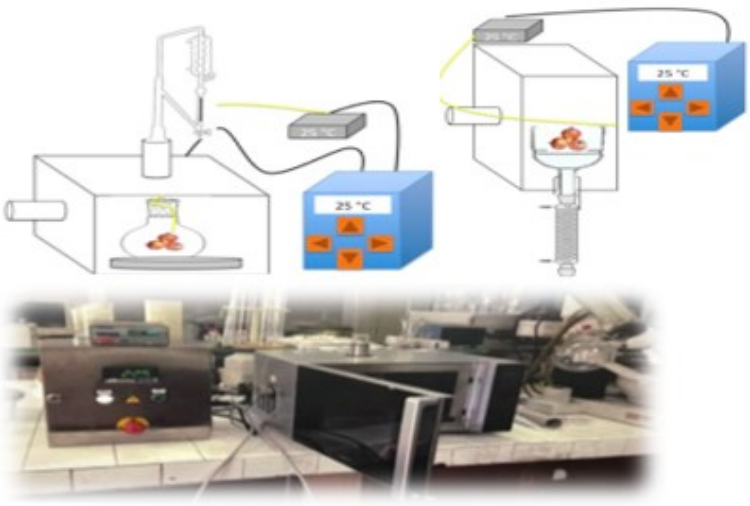

Figure 28. Multimode microwave prototype.

Microwave assisted solvent extraction (MAE)

MAE is a rapid and efficient extraction technique based on the use of microwaves to heat the sample/solvent mixture to facilitate and speed up the extraction of the analyte. In conventional separations (**Figure 29**), mass transfer occurs from the inside of the matrix to the outside while heat transfer occurs from the outside to the inside.

For microwave extractions the two transport phenomena are in the same direction from the inside of the extracted material to the bulk solvent. The acceleration of extraction rates under microwaves could be due to a synergy combination of the two transfer phenomena mass and heat acting in the same direction. In Microwave assisted-extractions, heat is dissipated volumetrically inside the irradiated medium, while in conventional extraction heat is transferred from the heating medium to the interior of the sample.

Microwaves are volumetrically distributed, and heat transfer occurs from the sample to the colder environment. This causes an important difference between the two mechanisms. In conventional heating, heat transfer depends on thermal conductivity, on the temperature

difference across the sample, and, for fluids, on convection currents. As a result, the temperature increase is often rather slow. By contrast, in microwave heating, due to the volumetric heating effect, much faster temperature increases can be obtained, depending on the microwave power and the dielectric loss factor of the material being irradiated.

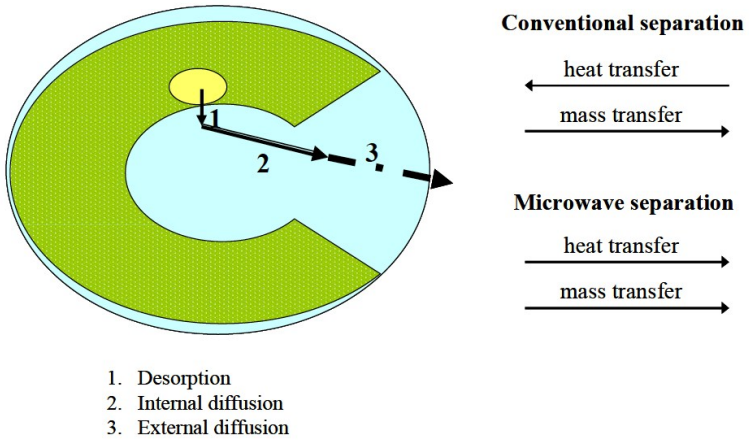

Figure 29. Comparison of Mass and Heat Transfer in Conventional and Microwave-Assisted Extraction [173].

The correct choice of extraction solvent is of paramount importance in ensuring the optimisation of the process. When making this choice, it is essential to consider the following: the solvent's ability to absorb microwaves, the interactions of the solvent with the matrix, the solubility of the analyte in the solvent, and the compatibility of the solvent with the final analytical method.

The solvent must demonstrate high selectivity for the analyte of interest [174]. Polar solvents with high dielectric constants exhibit rapid heating in a microwave field, while non-polar solvents remain transparent and do not undergo significant heating.

In contradistinction to conventional heat sources, which act on a surface from which heat spreads to the inner layers of the body by conduction and convection, a microwave heat source acts on the entire volume (if the medium is homogeneous) or on localized heating centres

consisting of polar molecules present in the product. It is evident that, in comparison to conventional heating, microwaves require a shorter duration to heat the container before the heat is transferred to the solution. This is due to the direct heating of the bulk by microwaves, which results in a minimal temperature gradient.

The rapid, internal heating provided by microwaves leads to a synergistic combination of heat and mass transfer that enhances the extraction process:

Cellular Disruption: the intense heating of the inherent moisture within plant cells causes the water to vaporize and generate high internal pressure. This pressure causes the cell walls and membranes to rupture, facilitating the release of intracellular components (analytes) into the surrounding solvent.

Enhanced Mass Transfer: the heating increases the kinetic energy of the molecules and lowers the solvent's viscosity and surface tension, which improves the penetration of the solvent into the sample matrix. The mass transfer gradient works in the same direction as the heat transfer (from the inside of the particle to the bulk solution), which dramatically speeds up the process.

Increased Solubility: higher temperatures (especially in closed-vessel systems where the solvent can be heated above its atmospheric boiling point) increase the solubility of the target compounds in the solvent.

Speed: extraction times are significantly shorter, often reduced from hours (for Soxhlet) to minutes.

Reduced Solvent Consumption: MAE typically requires smaller volumes of solvent, making it a "greener" and more cost-effective technique.

High Efficiency and Yield: the method often results in comparable or higher extraction yields of target analytes.

Automation and Control: commercial MAE systems offer precise control over temperature and pressure, which improves reproducibility and allows for automated, batch processing of samples.

MAE is typically performed in specialized equipment, which can be either **open-vessel** (atmospheric pressure with reflux condensation) or **closed-vessel** systems (controlled high temperature and pressure). Key parameters requiring optimization for efficient extraction include solvent type (polarity and dielectric properties), temperature, extraction time, and sample particle size.

Different procedures can be selected:

1) Microwave extraction with polar solvents
2) Microwave extraction with a mixture of polar and non apolar solvents
3) Microwave extraction with apolar solvents

1. In the first case the sample is immersed in a solvent or mixture of solvents that exhibit a high degree of absorption of microwave energy. This mechanism is considered appropriate for the extraction of analytes that are essentially polar or moderately polar in nature. (organic solvents, water, NaDES)
2. The sample is extracted using a combination of two solvents: one non-polar, transparent to microwaves, but capable of extracting the analyte; the other polar (high dielectric constant), capable of rapidly heating the sample/solvent mixture. This mechanism is used for applications (extraction of essentially non-polar organic compounds) that require the use of non-polar solvents that are transparent to microwaves and has the disadvantage of being poorly selective (analytes are extracted across a wide spectrum of polarities) [174].
3. The sample, with a high dielectric constant, is extracted using a microwave-transparent solvent. This mechanism is particularly well suited to the extraction of thermolabile analytes

(e.g., sulfur compounds in garlic) and essential oils from plant matrices with a high-water content. Microwaves interact with the free water present in the plant tissue, causing considerable expansion and consequent breakdown of the tissue. In this way, the essential oil or analytes of interest flow towards the organic solvent, which remains cold (or heats up slightly).

In any case the choice of solvent must be made taking into account:

- solubility of the substances to be extracted in the solvent;
- interaction between the solvent and the matrix;
- microwave absorption properties of the extractant.

The degree of interaction of the solvent with microwaves is expressed by the dissipation coefficient (tan δ), which is given by the following equation:

$$tan\delta = \varepsilon'' / \varepsilon$$

where ε'' is the dielectric loss (a measure of the efficiency of converting microwave energy into thermal energy) and ε is the dielectric constant (a measure of a molecule's ability to polarize in an electric field).

Microwave assisted solvent-free extraction

SFME – Solvent Free Microwave Extraction

SFME is a combination of microwave heating and dry distillation, conducted at atmospheric pressure, without the addition of external water or organic solvents.

Microwaves selectively interact with the water naturally present within the plant matrix. This volumetric heating is very rapid and uniform. The rapid vaporization of water inside the cells generates internal pressure that leads to the breaking of cell walls and oil glands. The volatile compounds (such as essential oils) released are carried by the **Internal Azeotropic Distillation**

generated water vapour. The vapour/oil mixture is then condensed by an external cooling system. The collected distillate naturally separates into an aqueous phase (hydrosol/hydrolate) and an oil phase, due to their immiscibility and different densities.

SFME offers significant advantages over conventional methods such as hydrodistillation (HD):

- Eliminates the use of solvents, resulting in a final product free of chemical residues.
- Extraction times are significantly reduced, often from several hours to just 30 minutes, sometimes with higher yields.
- Lower thermal exposure and the speed of the process preserve volatile and heat-labile compounds, leading to a superior quality essential oil.
- Reduces energy and water consumption and waste production, perfectly aligning with green chemistry principles.

MHG (Microwave Hydrodiffusion and Gravity)

MHG is an original "upside-down" microwave alembic combining microwave heating and earth gravity at atmospheric pressure. MHG is conceived for laboratory and industrial scale applications. It exploits warming of the water contained into the matrix, causing the expansion and consequent rupture of the matrix cells. This phenomenon, known as hydrodiffusion, allows the extract to diffuse outside the matrix. Moreover, microwaves increase tissue softness, cel permeability and cell disruption, thus enhancing the mass transfer within and outside the plant tissue. The extract recovered by gravity, dropping out of the microwave reactor by a hole positioned at the bottom of the applicator. The original extracts are not achievable by any other known method.

The MHG technique (acronym for Microwave Hydrodiffusion and Gravity) is an innovative and environmentally friendly extraction methodology, which represents a specific variant of solvent-free microwave extraction (SFME).

MHG combines the action of volumetric microwave heating with the force of Earth's gravity to rapidly extract natural compounds - primarily essential oils, pigments, and antioxidants from plant material.

The system functions on the principle of an inverted microwave alembic, operating at atmospheric pressure without the necessity of water or organic solvents.

The fresh (or rehydrated) plant material is placed inside the microwave reactor. In contradistinction to standard configurations, the sample container is generally positioned above a condenser and a collecting vessel.

Microwaves are able to penetrate the plant tissue and selectively heat the water naturally contained within the cells (*in situ* moisture).

The rapid heating of the intracellular water generates internal pressure, which leads to the expansion and rupture of the cell walls and oil glands (in the case of essential oils). This physical phenomenon is known as hydrodiffusion.

The liberated target compounds and water vapour migrate outwards from the sample. The inverted configuration of the system enables the diffused extract to fall by gravity through a perforated disk, and to be collected in a continuous cooling system positioned beneath the reactor.

The reduction in extraction time is significant (from hours to minutes) when compared with conventional methods such as hydrodistillation. The device exhibits a substantial reduction in energy consumption, reaching a maximum of 90% reduction, thereby eliminating the financial burden and risks associated with the utilisation of solvents.

The accelerated extraction process, in conjunction with the absence of protracted overheating, results in the preservation of volatile and heat-labile compounds.

4) GREEN EXTRACTS WITH A HIGH GREEN VALUE

Cosmetic Efficiency Evaluation

The evaluation of a plant extract for potential utilisation in cosmetics entails a comprehensive assessment of its purported benefits and safety. This concern also considers the extract's specific composition, which can vary based on factors such as cultivation and extraction method or conditions, and then how it integrates with other cosmetic ingredients.

In general, botanical matrices are a good source of phytochemical compounds, such as vitamins, polyphenols, tocopherols, and carotenoids that provide several interesting biological activities to the extracts, including antioxidant, anti-inflammatory, and antimicrobial properties [175].

One of the main focus on novel natural bioactivities is related to the protection from UV rays and free radicals, while enhancing skin health. Free radicals significantly contribute to skin damage and hasten ageing by interfering with defence and restorative processes. Plants contain natural chemicals that can scavenge free radicals and have antioxidant capabilities [176].

Phenolic compounds have been found to exhibit significant antioxidant activity *in vitro* spectrophotometric assays, primarily due to the chemical structure of these compounds and the presence of aromatic rings capable of stabilising or delocalising unpaired electrons [177].

Total Phenolic content and Antioxidant activity

Several methods for evaluating the antioxidant potential have been widely described in the literature. These methods are generally classified into two main categories: chromatographic and spectrophotometric techniques. Nevertheless, spectrophotometric methods (especially electron transfer-based assays) are the most widely used due to their simplicity and speed of execution. These assays involve the donation of a single electron from an antioxidant to a free radical. The reaction solution is characterized by a color change; the magnitude of absorbance

change, recorded at a specific wavelength, correlates with the concentration of antioxidants in the sample.

Among the different available methods, depending on the standard used, my research focused on the application of DPPH and Folin-Ciocalteau assays.

Folin-Ciocalteu test

The method is based on the addition of a specific oxidizing agent (Folin-Ciocalteu reagent) to the sample solution to be analyzed. The reagent consists of a yellow mixture based on phosphotungstic acid ($H_3PW_{12}O_{40}$) and phosphomolybdic acid ($H_3PMo_{12}O_{40}$), capable of oxidizing phenolic substrates and other antioxidant molecules. The reagent is reduced to the respective oxides (W_8O_{23} and Mo_8O_{23}), imparting a blue coloration to the solution, the intensity of which is measured spectrophotometrically at a wavelength of 765 nm (**Figure 30**) [178]. Gallic acid is employed as the reference standard to construct the calibration curve; the values determined for the samples are expressed as milligrams of gallic acid equivalents per gram of sample (mGAE).

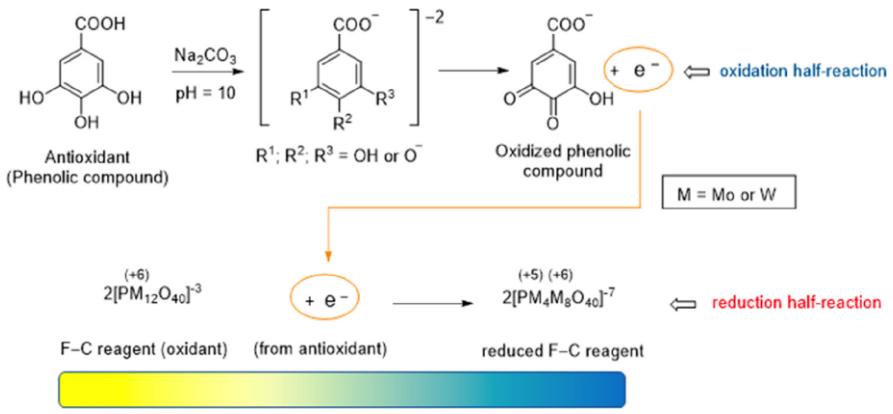

Figure 30. General redox reaction in the Folin-Ciocalteu test [178].

DPPH Assay - Radical Scavenging Activity

The antiradical activity of the sample can be measured using the DPPH assay (2,2-diphenyl-1-picrylhydrazyl), a stable radical reagent that appears in solution with an intense violet color. The assay exploits its ability to be reduced to 2,2-diphenyl-1-hydrazine (DPPH-H), which exhibits a pale-yellow color (**Figure 31**). This color change corresponds to a decrease in absorbance, proportional to the antioxidant activity of the sample under investigation, evaluated by UV-visible spectrophotometry at 516 nm [179]. The result of the assay is expressed as percentage antioxidant activity in comparison with that of a known, highly antioxidant compound (for example Trolox, 6-hydroxy-2,5,7,8-tetramethylchroman-2-carboxylic acid), with which a calibration curve is previously obtained at scalar concentrations using the same method.

Figure 31. DPPH reduction reaction [180].

The results are express as Trolox equivalents in mg/L, and the percentage of antioxidant activity (AA%) was calculated from the ratio of decreasing absorbance of sample solution (A0−As) to absorbance of blank DPPH solutions (A0), as expressed in expressed in Equation (1) [181].

$$AA\% = \frac{(A0-As)}{A0} * 100 \qquad (1)$$

Microbiological studies: antimicrobial activity

Microbiological quality is a fundamental aspect in the production of cosmetic, as the presence of undesirable microorganisms can compromise their efficacy, stability, and safety for the end consumer. Sources of contamination include raw materials, the production environment, inadequately sanitized equipment, and non-compliant packaging processes [182]. European Regulation No. 1223/2009 requires that products placed on the market be safe under normal conditions of use, requiring assessment of microbiological stability, the adoption of effective preservation systems, and verification of the absence of contamination. In addition, to microbiological quality control, a further emerging criticality is represented by multidrug resistance (MDR). Since 2012 the phenomenon of antibiotic resistance has grown exponentially, as a result of an excessive and not always rational use of such drugs [183]. In this alarming antibiotic resistance, the identification of novel bioactive ingredients represents a significant research aim.

Microbiological studies are essential, as they provide evidence of the extracts' potential as functional ingredients in cosmetic formulations (e.g., natural preservatives) or in pharmaceutical applications (e.g., therapeutic agents). These investigations typically aim to determine both the inhibitory and bactericidal properties of bioactive compounds, thus establishing their relevance for the development of safe and effective products. Several well-established tests are commonly used in this field:

- Minimum Inhibitory Concentration (MIC), which defines the lowest concentration of an extract capable of inhibiting visible microbial growth.
- Minimum Bactericidal Concentration (MBC), which measures the concentration necessary to kill the majority of the bacterial population (a bactericidal effect).

- Time-kill assays, which monitor the kinetics of bacterial reduction over time in the presence of the extrac.t
- Agar diffusion methods, such as the Kirby-Bauer disk diffusion test, provide a qualitative and semi-quantitative measure of antimicrobial activity based on zones of inhibition.
- Antibiofilm assays, which evaluate the ability of extracts to prevent biofilm formation or destroy mature biofilms, a particularly important aspect given the role of biofilms in microbial resistance and persistence.
- Sowing by inclusion, involves incorporating the test substance directly into the molten agar before inoculation, ensuring a homogeneous distribution of the compound and allowing the evaluation of the inhibitory effects.

In the following sections, the specific antimicrobial protocols employed during this research will be described in detail, highlighting the experimental conditions and methodological choices applied to each assay.

Minimum inhibitory concentration

The minimum inhibitory concentration (MIC) test is the primary quantitative method used to determine the *in vitro* activity of an antimicrobial agent against a target microorganism, representing the lowest concentration that visibly inhibits microbial growth. The broth microdilution method is the gold standard for this determination, conducted in multiwell plates according to international guidelines such as those provided by the European Committee on Antimicrobial Susceptibility Testing (EUCAST) [184]. The process begins with standardization of a fresh bacterial culture to produce a specific and reproducible inoculum concentration, often around 5×10^5 cells/mL in the final test volume. The test compound is prepared through a range of serial two-fold dilutions. These dilutions, covering the concentration range of interest, are

dispensed into the wells of the microtiter plate and combined with the standardized bacterial suspension. Essential controls are incorporated, including a bacterial-only growth control (compound-free) and a dedicated control to assess the potential intrinsic antimicrobial activity of the solvent or vehicle itself, at all concentrations used. After incubation under optimal growth conditions, typically at 37°C for 24 hours, the MIC value is recorded visually as the lowest concentration that results in complete inhibition of visible bacterial growth compared to the compound-free control. To ensure the reliability and statistical validity of the determined value, all tests are performed as multiple independent experiments, often including at least three biological replicates, with final MIC values typically expressed as the median or modal result.

Minimum Bactericidal Concentration

Minimum Bactericidal Concentration (MBC) The Minimum Bactericidal Concentration (MBC) is a critical parameter in microbiology, serving to definitively characterize the nature of an antimicrobial agent's action. Unlike the Minimum Inhibitory Concentration (MIC), which determines the minimum concentration necessary to prevent visible bacterial growth (a bacteriostatic effect), the MBC measures the concentration necessary to kill the majority of the bacterial population (a bactericidal effect). The MBC is narrowly defined as the minimum concentration of an antimicrobial agent that kills 99.9% of the initial bacterial inoculum after a standard incubation period, typically 18 to 24 hours [185]. The determination of the MBC is performed as an extension of the MIC assay. Following the initial MIC determination, broth aliquots are taken from the wells showing no visible growth (i.e., wells corresponding to the MIC concentration and higher concentrations). A small volume of these broths is subcultured onto fresh agar plates containing no antimicrobial agent. This crucial step aims to ascertain whether the bacteria were merely inhibited (bacteriostatic effect) or permanently destroyed (bactericidal effect).

Time-kill assay

The Time-Kill Curve assay is a fundamental microbiological method used to characterize the antimicrobial activity over a defined period of time [186]. This assay determines whether a compound's action against a target microorganism is bacteriostatic (inhibiting growth) or bactericidal (killing cells), typically over a 24-hour incubation period. In general, the procedure begins with the preparation of a standardized microbial culture, usually harvested during the mid-logarithmic growth phase. This culture is then added to a suitable nutrient medium (such as Mueller-Hinton broth) containing the test compound at predetermined concentrations, often expressed as multiples of the Minimum Inhibitory Concentration (MIC). A bacterial growth control, containing the inoculum without the antimicrobial agent, is always run in parallel under identical incubation conditions (typically at 37°C with shaking). To construct the curve, aliquots are collected from both the test and growth control samples at various predefined time intervals during the incubation period (e.g., t = 0, 2, 4, 6, 8, and 24 hours). To prevent residual antimicrobial agent from affecting the viable cell count (a phenomenon known as "carryover"), the collected aliquots must be immediately neutralized or sufficiently diluted, commonly using 0.9% sodium chloride solution. The remaining viable microbial population at each time point is quantified by seeding serial dilutions on appropriate agar plates. After the standard incubation, the resulting number of colonies is counted, yielding colony-forming units per milliliter (CFU/mL). The generated data is then used to plot the time-kill curve, which expresses the results as the $\log_{10}$ of the number of viable bacterial cells (CFU/mL) as a function of time. This graphical representation allows us to evaluate whether the compound under test achieves a significant reduction in bacterial load (for example, a 3 $\log_{10}$ reduction, which generally defines bactericidal activity). Experiments are always conducted with biological replicates (at least three times, n = 3) to ensure statistical robustness.

Biofilm inhibition

The Crystal Violet (CV) assay is a foundational microbiological method used to quantitatively assess the action of an antimicrobial agent on microbial biofilms. The assay is typically configured to evaluate two distinct aspects of activity: inhibition of initial biofilm formation and disruption of pre-formed (mature) biofilm. The methodology generally conforms to international standards [187]. For Inhibition of Formation, the assay begins with the standardization of a fresh bacterial culture to achieve a specific inoculum concentration. The diluted bacterial suspension is simultaneously introduced into the wells of a microplate along with the test compound at defined concentrations. Following an appropriate incubation period (often 24 hours), the compound's effect is measured, indicating its ability to prevent bacterial attachment and matrix synthesis. In contrast, the assay for Disruption of Mature Biofilm requires an initial incubation period where the bacteria are allowed to grow and establish a robust, adherent biofilm (often 48-72 hours) in the absence of the test compound. Once the mature biofilm is formed and the planktonic cells are removed, the compound is then added to the wells for a second incubation period, allowing its activity against the established structure to be assessed. In both methods, the subsequent steps are identical: the culture supernatant is removed, and the wells are extensively washed with a buffer solution to detach loosely adherent cells. The remaining adherent biomass is stained using a Crystal Violet solution, which binds to the negatively charged cell wall components and the extracellular polymeric substance (EPS) matrix. Excess stain is removed by further washing. The retained, bound stain is then solubilized using an organic solvent (such as ethanol), and the resulting solution's absorbance is quantified spectrophotometrically, typically at 570 nm. The optical density (OD) values, corrected against solvent and medium blanks, are directly proportional to the amount of viable or non-viable biomass present, allowing the calculation of the percentage of inhibition or

disruption relative to the untreated bacterial control. All assays are typically executed using at least three biological replicates to ensure statistical reliability.

Kirby-Bauer disk diffusion

The Kirby-Bauer disk diffusion method is a widely employed and highly standardized qualitative test used for assessing the *in vitro* antimicrobial activity of compounds against various bacterial strains. In its conventional form, the procedure begins by preparing a Mueller-Hinton agar plate that is inoculated with a standardized bacterial suspension, typically adjusted to a 0.5 McFarland turbidity standard (approximately 1-2 x 10^8 CFU/mL), ensuring the eventual formation of a confluent microbial growth layer. Sterile paper disks, generally 6 mm in diameter, are impregnated with known, defined concentrations of the antimicrobial agents being tested and are subsequently placed onto the surface of the inoculated agar. During the prescribed incubation period, usually 18-24 hours at a controlled temperature between 35-37 °C, the antimicrobial compounds radially diffuse into the agar medium. This diffusion process creates concentration gradients, leading to the formation of clear zones of inhibited bacterial growth around the disks, known as zones of inhibition. The diameter of the zones of inhibition is measured and interpreted according to established guidelines to determine the susceptibility or resistance of the bacterial strain to the specific agent, thus providing a rapid qualitative assessment of antimicrobial potential [188].

Sowing by Inclusion

The Agar Incorporation Method, often referred to as "Sowing by Inclusion," is an established antimicrobial susceptibility test used to evaluate the inhibitory potential of compounds, offering a complementary approach to diffusion-based assays. This technique is designed to ensure a homogeneous distribution of the test compound throughout the solid growth medium [189]. The general procedure involves preparing and sterilizing a suitable agar medium, such as

Mueller-Hinton agar, and subsequently cooling it to a temperature safe for the test compounds (typically 40°C to 45°C) to prevent thermal degradation. At this stage, appropriate volumes of the extracts or antimicrobial agents are incorporated directly into the molten medium. The mixture is then poured into Petri dishes and allowed to solidify. Once the compound is uniformly distributed and the medium is solid, the plates are inoculated on the surface with a standardized bacterial suspension, commonly adjusted to a 0.5 McFarland standard (approximating 1-2x10^8 CFU/mL), achieving an appropriate final inoculum density. After incubation, generally 24 hours at 35°C to 37°C, the presence or absence of bacterial growth on the test plates is qualitatively assessed by direct comparison with control plates containing no test compound. This visual observation serves as a direct indicator of the inhibitory potential of the agents under evaluation.

Matrix-assisted laser desorption ionization time-of-flight analysis

Matrix-assisted laser desorption ionization time-of-flight (MALDI-TOF) mass spectrometry has become a revolutionary high-throughput technology in clinical and environmental microbiology for the rapid and accurate identification of microorganisms, including bacteria, yeasts, and fungi [190]. This method uses a molecular fingerprinting approach, in which microbial identification is based on the distinctive profile of highly abundant cellular proteins, primarily ribosomal proteins [191]. The general principle involves applying a small amount of the intact microbial sample to a target plate and co-crystallizing it with a matrix chemical. A pulsed laser then strikes this co-crystallized mixture, causing the proteins to desorb and ionize. These generated ions are accelerated through a vacuum tube, the time-of-flight (TOF) analyzer, where they are separated based on their mass-to-charge ratio (m/z). Lighter ions travel faster and reach the detector before heavier ions. The time it takes for ions to reach the detector is converted into a mass spectrum, which graphically represents the ion intensity as a function of the m/z ratio. This spectrum constitutes a unique and reproducible protein fingerprint,

characteristic of the species, subspecies, or strain under investigation. Final identification is achieved by comparing the generated spectrum to a large and validated reference library of known microorganisms, using sophisticated proprietary software [190] The high throughput, minimal sample preparation, cost-effectiveness, and high discriminatory power of MALDI-TOF have made it an essential tool for microbial identification, often replacing traditional biochemical and genetic methods [191].

Microbiological studies: strains

To evaluate antimicrobial activity, multidrug-resistant clinical strains of both Gram-positive and Gram-negative bacteria were selected. All strains were obtained from the School of Medical and Pharmaceutical Sciences (University of Genoa) and identified by VITEK® 2 (Biomerieux, Florence, Italy) or matrix-assisted laser desorption/ionization time-of-flight (MALDI-TOF) mass spectrometry (Biomerieux, Florence, Italy).

Gram-positive strains included *Staphylococcus aureus*, the main pathogen of the genus, responsible for a broad spectrum of infections ranging from superficial skin lesions [192] to invasive diseases such as bacteremia and endocarditis [193]. Methicillin-Resistant *Staphylococcus aureus* strains (MRSA) are particularly relevant due to their reduced susceptibility to β-lactam antibiotics [194]. Among coagulase-negative staphylococci (CoNS), *Staphylococcus epidermidis* and certain *Staphylococcus saprophyticus* were considered for their role in biofilm-associated infections and urinary tract infections, respectively [192,195]. Other CoNS species, such as *Staphylococcus warneri, Staphylococcus simulans, Staphylococcus hominis* [196], *Staphylococcus haemolyticus* [197], *Staphylococcus lugdunensis* [198] and *Staphylococcus capitis* [199], were included as opportunistic pathogens multidrug resistant increasingly reported in nosocomial settings. Finally, *Enterococcus faecalis*

and *Enterococcus faecium* were tested as representatives of intestinal commensals with high levels of intrinsic and acquired resistance, including Vancomycin-Resistant Enterococci (VRE).

Gram-negative strains were also included to broaden the evaluation spectrum. *Escherichia coli* was selected as a representative of enteric bacteria, frequently implicated in urinary tract and systemic infections. *E. coli* exhibits high levels of resistance to antibiotics, particularly beta-lactams, through the production of beta-lactamases. An emerging problem is carbapenem resistance, due to the production of plasmid carbapenemases [200]. *Pseudomonas aeruginosa* was included due to its strong biofilm-forming ability and intrinsic resistance mechanisms, making it a critical opportunistic pathogen in hospital settings [201]. *Klebsiella pneumoniae* was tested as another clinically relevant strain, known for its role in respiratory and bloodstream infections and the emergence of carbapenem-resistant isolates [192].

These Gram-positive and Gram-negative strains provided a comprehensive panel for evaluating the antimicrobial potential of plant-derived extracts, ensuring representation of both common pathogens and resistant opportunistic species.

RESULTS

Bioactive Potential Cosmetic Ingredients

Applying the multidisciplinary approach that takes into account all the points outlined above, my research led to different results presented at cosmetic and pharmaceutical congresses and published in international scientific journals.

In the following section, for each research topic a short paragraph highlights the results obtained accompanied by a brief discussion. The experimental data related to materials, procedure and protocols in general, when available in the corresponding research article, are not reported.

NaDES-Based Extracts by Microwave Activation from *Laurus nobilis* L. Leaves: Sustainable Multifunctional Ingredients for Potential Cosmetic and Pharmaceutical Applications

As described above, *Laurus nobilis* L. is a plant of considerable industrial importance, widely used as an ornamental species, a culinary spice, and a source of aromatic compounds in the flavour and fragrance industry. Due to its broad spectrum of bioactive constituents, it also plays a significant role in traditional medicine for the treatment of various health conditions. Based on this, the objective of this study was to develop a sustainable and efficient extraction process (based on natural deep eutectic solvents combined with microwave-assisted extraction) to obtain a ready-to-use multifunctional ingredient, exploiting the synergistic properties of the NaDES components and the bioactivity of laurel-derived phytochemicals. Natural eutectic solvents obtained by combining the hydrogen bond acceptor (betaine and choline chloride) with two different hydrogen bond donors (including glycerol and lactic acid), used in defined molar ratios, were analyzed. Extraction efficiency was assessed using the total phenolic content

recovered, and the ingredients cosmetic evaluation were evaluated using DPPH. The antibacterial activity of the extract was analyzed using the MIC test. Furthermore, gas chromatography-mass spectrometry (GC-MS) analysis was conducted to study the volatile aromatic components, which contribute to the extract's pleasant and characteristic fragrance. The results highlighted the potential of this NaDES-based system as an environmentally friendly and multifunctional ingredient with preservative, antioxidant, and aromatic functions, suitable for use in modern cosmetic and therapeutic formulations.

Results and Discussion

Microwave-Assisted Preparation of NaDES-Based Extracts

In accordance with the methodology described in a previously published study [131], four NaDES-based extracts (BGs, BGAs, CGs, and CGAs) were successfully prepared within five minutes [202] using a modified extraction process. The extracts displayed advantageous rheological characteristics, characterised by their low viscosity, in addition to a distinctive and agreeable olfactory profile. The rapid increase in temperature observed during the extraction process can be attributed to the polarity of both the solvent components and the bioactive compounds, in combination with the efficient dielectric heating promoted by microwave irradiation. The target temperature of 75°C was rapidly attained within a time range of 10 to 15 seconds. The maintenance of thermal stability was achieved through the dynamic modulation of microwave power, ranging from 0 to 300 watts. The regulation was achieved through an integrated feedback control system within the microwave apparatus, ensuring precise temperature management. This control effectively prevents the thermal degradation of the plant matrix and the extracted compounds and consequently preserves their structural and functional integrity throughout the process.

Total Phenolic Content and Radical Scavenging Activity

All NaDES-based extracts exhibited pronounced and stable antioxidant activity (RSA), with values ranging from 62% to 88%. These results demonstrated a strong correlation with the corresponding total phenolic content (TPC), which exhibited a range from 10.12 to 11.72 milligrams of gallic acid equivalents (GAE) for gram of fresh laurel leaves. It is interesting to note that the formulations employing betaine as the hydrogen bond acceptor demonstrated superior performance in both assays. The following table (**Table 1**) presents a summary of the key results for each extract.

Table 1. TPC, expressed as mg equivalents of gallic acid for of fresh laurel leaves and RSA% of NaDES-based samples (BGs, BGAs, CGs, and CGAs), as determined by the Folin–Ciocalteu and DPPH assays, respectively. Numbers followed by different letters within the same column indicate significant differences among results ($p < 0.001$, Bonferroni test).

NaDES Sample	TPC (mg GAE/g ± SD)	RSA (% ± SD)
BGs	11.72 ± 0.02^{a}	88.1 ± 0.1^{a}
BGAs	11.57 ± 0.02^{a}	80.9 ± 0.3^{b}
CGs	10.38 ± 0.07^{b}	77.8 ± 0.4^{b}
CGAs	10.12 ± 0.03^{b}	62.2 ± 1.0^{c}

Despite the positive and comparable results obtained with the CGAs sample, the betaine-based BGAs were identified as the most promising candidate for a cosmetic-ready ingredient, due to their excellent performance and fragrant profile. A notable limitation to consider is the faint amine or "fishy" odour associated with choline chloride, which is present in both the eutectic solvents (CG and CGA) and their corresponding extracts (CGs and CGAs). Moreover, from a regulatory perspective, the European Cosmetic Regulation 1223/09 (Annex II, entry no. 168) prohibits the use of choline chloride in cosmetic products. However, it should be noted that this restriction does not apply to pharmaceutical formulations intended for topical application. This aspect may therefore be considered a potential area for future research and development.

As a preliminary stability test, for compound **BGAs**, the TPC and DPPH assay values were also verified after 180 days of storage at room temperature (**BGAs** t180). The sample appears to be

stable, with only a slight decrease in phenolic content (from 11.57 ± 0.02 to 11.35 ± 0.02 mg GAE/g) and not affecting its antioxidant capacity (from 80.9 ± 0.3 to 80.5 ± 0.4%).

Minimal Inhibitory Concentrations (MICs)

The antimicrobial activity of the NaDES-based extracts was assessed against six clinically relevant multidrug-resistant (MDR) bacterial strains, as summarized in **Table 2**. The panel included four Gram-positive and two Gram-negative isolates: two methicillin-resistant *Staphylococcus aureus* (MRSA) strains, two methicillin-resistant *Staphylococcus epidermidis* (MRSE) strains, one *Escherichia coli* a strain producing class A *Klebsiella pneumoniae* carbapenemases - KPC, and resistant to carbapenems - CR), and one strain of *Pseudomonas aeruginosa* (resistant to ceftazidime- avibactam KAZ-AVI R, and CR). All extracts tested exhibited antibacterial activity against Gram-positive strains (**Table 2**). However, only those formulations containing lactic acid (CGAs and BGAs) demonstrated significant antimicrobial efficacy against both Gram-positive and Gram-negative clinical isolates, with MIC values ranging from 3.5 to 7.1 mg/mL. BGs showed comparable activity, though restricted to Gram-positive strains, within the same MIC interval (3.5–7.1 mg/mL). In contrast, CGs displayed the weakest antibacterial effect among the four NaDES-based samples, being active solely against Gram-positive strains and predominantly at concentrations of 57.7 mg/mL. The eutectic solvents incorporating lactic acid (BGA and GCA) exhibited intrinsic antimicrobial properties, with MICs between 13.5 and 27.8 mg/mL, although their activity was lower than that observed for the corresponding extracts. Neither BG nor CG displayed any inhibitory effect within the concentration range investigated.

Table 2. Minimum inhibitory concentrations (MICs), expressed as mg/mL of NaDESs (BG, BGA, CG, CGA) and NaDES-based extracts (BGs, BGAs, CGs, and CGAs) against selected multidrug-resistant Gram-positive and Gram-negative bacterial strains. Experiments were carried out in triplicate. The degree of concordance in all the experiments was 3/3. Variation among triplicate samples was less than 10%.

		MICs (mg/mL)							
Strains	**Strain**	**BG ***	**BGs**	**BGA**	**BGAs**	**CG ***	**CGs**	**CGA**	**CGAs**
***S. aureus* (MRSA)**	17	na	7.0	27.8	7.1	na	55.7	27.1	7.0
	18	na	3.5	27.8	3.5	na	55.7	27.1	3.5
***S. epidermidis* (MRSE)**	2	na	3.5	27.8	3.5	na	55.7	27.1	3.5
	22	na	3.5	27.8	3.5	na	27.9	27.1	3.5
***E. coli* (CR)**	477	na	na	13.9	3.5	na	na	13.5	3.5
***P. aeruginosa* (CR, K)**	259	na	na	13.9	3.5	na	na	13.5	3.5

* na= no activity detected in the range of concentrations studied (from 110 to 0.2 mg/mL); MRSA = methicillin-resistant *Staphilococcus aureus*; MRSE = methicillin-resistant *Staphilococcus epidermidis; CR* = carbapenemase resistant; K = strain producing class A *Klebsiella pneumoniae.*

As reported in **Table 2**, all tested extracts demonstrated antibacterial activity against Gram-positive strains. Notably, only the extracts containing lactic acid (CGAs and BGAs) exhibited significant antimicrobial effects against both Gram-positive and Gram-negative clinical isolates, with minimum inhibitory concentrations (MICs) ranging from 3.5 to 7.1 mg/mL BG extracts displayed comparable activity exclusively against Gram-positive bacteria, within the same MIC range, whereas CG extracts showed the lowest antibacterial efficacy among the four NaDES-based formulations, being active solely against Gram-positive strains and predominantly at higher concentrations (57.7 mg/mL).

Eutectic solvents containing lactic acid (BGA and GCA) showed intrinsic antimicrobial properties, although at higher MIC values (13.5-27.8 mg/mL) than the corresponding extracts. In contrast, neither BG nor CG solvents showed measurable activity in the concentration range tested. The MIC comparison clearly indicates that the inclusion of lactic acid in the blend strengthens and broadens the antimicrobial activity of the extract, showing effectiveness not only against Gram-positive microorganisms but also against Gram-negative ones. This trend is further supported by the data obtained with the respective solvents, especially when betaine is employed as the hydrogen bond acceptor (HBA). However, it should be emphasized that in this

case the inhibitory effect is achieved only at substantially higher concentrations (13.9-27 mg/mL compared to 3.5-7.1 mg/mL).

Gas Chromatography-mass spectrometry of the BGA extract

Gas chromatography-mass spectrometry (GC-MS) analysis of the volatile fraction obtained from the BGA sample identified as the most promising formulation revealed the presence of 21 volatile constituents. These compounds are reported in **Table 3**, in order of elution, along with their corresponding retention indices (Ri) as determined on an Elite-5 MS capillary column. In **Figure 32**, the typical chromatogram related to BGAs GC-MS analysis is reported as an example; while the distribution of compounds by chemical classes, with the relative percentage contributions of each group, is reported in **Figure 33**.

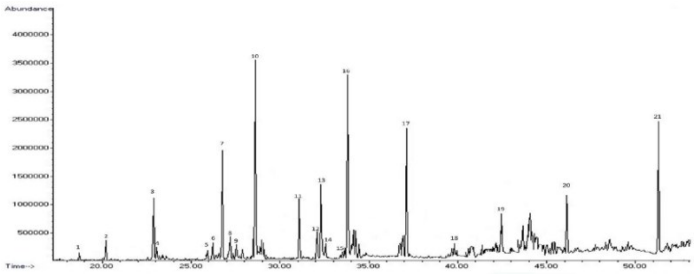

Figure 32. Representative GC-MS chromatograms of the volatile fraction of BGAs. The major compounds are indicated by number; compound identification is provided in **Table 3**.

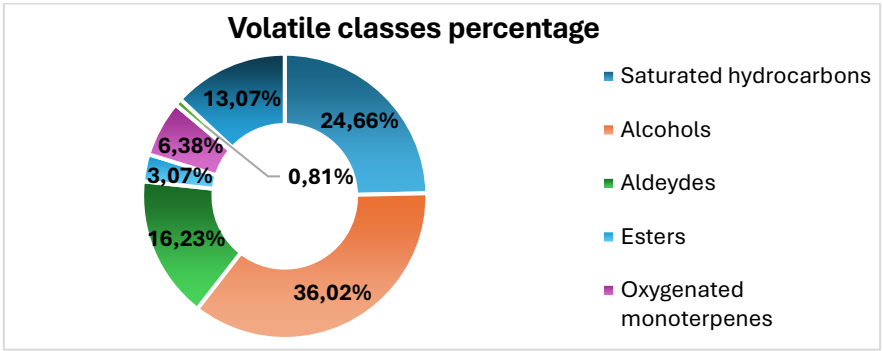

Figure 33. Graphical representation of the mean percentages related to the volatile compounds classes, identified by GC -MS in sample BGAs.

Table 3. GC-MS analysis of the volatile fraction of BGAs: retention indices, relative percentages, identification methods, and olfactory descriptions of the compounds detected across three analytical replicates (BGAs1, BGAs2, BGAs3).

Compound[a]	Ri[b]	Ri[c]	Relative %			Mean % (± SD)	Identif. method	Olfactive description
			BGAs1	BGAs2	BGAs3			
Decane	1000	1000	0.48	-	0.58	0.53 ± 0.08	STD	alkane
1.8-cineole	1042	1043	1.34	0.50	1.06	0.96 ± 0.43	NIST, RI	mint, sweety
Linalool	1106	1109	5.60	3.72	3.67	4.33 ± 1.10	NIST, RI	flower, lavender
2,4-dimethyldecane	1115	1113	0.90	0.42	0.62	0.65 ± 0.24	NIST, RI	alkane
Borneol	1188	1186	0.73	0.90	-	0.81 ± 0.12	NIST, RI	camphor
Terpinen-4-ol	1192	1194	1.32	1.31	0.64	1.09 ± 0.39	NIST, RI	turpentine, nutmeg
Dodecane	1200	1200	8.28	5.70	7.47	7.15 ± 1.32	STD	alkane
4,8-dimethyl-undecane	1212	1221	2.30	1.43	2.49	2.08 ± 0.57	NIST, RI	alkane
2,4-dimethylundecane	1223	1230	1.60	0.66	1.31	1.19 ± 0.48	NIST, RI	alkane
1,3-di-tert-butylbenzene	1249	1259	15.77	9.17	14.44	13.13 ± 3.49	NIST, RI	-
Tridecane	1300	1330	4.06	3.13	5.02	4.07 ± 0.95	STD	alkane
□-terpinyl acetate	1356	1359	2.37	4.28	2.64	3.1 ± 1.03	NIST, RI	wax
Eugenol	1363	1365	6.44	9.04	3.38	6.29 ± 2.83	NIST, RI	clove, honey
2-methyl-tridecane	1366	1373	1.24	1.17	1.55	1.32 ± 0.20	NIST, RI	alkane
Tetradecane	1400	1400	0.41	0.48	0.69	0.53 ± 0.14	NIST, RI	alkane
Methyl eugenol	1408	1410	15.70	19.56	14.13	16.46 ± 2.80	NIST, RI	clove, spice
2,4-di-tert-butyl-phenol	1513	1517	10.97	13.70	15.14	13.27 ± 2.12	NIST, RI	-
Hexadecane	1600	1600	1.08	0.92	1.32	1.11 ± 0.20	STD	alkane
Heptadecane	1700	1700	5.31	5.86	7.31	6.16 ± 1.04	STD	alkane
Hexadecanal	1831	1830	4.57	6.18	5.36	5.37 ± 0.80	NIST, RI	alkane
Octadecanal	2037	2036	9.53	11.89	11.16	10.86 ± 1.21	NIST, RI	oil

[a]Compounds listed in order of their elution on an Elite-5 column. [b]Retention Indices according to Adams [203] and with published data [204]. [c]Retention indices determined on an Elite-5 column using a homologous series of n-hydrocarbons. [d]Method of identification: STD = pure compound; MS = mass spectrum; NIST = comparison with library [205]; RI = retention indices in agreement with literature values. [203,204]

The most represented class of volatile compounds in the BGA extract was that of alcohols, representing 36.02% of the total volatile profile. Within this group, the most abundant constituents were methyl eugenol (16.46%), 2,4-di-tert-butylphenol (13.27%), and eugenol (6.29%). Saturated hydrocarbons formed the second most abundant class (24.77%), with dodecane (7.15%), heptadecane (6.16%), and tridecane (4.07%) as the main compounds. Aldehydes constituted 16.23% of the profile, primarily due to 4-octadecanal (10.86%) and hexadecanal (5.37%). The miscellaneous category (13.13%) included only 1,3-di-tert-butylbenzene. Lastly, oxygenated monoterpenes comprised 6.38%, with linalool (4.33%), terpinen-4-ol (1.09%), and 1,8-cineole (0.96%) as key representatives.

As expected, the number of volatile compounds identified by gas chromatography-mass spectrometry (GC-MS) is markedly lower and shows significant differences in relative abundance compared to those found in conventional bay laurel essential oil [206]. However, these constituents still contribute to the sample's characteristic and pleasant aroma, which combines herbaceous, fresh, and subtly spicy notes. The aromatic profile appears to be primarily influenced by the presence of linalool, eugenol, methyl eugenol, α-terpinyl acetate, and 1,8-cineole.

Conclusions

In the context of green extraction methodologies, NaDES have emerged as a rapid and efficient strategy for improving the recovery of bioactive compounds from *Laurus nobilis* leaves in a sustainable manner. The combination of the intrinsic biological properties of both NaDES components and *Laurus nobilis* phytoconstituents results in a synergistic effect, leading to multifunctional NaDES-based extracts. These preparations, in addition to having a good and diversified antibacterial activity, can serve as ready-to-use natural ingredients with antioxidant and self-preserving activity, suitable for direct incorporation into cosmetic formulations.

Additionally, they contribute to the sensory characteristics of the final product through the selective extraction of volatile aromatic compounds. The substitution of traditional organic solvents with these eutectic systems aligns with the increasing demand for natural and eco-compatible ingredients, while fulfilling functional and dermatological efficacy requirements in modern dermocosmetic applications.

Dissemination of Results

The research outcomes were disseminated through publication in the international peer-reviewed journal Molecules, with the article entitled NaDES-Based Extracts by Microwave Activation from *Laurus nobilis* L. Leaves: Sustainable Multifunctional Ingredients for Potential Cosmetic and Pharmaceutical Applications [207]. Moreover, the study was selected for presentation as an invited oral contribution at the 8th Intercontinental Personal Care Excellence Conference held in Verona. A part of this research also investigated the anti-acne potential of the selected NaDES-based extract; however, the detailed data and results pertaining to this aspect cannot be disclosed at this time as they are covered by a patent application.

Evaluation of the Biological Activity of Manna Exudate, from *Fraxinus ornus* L., and Its Potential Use as Hydrogel Formulation in Dermatology and Cosmetology

Manna, a medicinal plant, has been extensively researched and is known to contain a complex mixture of sugar derivatives and polyphenolic compounds. These compounds contribute to the notable bioactive profile of Manna, which is characterised by antioxidant and anti-inflammatory properties. The purpose of the present study was to explore the incorporation of Manna extract from the plant *Fraxinus ornus* within a pectin-based hydrogel matrix, and to evaluate its potential as a synergistic delivery system for applications in cosmetic and dermatological fields. The present study specifically focused on the wound healing efficacy of the Manna extract, emphasising its tissue reparative activities in the context of wounds. In addition, considering the well-documented relationship between antioxidant capacity and anti-aging effects, the extract was also assessed for its potential anti-elastase activity and skin depigmentation potential. The quantification of the total phenolic content was conducted for each extract, together with comprehensive *in vitro* assays to evaluate the safety profile of the formulation. These findings emphasise the potential of pectin hydrogels as effective vehicles for the management of skin disorders, supporting their use as wound dressings and in anti-aging cosmetic formulations.

Results and Discussion

Microscopic Characterization of the Manna Exudate extract

Microscopic examination of the Manna exudate extract revealed the presence of a distinct crystalline structure, detectable through both optical microscopy and scanning electron microscopy (SEM). In **Figure 35 A**, several starch granules are identifiable under light microscopy. Following Lugol's iodine staining, these granules exhibit a characteristic dark blue

coloration, confirming their polysaccharide nature (**Figure 34 B**). SEM images (**Figures 34 C** and **D)** further illustrate the crystalline morphology of Manna at different magnifications.

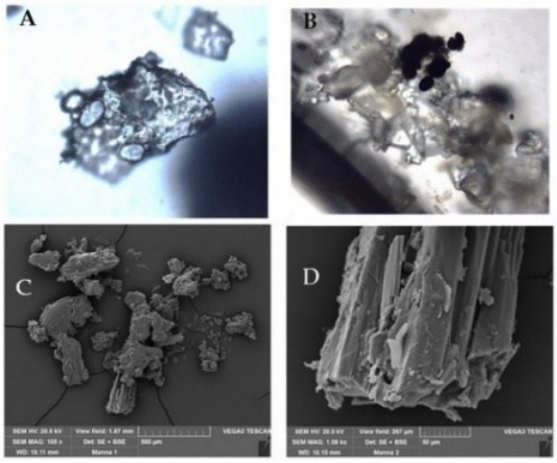

Figure 34. Micrographs of Manna samples acquired through optical microscopy (A, B) and scanning electron microscopy (C, D).

Quantification of Mannitol, Sugars and Total Starch Content

Table 4 presents the proximate composition of Manna, including the contents of mannitol, simple sugars, and total starch. These components were quantified through specific analytical assays, as described in detail in section 4.2.1.

Table 4. Phytochemical composition of lyophilized Manna extract, expressed as g per 100 g of dry weight. Values are reported as means ± standard deviation (SD) from three independent measurements.

Compound	Quantity (g/100g)
Glucose	2.43 ± 0.04
Fructose	5.84 ± 0.27
Resistant Starch	1.93 ± 0.08
Starch	1.34 ± 0.08
Mannitol	75.78 ± 0.68
Total polyphenols	0.21 ± 0.03
Hydroxycinnamic Acids	0.04 ± 0.01
Flavonoids	0.02 ± 0.01
Tannins	0.06 ± 0.03

According to previously published studies, mannitol is identified as the predominant saccharide in Manna extracts, with lower concentrations of fructose, glucose, and starch also detected. Notably, the total polyphenol content is substantial and comparable to that typically found in extra virgin olive oil. This observation is consistent with the chemotaxonomic relationship between the genera *Fraxinus* and *Olea* [208].

Radical Scavenging Capacity and Anti-Tyrosinase activity of Manna

The Manna extract exhibited a dose-dependent scavenging activity against reactive oxygen species (ROS), as shown in **Figure 35**. The highest antioxidant effect was observed at a concentration of 40 mg/mL, resulting in a mean ROS-scavenging activity of 23.71 ± 1.81%.

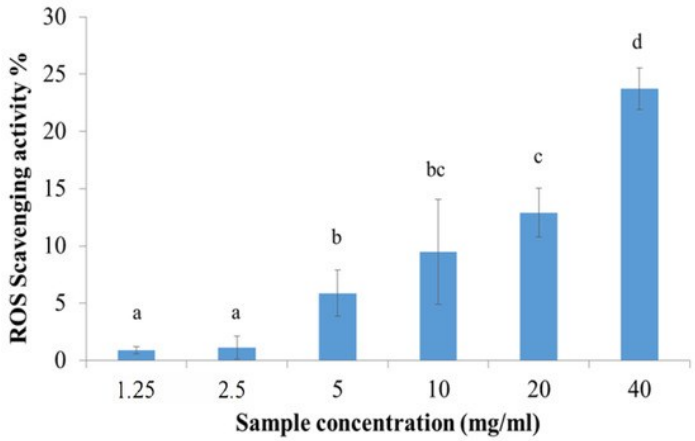

Figure 35. ROS-scavenging capacity of Manna extract at increasing concentrations. Data are presented as mean percentage values ± standard deviation (SD). Different letters indicate statistically significant differences among groups ($p < 0.05$).

The significant free radical-scavenging capacity and the tyrosinase-inhibitory activity appear to increase proportionally with the concentration of antioxidant compounds. **Table 5** summarizes the anti-tyrosinase activity of Manna extract. Overall, the extract exhibited a relatively low inhibitory effect on tyrosinase. Statistical analysis revealed a significant influence of sample

concentration ($p < 0.05$). Specifically, the samples at concentrations of 20 and 40 mg/mL demonstrated the highest inhibitory activities, with no significant difference observed between these two concentrations ($p > 0.05$).

Table 5. Evaluation of anti-tyrosinase effects of Manna extracts across different concentrations. Values represent the mean inhibition percentage, along with Km and Vmax parameters, expressed as mean ± standard error (SE). CTR denotes the negative control. Superscript letters indicate statistically significant differences within each measured variable ($p < 0.05$).

Sample Concentration	Anti-Tyrosinase Activity	Km (µM)	Vmax (µmol/min)
CTR	-	19.75 ±	1.43 ± 0.022 [a]
1.25	0.46 ± 0.069 [a]	25.47 ±	1.58 ± 0.034 [a]
2.5	2.33 ± 1.122 [a]	19.92 ±	1.43 ± 0.029 [a]
5	3.63 ± 1.401 [a]	20.29 ±	1.45 ± 0.022 [a]
10	5.47 ± 1.152 [a]	19.91 ±	1.45 ± 0.022 [a]
20	10.08 ± 3.584 [b]	19.54 ±	1.42 ± 0.033 [a]
40	10.96 ± 4.051 [b]	18.78 ±	1.31 ± 0.029 [a]

Anti-elastase Activity of Manna

As illustrated in **Table 6**, the inhibitory effects of Manna extract on elastase activity are observed as a function of varying concentrations. The results demonstrate a significant capacity of the extract to inhibit elastase, with the level of inhibition showing a notable response to concentration ($p < 0.05$). At lower concentrations (1.25 to 10 mg/mL), the inhibition remained around 10% while higher concentrations yielded approximately 25% elastase inhibition.

Table 6. Inhibitory effects of Manna extract on elastase activity at different concentrations. Data are presented as mean values ± standard error (SE) for inhibition percentage, Km, and Vmax. CTR refers to negative control. Superscript letters indicate statistically significant differences for each parameter ($p < 0.05$).

Sample Concentration	Anti-Elastase Activity %	Km (µM)	Vmax (µmol/min)
CTR	-	6.63 ± 0.387 [a]	0.98 ± 0.016 [a]
1.25	10.69 ± 4.086 [a]	12.57 ± 4.166 [b]	0.87 ± 0.112 [a]
2.5	10.16 ± 3.140 [a]	8.45 ± 0.389 [b]	1.06 ± 0.016 [a]
5	11.57 ± 2.772 [a]	8.48 ± 0.287 [b]	1.03 ± 0.011 [a]
10	16.13 ± 3.003 [a]	8.18 ± 0.525 [b]	1.00 ± 0.020 [a]
20	26.00 ± 3.452 [b]	11.63 ± 0.456 [b]	1.08 ± 0.016 [a]
40	25.05 ± 5.110 [b]	12.16 ± 0.794 [b]	1.11 ± 0.028 [a]

The Manna extract demonstrated a significant increase in Km values in comparison to the negative control, while Vmax values remained constant. These results are indicative of a competitive inhibition mechanism, in which the extract interacts with the active site of elastase.

Cytotoxicity of Manna (MTT Assay)

MTT assay results (**Figure 36**) indicated that HaCaT cell viability was preserved at all tested concentrations of Manna extract, confirming the absence of cytotoxic effects.

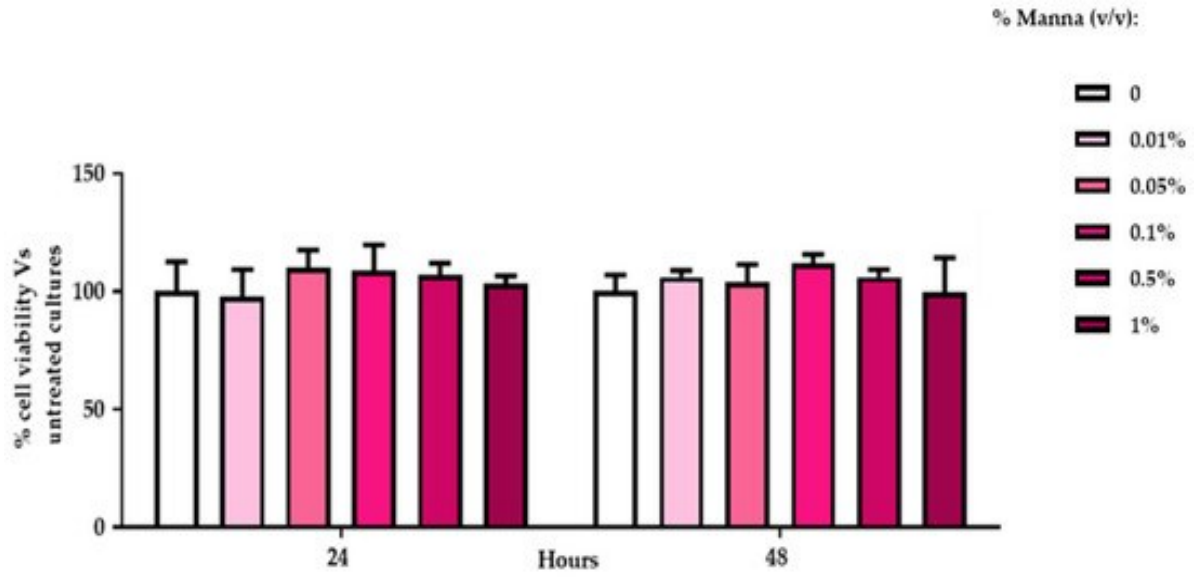

Figure 36. HaCaT cell viability following exposure to Manna extract for 24 and 48 hours. Cells were treated with increasing concentrations of Manna solution, and viability was assessed using the MTT assay. Results are expressed as the percentage of viable cells relative to untreated controls. Data represent the mean ± SD from two independent experiments, each performed in triplicate. Statistical analysis was carried out using ANOVA and Dunnett's test.

Cell proliferation index (DNA Assay)

The Manna extract influenced the proliferative behavior of both HaCaT and DLD-1 cell lines, with more pronounced effects observed after 48 hours of treatment. Following 24 hours of exposure to Manna at concentrations of 0.01% and 0.05%, HaCaT cells exhibited a dose-dependent decrease in proliferation. Specifically, a significant reduction in proliferation was detected at the lower concentration (0.01%), whereas at the higher concentration (0.05%),

proliferation levels were comparable to untreated controls. After 48 hours, Manna treatment resulted in a significant increase in HaCaT cell proliferation, which displayed an inverse trend (**Figure 37**).

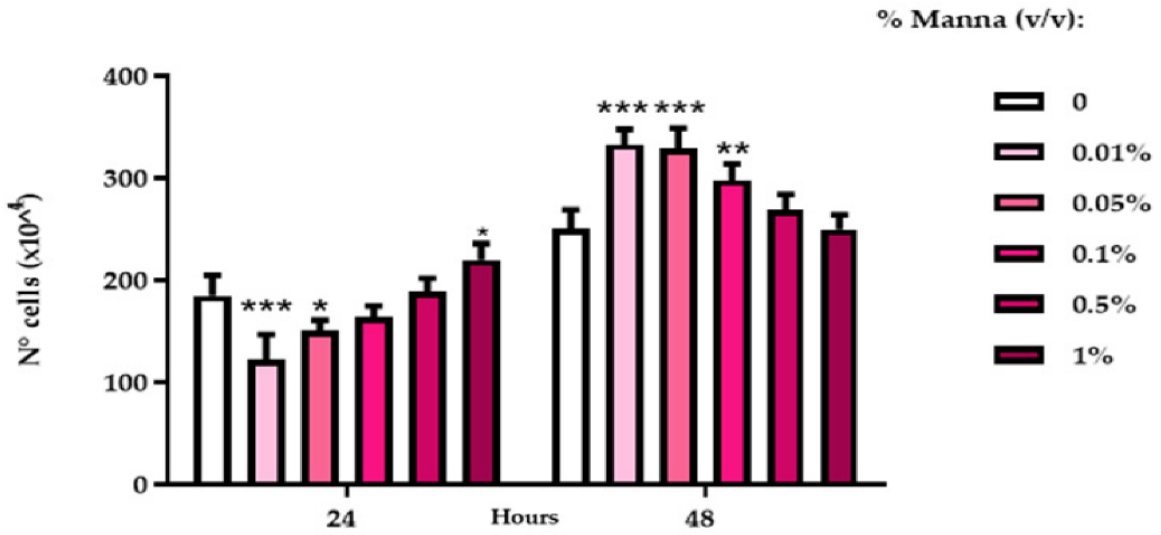

Figure 37. Proliferation indices of HaCaT cells following treatment with liquid Manna formulation. Proliferation was quantified by spectrofluorimetric analysis of DNA content (DNA assay), calibrated against a standard curve of known cell concentrations prepared for each assay. Data are expressed as mean ± SD from two independent experiments, each conducted in triplicate. Statistical significance compared to control is indicated as ***$p < 0.001$, **$p < 0.01$, *$p < 0.05$ (Two-Way ANOVA).

Healing abilities of Manna extract (Scratch wound assay)

In **Figure 38**, it is possible to observe that no wound closure occurred in the negative control HaCaT cultures, while the positive controls achieved complete healing within 48 hours. Treatment with Manna solutions resulted in progressive, dose-dependent wound repair, with the 1% Manna concentration promoting near-complete closure of the scratch.

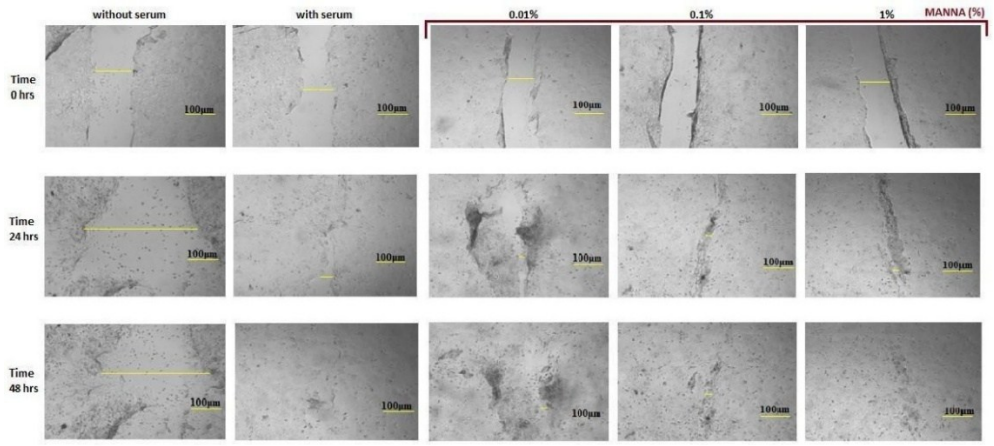

Figure 38. Representative digital images showing the wound incision and subsequent cell migration in HaCaT cultures untreated and treated with Manna formulation at concentrations of 0.01%, 0.1%, and 1% for 24 and 48 hours. Images were captured at 5× magnification at each time point. Scale bar represents 100 µm.

Data obtained from ImageJ 2.15.1 were quantified by calculating the percentage of wound closure (**Figure 39**) in HaCaT cells treated with varying concentrations of Manna solution, using the following formula:

$$Wond\ closur\ (\%) = 100 - \frac{(mean\ \mathrm{T48} * 100)}{maen\ T0}$$

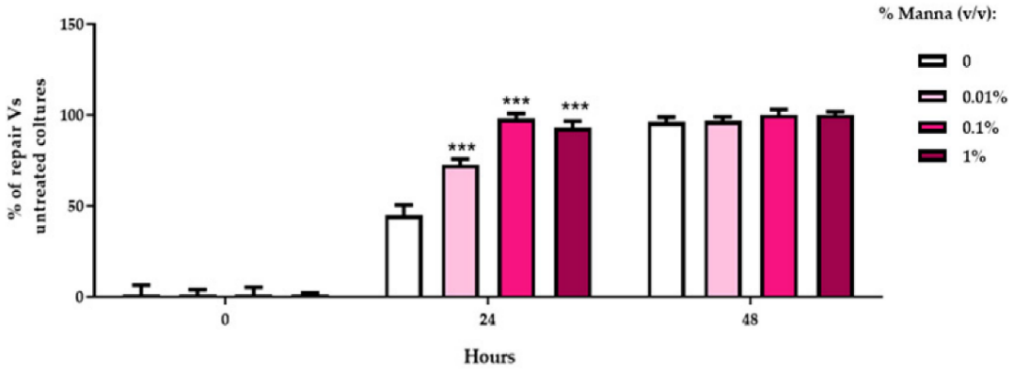

Figure 39. Percentage of wound closure in HaCaT cells treated with different concentrations of Manna liquid formulation (0.01%, 0.1%, and 1%). The measurements refer to the reduction in the distance between wound edges, expressed as a percentage relative to the initial value recorded at time zero. Images were analyzed using ImageJ software, and data are presented as mean ± SD from two independent experiments performed in duplicate. Statistical significance compared to the respective positive control is indicated as ***$p < 0.001$ (ANOVA followed by Dunnett's test).

The collective results suggest that Manna-based solutions do not have a negative effect on mitochondrial function, as demonstrated by the absence of cytotoxic effects in the MTT assay. This observation is supported by DNA assay, which indicates an absence of evidence of cellular stress. It is interesting to note that the lowest concentrations of the substance tested (0.01% and 0.05%) resulted in an increase in HaCaT cell proliferation. These results serve to support the hypothesis of a regenerative role for Manna, a theory that is also supported by the enhanced wound closure observed in the scratch assay.

pH values and rheological properties of Manna-based hydrogel

Table 7. shows the pH values of the hydrogel formulations, which were measured using a calibrated pH meter and found to be within the physiologically acceptable range for skin (5.50–6.80).

Table 7. Mean pH values ± standard deviation (SD) of the hydrogels tested, based on three independent experiments (n = 3).

Hydrogel Sample	pH
BN PEC-D	5.04 ± 0.02
BN PEC-K	6.10 ± 0.01
PEC-D	5.50 ± 0.01
PEC-K	6.80 ± 0.02

Understanding the flow characteristics of a hydrogel is essential to predict its behavior in vivo, especially its capacity to distribute homogeneously and form a coating on the skin surface.

Regarding the rheological behavior of the samples, Manna-based gel formulations demonstrated non-Newtonian flow behavior under room temperature conditions **Figure 40** PEC-D was more viscous than PEC-K throughout the entire shear rate range. In both systems, the viscosity (η) decreased noticeably with a slight increase in shear rate (γ), up to approximately $\gamma = 20\ s^{-1}$. Beyond this threshold, the viscosity stabilized and remained nearly constant up to $\gamma = 100\ s^{-1}$. This rheological behavior is characteristic of shear-thinning fluids

(pseudoplastics), where the flow behavior index (n) is less than 1. In contrast, fluids that exhibit increasing viscosity with increasing shear rate at high γ values are referred to as shear-thickening or dilatant systems, for which n > 1.

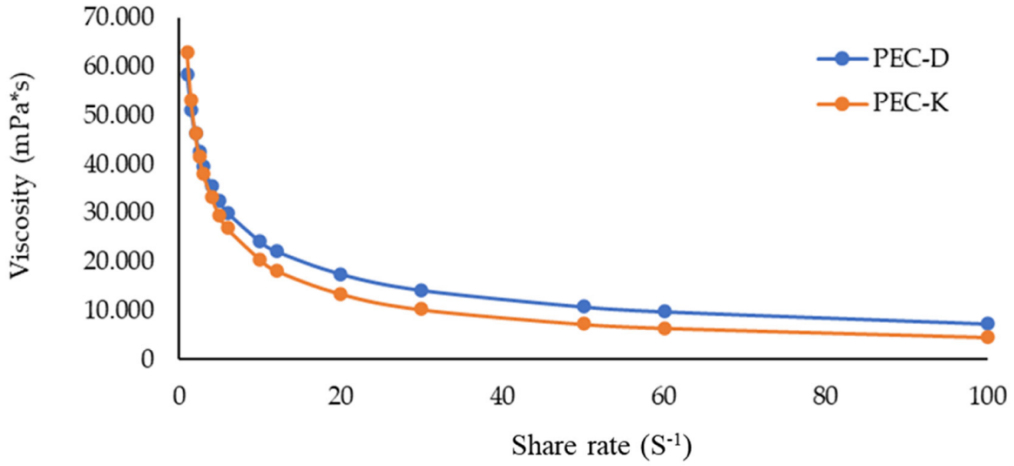

Figure 40. Viscosity profiles of PEC-D and PEC-K as a function of shear rate.

For shear rate (γ) values up to 100 s^{-1}, both PEC-D and PEC-K exhibit shear-thinning behavior, characterized by a decrease in viscosity with increasing shear rate.

Antioxidant Activity and Total Phenolic Content of Manna-based hydrogel

The antioxidant activity (AA%) of the formulated gels was assessed using the DPPH assay, and the corresponding results are presented in **Table 8** The total polyphenolic content was determined by the Folin-Ciocalteu method and the results are reported in **Table 9**. A slight reduction in antioxidant activity was observed in the Manna-pectin hydrogels compared to the Manna exudate solution alone (see **Table 8** and **Figure 36**). This phenomenon may be attributed to the partial degradation of polyphenolic compounds during storage at room temperature. However, the hydrogels exhibited an overall satisfactory level of antioxidant activity, indicating their potential for *in vivo* topical application. In particular, such formulations may support tissue regeneration and exert a mild depigmenting effect, properties that are highly desirable in cosmetic products.

Table 8. Antioxidant activity (AA%) of the samples determined by the DPPH assay. Data are expressed as mean values ± standard deviation (SD) from three independent experiments (n = 3).

	Absorbance λ = 515 nm	% DPPH	AA%
DPPH	0.443	100	-
PEC-K	0.340	76.75 ± 0.3	11.71 ± 0.3
PEC-D	0.351	79.23 ± 0.2	10.33 ± 0.2

Table 9. Total phenolic content of the samples determined using the Folin–Ciocalteu assay. Data are expressed as mean values ± standard deviation (SD) from three independent experiments (n = 3).

	Absorbance λ = 750 nm	mg/GAE/g gel
PEC-K	0.436	35.66 ± 0.15
PEC-D	0.361	29.51 ± 0.22

Conclusions

The primary objective of this study was to investigate the *in vitro* biological activity of Manna exudate for potential application in hydrogel-based formulations within the cosmetic and dermatological fields. To evaluate the possible effects of manna exudate such as cytotoxic, antiproliferative, and antioxidant effects, a human keratinocyte cell line (HaCaT) was used in this study.

No evidence of mitochondrial toxicity was observed, and DNA quantification assays confirmed the absence of proliferative stimulation. Furthermore, the results of the scratch assay demonstrated a significant enhancement in wound closure after 24 hours of exposure to various concentrations of Manna. Radical-scavenging, anti-tyrosinase, and anti-elastase assays further supported the capacity of Manna, when appropriately delivered within a pectin-based hydrogel, to mitigate oxidative stress and exert anti-inflammatory effects.

Collectively, these findings suggest that Manna exudate has potential as a natural plant-derived bioactive compound for incorporation into topical formulations with antioxidant activity. Pectin hydrogels have been identified as a suitable delivery platform for the development of novel skincare products and therapeutic treatments for dermatological diseases, particularly in the context of wound healing.

Dissemination of Results

The outcomes of this research were disseminated through publication in the international peer-reviewed journal Gels, with the article entitled Evaluation of the Biological Activity of Manna Exudate, from *Fraxinus ornus* L., and Its Potential Use as Hydrogel Formulation in Dermatology and Cosmetology [209].

In situ NADES microwave-mediated extraction of bioactive compounds from *Beta vulgaris* L. var. *rubra* waste

This research focused on the valorization of beetroot processing residues, specifically fresh stalks, through the recovery of bioactive compounds using an innovative microwave-assisted methodology. The approach involved the simultaneous *in situ* formation of natural deep eutectic solvents (NaDES) and extraction of phytochemicals, thereby streamlining traditional multi-step NaDES-based procedures. The overarching aim was to develop a fast, efficient, and sustainable "one-pot" extraction technique capable of generating non-toxic, ready-to-use bioactive ingredients with potential applications in cosmetic, and pharmaceutical fields.

To this end, a range of food-grade eutectic systems was investigated, combining hydrogen bond acceptors (choline chloride or betaine) with various hydrogen bond donors (including fructose, citric acid, glycerol, and urea) in specific molar ratios. The process was carried out under microwave irradiation, optimizing key parameters such as reaction time, temperature, and solvent-to-matrix ratio. The efficiency of extraction was primarily assessed by evaluating the total phenolic content recovered from the plant matrix. This strategy not only facilitates the sustainable recovery of high-value compounds from agricultural waste but also supports a circular economy model by converting beetroot residues into functional ingredients ready-to-use.

Results and Discussion

NaDES Preparation

In the initial phase of optimising the novel *in situ* methodology, a preliminary investigation was conducted on the microwave-assisted synthesis of NaDES. In this investigation, a selection of naturally occurring, food-grade components hydrogen bond acceptors (HBA) and hydrogen

bond donors (HBD) were combined (**Table 1**), according to the extraction method reported by Souza et al. (2022) [210] and our green sustainable target. The mixtures were subjected to two different methods of preparation. Firstly, they were subjected to a slightly modified version of the microwave protocol described by Souza et al. [210] (70°C, 30-180 sec). Secondly, they were prepared using a conventional method that involved a thermostatic water bath (70°C, 3600 sec). The formation time of NaDES is a crucial factor to consider, given the aim to modify microwave-assisted NaDES procedures into an *in situ* "one-pot" method, where solvent preparation and matrix extraction occur simultaneously. These aspects were identified as fundamental in a preliminary evaluation to identify the most effective eutectic system, based on the following criteria: rapid formation (within 120 seconds), low viscosity (under 0.35 Pa·s for optimal sample handling), storage stability.

Among the tested eutectic mixtures, choline chloride/glycerol (CG), choline chloride/urea (CU), betaine/fructose/water (BF), and betaine/glycerol (BG) were the most suitable food-grade mixture. The combinations of choline chloride/citric acid and betaine/citric acid were excluded from further analysis due to their observed physical instability over storage periods. Moreover, the choline chloride/fructose system was disregarded because its synthesis required a reaction time exceeding 120 seconds. Therefore, based on different criteria (rapid preparation, appropriate viscosity, and satisfactory stability) CG, CU, BF and BG were identified as the most promising NaDES formulations for subsequent solvent screening to optimize extraction performance.

Screening of NaDES for Optimized Extraction Performance

NaDES, characterized by different polarities, viscosities, and intermolecular interactions due to their constituent (HBD and HBA), are promising new media for extraction processes. The variability in these physicochemical properties influences the extraction kinetics and efficiency,

leading to the need for identification of the most effective eutectic system optimized for the target compounds.

To achieve this, a preliminary comparative study was conducted to evaluate the extraction capabilities of four selected NaDES formulations choline chloride/glycerol (CG), choline chloride/urea (CU), betaine/fructose/water (BF), and betaine/glycerol (BG) with water used as a control solvent. The experimental parameters were set in accordance with established protocols from the literature [211, 212] employing a solvent-to-solid ratio of 15:1 (w/w), a temperature of 50°C, and an extraction time of 30 minutes.

The screening results, summarized in **Figure 41**, demonstrate that among the NaDES tested, CU exhibited the highest TPC recovery, with a value of 0.39 mg GAE/g. This was followed by CG (0.29 mg GAE/g), BG (0.22 mg GAE/g), and BF (0.17 mg GAE/g). Notably, the aqueous extraction performed under the same conditions yielded the lowest TPC (0.09 mg GAE/g). Based on these results, CU was selected as the optimal solvent for successive extraction experiments.

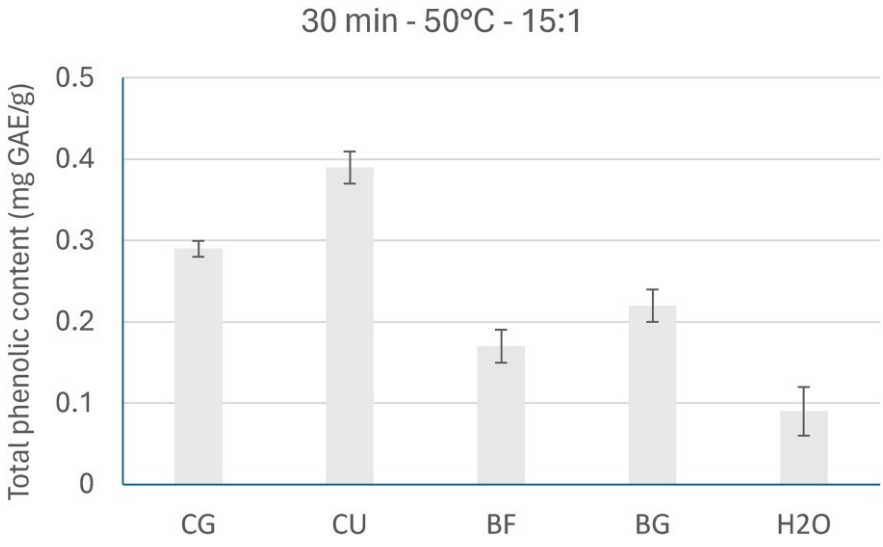

Figure 41. Comparative evaluation of extraction efficiency using microwave-assisted NaDES systems (CG, CU, BF, and BG) and water (H_2O) as solvents. Experimental conditions: 50 °C, 30 minutes, and a solvent-to-matrix ratio of 15:1 (w/w). Results are expressed as milligrams of gallic acid equivalents (GAE) per gram of fresh beetroot stalk. Data represents the mean ± standard deviation (n = 3).

Single-Factor Experimental Analysis

Data of the single-variable optimization experiments, conducted under microwave irradiation using choline chloride/urea (CU) as the extraction solvent, are presented in **Figures 42a-c**. **Figure 42a** represented the influence of varying solvent-to-matrix ratios (ranging from 10:1 to 30:1 w/w) on TPC, with all extractions performed at 50 °C for 30 minutes. An evident increase in TPC is observed when the ratio increases from 10:1 to 15:1. However, the enhancement in TPC becomes progressively less marked as the solvent-to-matrix ratio increases from 15:1 to 20:1, and no appreciable change is observed between 20:1 and 30:1.

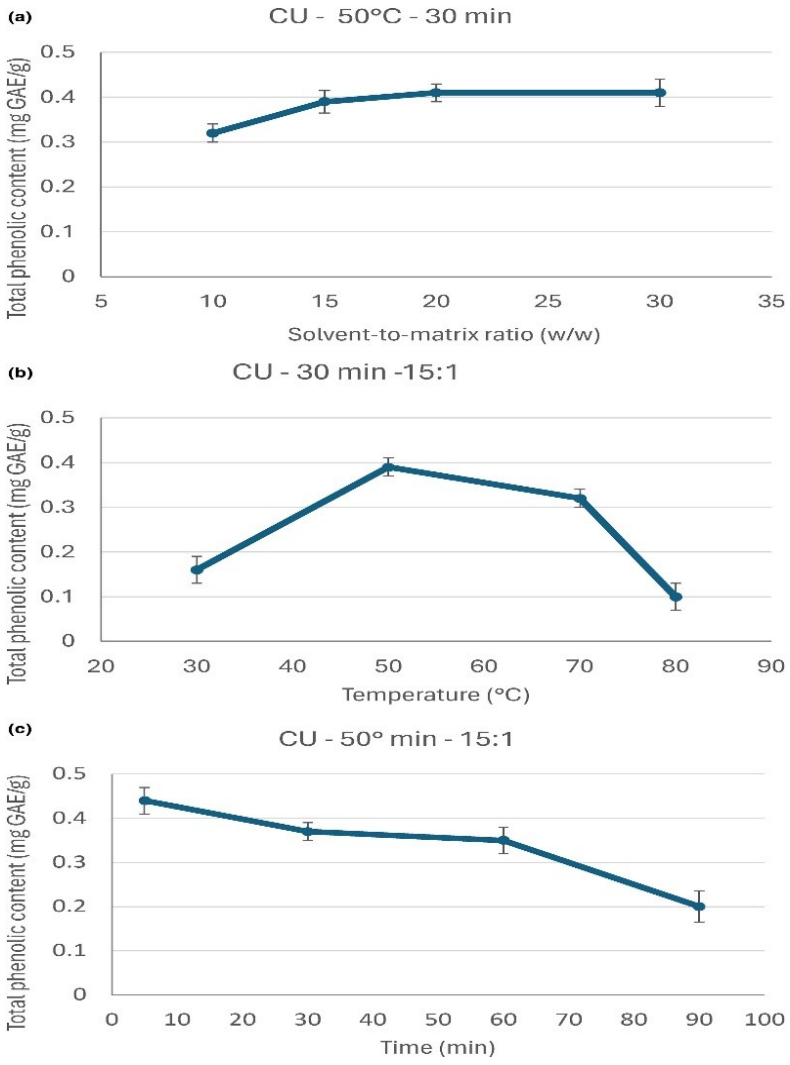

Figure 42. Influence of individual extraction parameters on total phenolic content (TPC) under microwave-assisted extraction using choline chloride/urea (CU) as the solvent. (**a**) Solvent-to-matrix ratio (50 °C, 30 min); (**b**) Extraction temperature (30 min, 15:1 w/w); (**c**) Extraction time (50 °C, 15:1 w/w). Data are presented as mean values ± standard deviation (n = 3).

This effect can be attributed to the initial formation of a larger contact area between the solvent and the sample matrix, which enhances mass transfer and facilitates phenolic release in the early stages of extraction.

Figure 42b shows the influence of temperature (ranging from 30 to 80 °C) on TPC yield, with fixed extraction conditions (30 min, 15:1 solvent-to-matrix ratio w/w). TPC values rise significantly from 0.16 mg GAE/g at 30 °C to a maximum of 0.39 mg GAE/g at 50 °C. However, a further increase in temperature results in a significant decrease in TPC, reaching 0.1 mg GAE/g at 80 °C. This trend may initially be due to the reduced viscosity of the solvent at higher temperatures, which improves contact with the chopped plant material. On the other hand, a long exposure to temperatures above 50 °C appears to cause degradation of phenolic compounds, lowering the yield.

This degradation is also reflected in the results related to extraction time (**Figure 42c**), where durations from 5 to 90 minutes were tested under fixed conditions (50 °C, 15:1 w/w). TPC levels decrease steadily from 0.44 mg GAE/g at 5 min to 0.35 mg GAE/g at 60 min, followed by a drastic reduction to 0.2 mg GAE/g at 90 min.

The high phenolic content recovered after only 5 minutes may be explained by the rapid increase in temperature induced by microwave dielectric heating, which ensures efficient and uniform energy transfer to the extraction medium. This heating mechanism, facilitated by solvent and matrix polarity, allows an accelerated mass transfer and effective release of target compounds in a short time frame.

Results of the design of experiments (DOE)

The experimental design with the corresponding TPC responses and the predicted TPC values obtained from the extraction of fresh beetroot stalks via ISMWE are summarized in **Table 10**. Data indicates that the maximum TPC was observed in run 8, conducted at 5 minutes, 70 °C,

and a solvent-to-solid ratio of 20:1, whereas the minimum TPC value was recorded in run 7, under conditions of 5 minutes, 30 °C, and 10:1 ratio.

Table 10. TPC Response and Predicted TPC Values Obtained from the Nine Samples Proposed by the DOE-

Run	Time	Temperature	Solvent/matrix ratio	TPC response	Predicted TPC
1	5	30	20	0.13	0.15
2	60	70	10	0.32	0.30
3	60	70	20	0.33	0.33
4	5	70	10	0.52	0.49
5	60	30	10	0.13	0.14
6	60	30	20	0.15	0.16
7	5	30	10	0.11	0.11
8	5	70	20	0.55	0.54
C	32.5	50	15	0.38	0.36

The interaction profiles between the parameters are shown in the graph in **Figure 43**. The pink lines represent low levels, while the blue lines indicate high levels of each factor. The parallel and do not cross lines, this suggests that the interaction between the factors is weak. A crossing of lines, such as that between temperature and time, indicates a strong interaction that affects the TPC extraction efficiency.

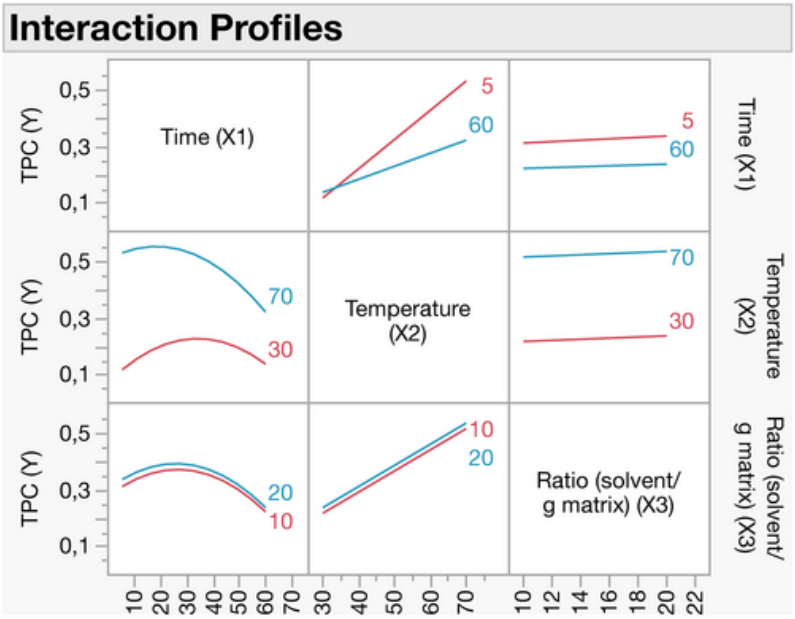

Figure 43. Interaction profiles of the factors Time (X1), Temperature (X2), and Solvent-to-Matrix Ratio (X3) with the response Total Phenolic Content (TPC, Y).

Table 11 reports the results of the analysis of variance (ANOVA), performed using JMP software and based on the full factorial design. The statistical analysis highlights the main factors that influence the extraction efficiency, identified by P-values lower than 0.05. In particular, the lowest P-values (indicated in red) point to time and temperature as significant variables, both individually and in combination.

Table 11. Analysis of Variance (ANOVA) of the Main Experimental Factors Performed with JMP Software.

Sorted parameter estimates					
Term	**Estimate**	**Std error**	***t* ratio**		**Prob > |*t*|**
Temperature (X2)(30,70)	0.15	0.0025	60.00		0.0106*
Time (X1) * Temperature (X2)	−0.0575	0.0025	−23.00		0.0277*
Time (X1)(5,60)	−0.0475	0.0025	−19.00		0.0335*
Time (X1) * Time (X1)	−0.1	0.0075	−13.33		0.0477*
Ratio (solvent/g matrix) (X3)(10,20)	0.01	0.0025	4.00		0.1560
Time (X1) * Ratio (solvent/g matrix) (X3)	−0.0025	0.0025	−1.00		0.5000
Temperature (X2) * Ratio (solvent/g matrix) (X3)	0	0.0025	0.00		1.0000
Temperature (X2) * Temperature (X2)	0	0			
Ratio (solvent/g matrix) (X3) * Ratio (solvent/g matrix) (X3)	0	0			

* Significant data with *P*-values < 0.05

The analysis of experimental data indicates that high temperatures in combination with minimal treatment times are the most significant parameters to enhancing the extraction yield. Microwave-assisted extraction (MAE) has proven to be a highly effective technique for

accelerating the extraction process, particularly due to its strong compatibility with NaDES, allowing a short heat exposure. This approach reduces the degradation of thermolabile compounds and allows efficient recovery of phenolic constituents.

Therefore, based on the promising results obtained using CU, the following experimental conditions were chosen for the subsequent *in situ* microwave extraction (ISMWE): 20:1 g/g, at 70 °C for 5 min. This extraction was then compared with the conventional microwave extraction (MWE) where pre-synthesized NaDES were used, and with a microwave water extraction conducted under identical conditions.

Due to the polar nature of the components involved, microwave dielectric heating quickly brought the temperature up to 70 °C within 10-15 seconds coinciding with the beginning of the formation of NaDES and maintained it consistently through power modulation ranging from 0 to 300 Watts. The microwave system used is equipped with two fiber optic probes placed within the extraction vessel, allowing continuous real-time temperature monitoring and precise control of thermal feedback via adaptive power regulation. Under these defined conditions (70 °C for 5 minutes using 20 g of eutectic mixture and 1 g of freshly chopped beet stalks), the ISMWE technique demonstrated the highest extraction efficiencies, with CU emerging as the most effective solvent among those evaluated. Although the MWE approach yielded comparable results, it necessitates additional time for pre-formulating the solvent system, which must be factored into the overall process efficiency. In contrast, microwave-assisted water extraction under the same parameters produced lower yields (0.14 mg GAE/g), underscoring the critical role of solvent selection in optimizing extraction outcomes. A summary of these results is provided in **Figure 44**.

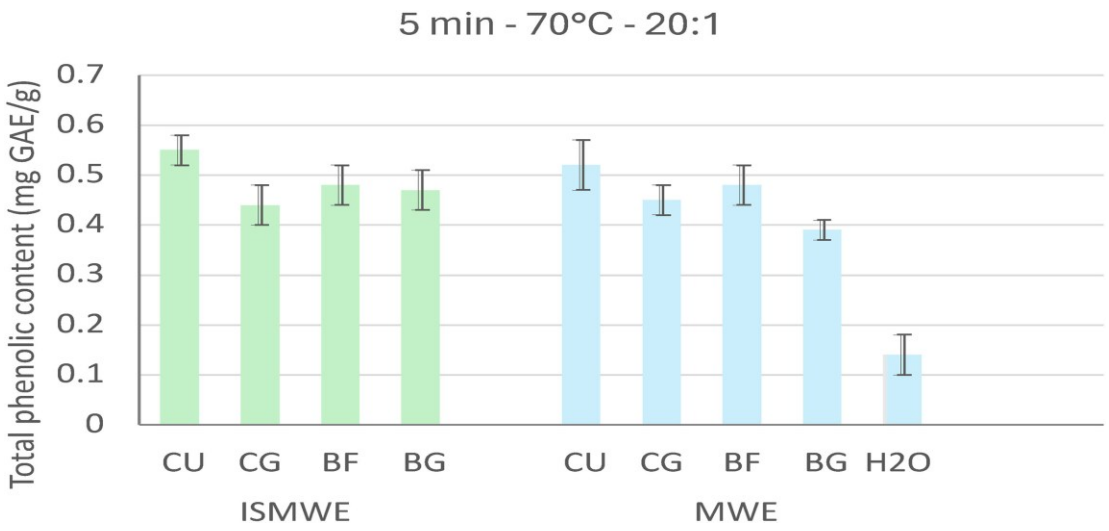

Figure 44. The recovery TPC achieved through microwave-assisted extraction methods (ISMWE and MWE) under the most favorable experimental conditions was evaluated using all selected NaDES and compared to microwave extraction with water (MWE H_2O). Data are reported as mean values (n = 3) with their respective standard deviations (± SD).

Radical Scavenging Activity: DPPH Assay

The antioxidant activity of MW CU extracts was evaluated through the DPPH assay, using Trolox as the reference standard. The results, presented in **Table 12**, include a comparison with microwave water extracts processed under identical conditions. Both NaDES-based extracts (ISMWE CU and MWE CU) demonstrated notable radical scavenging activity, exhibiting RSA values of 53% and 59%, respectively. These results underline the effectiveness of NaDES as extraction media for antioxidant compounds. Moreover, the RSA values were in good agreement with TPC of each extract, supporting the correlation between phenolic concentration and antioxidant activity. Notably, the bioactivity of the extracts was preserved without the need for solvent removal prior to use, highlighting their potential as ready-to-use ingredients.

Table 12. Percentage RSA values for the most effective NaDES-based extractions compared to water-based extractions, all conducted under the same experimental conditions (5 minutes, 70 °C, 20:1 solvent to-matrix ratio).

Extraction Methods	RSA (% ± SD)
ISMWE CU	53 ± 3
MWE CU	59 ±4
MWE H_20	12 ± 1

Mean values (n = 3) ± standard deviation (SD).

Stability studies: betacyanins Content

All extracts exhibited a vivid red coloration immediately after extraction process (**Figure 45a**), due to the presence of betalain pigments. As previously discussed, these are primarily composed of betacyanins (75-95%) and, to a less significant, betaxanthins (5-25%). It is well established that solvent composition plays a critical role in the stability of betalains either preserving or accelerating the degradation of betacyanins. Accordingly, the betacyanin content in both NaDES-based extracts and water-based samples was quantified and monitored over a three-month period, serving as a stability marker under storage conditions.

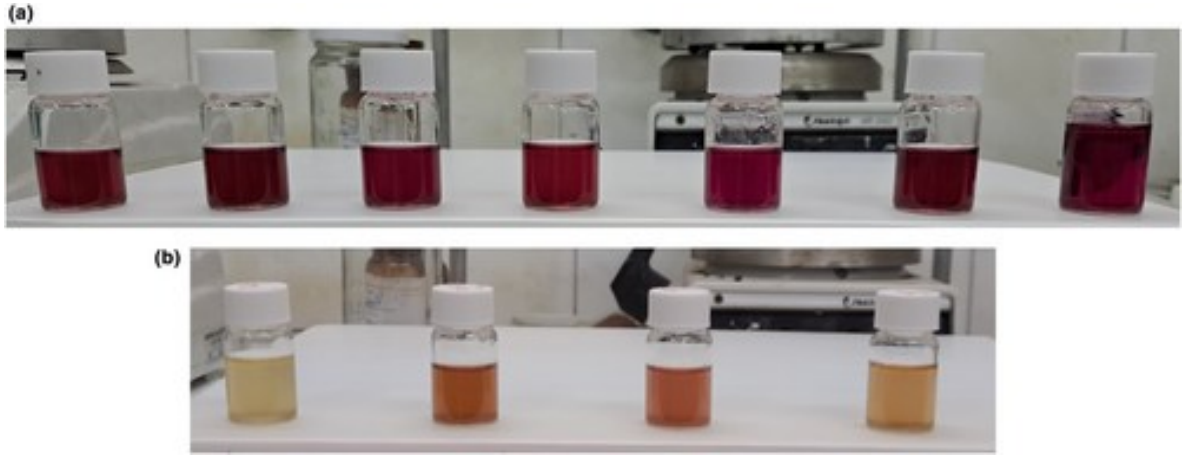

Figure 45 (a) NaDES-based and water-based extracts immediately following extraction; **(b)** water-based samples 24 hours post-extraction.

Figure 46 presents the trend in betacyanin content over time for both NaDES-based and water-based extracts. CU-based samples maintained a relatively stable betacyanin concentration throughout the observation period, ranging from 0.24-0.25 mg/g immediately after extraction to 0.15-0.20 mg/g after three months. In contrast, water extracts showed a marked decrease in betacyanin levels within the first 24 hours, dropping from 0.06 mg/g to 0.01 mg/g. These findings were consistent with visual observations: after 24 hours, the characteristic red hue had noticeably diminished in all water-based samples (**Figure 45b**).

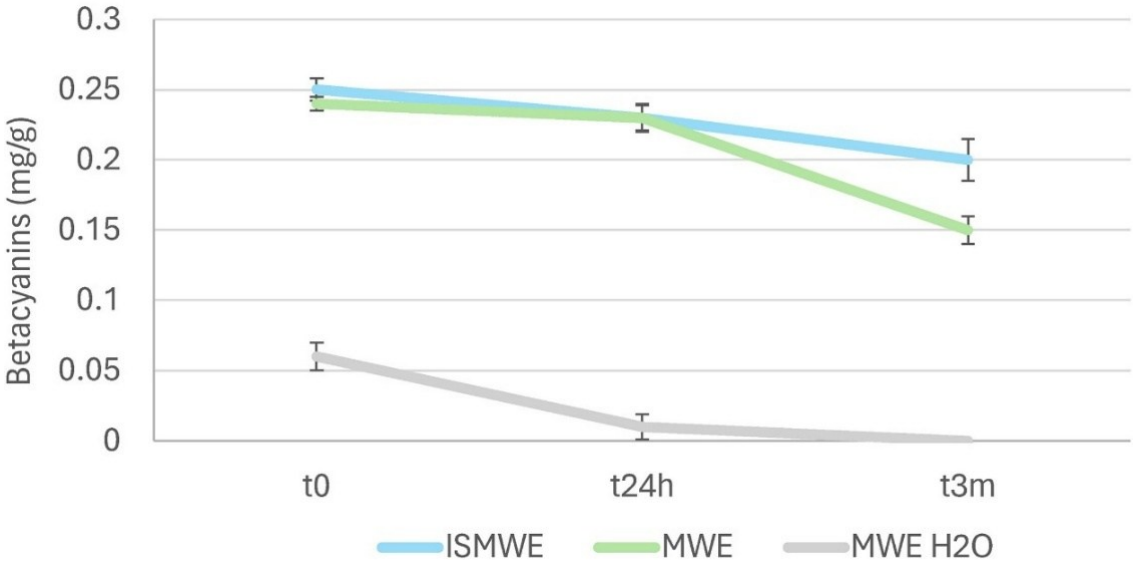

Figure 46. Betacyanin content (BC, mg/g) in choline/urea (CU) based extracts obtained via ISMWE and MWE, compared to water-based MWE, monitored over a three-month period (t_0, t_{24}h, t_3m). Results are reported as mean values (n = 3) ± standard deviation (SD).

Conclusions

In this study the potential direct application of natural extracts obtained from beetroot waste using microwave-assisted extraction with natural deep eutectic solvents (NaDES) under varying conditions was investigated. The innovative *in situ* extractive strategy proposed herein enabled the efficient recovery of bioactive compounds through a rapid (5-minute) and straightforward one-pot process. Extracts derived from NaDES exhibited notable antioxidant activity, attributable to the presence of diverse phenolic constituents, and demonstrated significantly improved long-term stability compared to water-based samples. Moreover, the possibility of preparing the solvent directly within the extraction vessel, simultaneously due to their natural composition, lack of toxicity, and enhanced stability, the NaDES extracts showed promising potential as active ingredients in food, cosmetic, and pharmaceutical applications while simultaneously contributing to the valorization of agro-food waste within a circular economy. with the processing of the matrix, presents an interesting approach for preliminary

screenings of other organic matrices, simplifying workup, streamlining the procedures, and reducing costs.

Dissemination of Results

The research results were disseminated through publication in the international peer-reviewed journal *International Journal of Food Science and Technology*, with the article entitled "*In situ* NaDES microwave-mediated extraction of bioactive compounds from *Beta vulgaris* L. var. *rubra* waste" [202]. This work was also presented as a poster at the 33rd IFSCC Congress in Barcelona. Subsequently, the poster was selected and the author was invited to deliver an oral presentation at the 7th IPCE (Intercontinental Personal Care Excellence) Conference, titled "Biodiversity & Sustainability-Rethinking Beauty," held in Venice.

Valorization and Potential Antimicrobial Use of Olive Mill Wastewater (OMW) from Italian Olive Oil Production

As stated previously, the production of olive oil leads to the generation of significant quantities of olive mill wastewater (OMW), which is primarily derived from the processes of washing, processing, and pressing olives in mills. Conventional milling processes require between 40 and 120 liters of water per quintal of olives processed, thereby producing significant volumes of wastewater. In the context of sustainable development objectives, particularly within the parameters of the circular economy, it is essential to reduce water consumption and valorise process water. To achieve this objective, the preliminary phase of the study concentrated on the purification of OMW by means of effective membrane-based filtration systems. The fractions obtained from the purification process were then evaluated for their antioxidant capacity using the DPPH assay, and their total phenolic content was quantified via the Folin-Ciocalteu method. Furthermore, infrared (IR) spectroscopy was utilised for the purpose of compositional characterisation. Furthermore, the fractions were assessed for antimicrobial activity against a panel of clinical isolates, including both Gram-positive and Gram-negative strains, many of which exhibited resistance or multi-resistance to conventional antibiotics. The findings highlighted the potential of this agro-industrial by-product as a bioactive source for applications in the (phyto)pharmaceutical field.

For clarity in the results of filtration procedure section, the samples collected at various stages of the process are defined as follows:

- **MF1:** sample obtained after microfiltration.
- **ROp1:** intermediate reverse osmosis permeate.
- **ROp2:** final reverse osmosis permeate.

- **MD1:** initial concentrate at the onset of membrane distillation (VMD).
- **MD2:** final VMD concentrate.
- **MDd1:** initial membrane distillation distillate at the onset of VMD.
- **MDd2:** final VMD distillate.

Results and Discussion

OMW Concentration from Membrane Processes

To evaluate the inorganic content of the samples, conductivity measurements were performed on untreated OMW and on the fractions obtained at different stages of the membrane-based purification process. The relationship between sample conductivity and the volume concentration ratio is illustrated in **Figure 47**. The untreated OMW exhibited a conductivity of approximately 7 mS/cm, corresponding to an estimated total dissolved solids (TDS) concentration of 4 g/L, expressed as NaCl equivalent. The microfiltration step did not significantly affect the ionic composition of the sample, as indicated by the comparable conductivity value observed in the MF1 fraction (**Figure 20**). Reverse osmosis (RO), known for its high selectivity in solute retention while allowing water permeation, resulted in a substantial increase in ionic concentration. At a volume concentration factor of 7.3, the RO1 concentrate displayed a conductivity of 30 mS/cm, equivalent to a TDS of approximately 19 g/L (NaCl equivalent). Further concentration was achieved via vacuum membrane distillation (VMD), applied to the RO concentrate. This step led to an overall volume concentration factor of around 15. As a result, the conductivity of the MD1 and MD2 (**Figure 20**) fractions increased to 41.8 mS/cm, corresponding to a TDS of roughly 27 g/L NaCl equivalent (**Figure 20**).

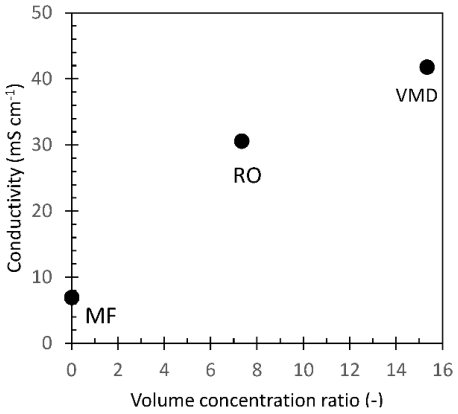

Figure 47. Electrical conductivity of OMW samples as a function of the volume concentration ratio obtained during each step of the membrane treatment process. The graph illustrates the progressive increase in conductivity from the untreated sample through microfiltration (MF), reverse osmosis (RO), and vacuum membrane distillation (VMD). The conductivity values reflect the concentration of total dissolved solids (TDS), expressed as NaCl equivalents, highlighting the efficiency of each step in concentrating the inorganic fraction of OMW.

To evaluate the effectiveness of the reverse osmosis (RO) and vacuum membrane distillation (VMD) processes in retaining dissolved inorganic electrolytes, permeate samples were collected at two stages during the RO concentration: one at the midpoint (ROp1, **Figure 20**) and one at the conclusion (ROp2, **Figure 20**) of the process. Similarly, distillate samples from the VMD concentration step were taken at the beginning (MDd1, **Figure 20**) and at the end (MDd2, **Figure 20**) of the operation. Conductivity measurements of these samples, as presented in **Table 13**, demonstrated that both RO and VMD methods achieved an approximate 98.5% reduction in electrolyte concentration within the treated fractions.

Table 13. Conductivity values of permeate samples collected during the RO concentration process (ROp1 and ROp2) and distillate samples from the VMD concentration step (MDd1 and MDd2).

Sample	Conductivity (mS/cm)
ROp1	0.14
ROp2	1.00
MDd1	0.42
MDd2	0.63

The composition of inorganic species in the MF1, RO, and MD samples was examined by subjecting the samples to drying and subsequent calcination at 600 °C, followed by

semiquantitative elemental analysis. The results indicated a uniform average composition of the inorganic residues across all samples, as illustrated in **Figure 48**. Potassium was found to be the major constituent, representing approximately 67% of the mass, with chlorine as the second most abundant element at about 15%. Other detected elements including sodium, magnesium, phosphorus, sulfur, calcium, and iron were present in similar amounts, each present at a weight percentage below 7%.

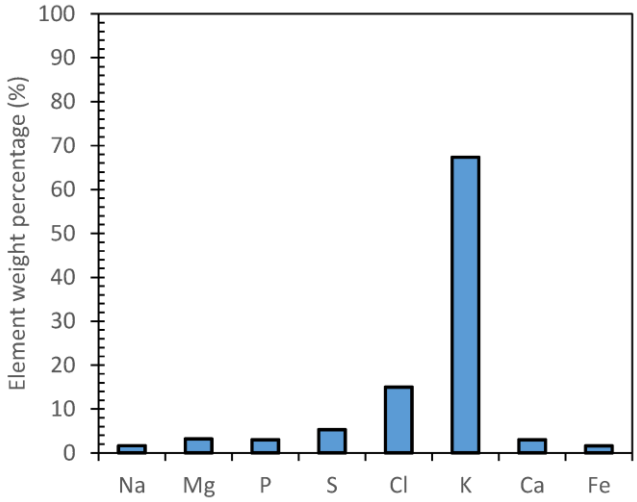

Figure 48. Semiquantitative elemental analysis of a representative sample obtained by EDX.

OMW Characterization: FTIR Analysis

Fourier-transform infrared (FTIR) spectroscopy was employed as a valuable analytical tool to investigate the functional groups present in the organic matrix of olive mill wastewater (OMW), as previously reported [212,213]. To determine whether the purification process altered the chemical composition of OMW, both the raw sample and the RO1-treated sample (**Figure 20**) were analyzed using FTIR spectroscopy (**Figure 49**).

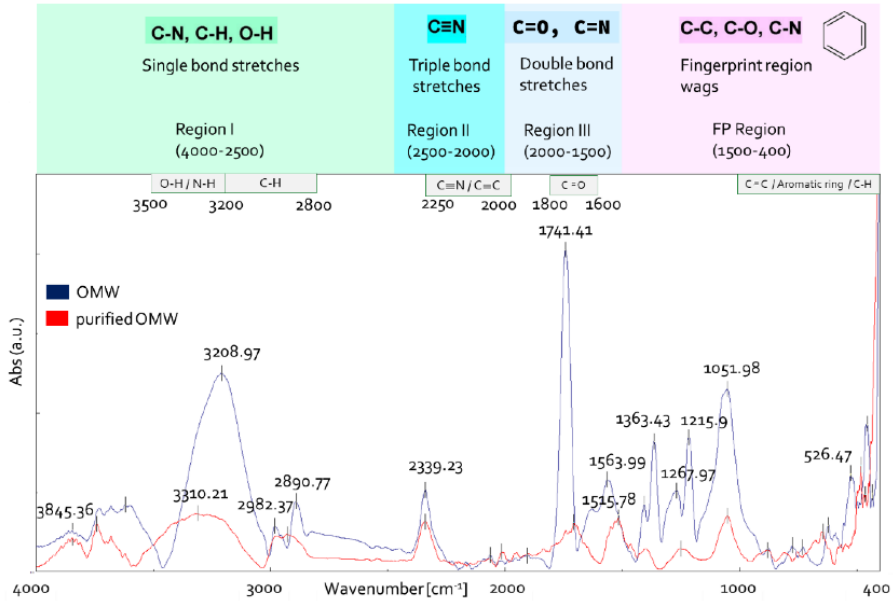

Figure 49. OMW IR spectra before and after purification.

The IR spectrum of untreated OMW (**Figure 49)** showed a broad absorption band in the 3500-3000 cm^{-1} region, which corresponds to O-H stretching vibrations, typically associated with hydroxyl-containing functional groups such as alcohols, phenols, and carboxylic acids (3670-2450 cm^{-1}) [214,215]. Peaks at approximately 2980 and 2890 cm^{-1} were attributed to the aliphatic C-H stretching of CH_2 and CH_3 groups. A smaller band observed around 2340 cm^{-1} likely resulted from atmospheric CO_2 present in the sample chamber during spectral acquisition.

A prominent absorption peak centered at 1740 cm^{-1} was observed and attributed to C=O stretching vibrations, commonly associated with carbonyl-containing groups such as carboxylic acids, esters, and ketones [216]. In the fingerprint region (1500-400 cm^{-1}), a band at 1363 cm^{-1} may be linked to C–H bending of methyl groups or asymmetric stretching of the carboxylate group (COO^-), as well as possible C=O deformation modes [217]. The band at 1216 cm^{-1} was indicative of C–O stretching in aryl ethers and phenolic compounds, along with potential in-plane deformations of carboxylic acid groups or vibrations in unsaturated esters [218].

Additionally, the absorption observed at 1052 cm^{-1} may be related to vibrational modes of polysaccharides, aromatic ethers, and carbohydrate structures [219].

Comparative analysis of the spectra revealed a general reduction in both the intensity and number of absorption bands in the RO1-treated sample, indicating a simplification of the organic composition after purification (**Figure 50**). Notably, a band at 1516 cm^{-1} was detected in the spectrum of the treated sample, which may correspond to C=C stretching vibrations in aromatic rings, associated with phenolic structures, flavonoids, and other polar aromatic compounds [212]. Spectral interpretation was carried out based on established assignments in literature [220,214].

Radical-Scavenging Activity and Total Polyphenol Contents

The total polyphenol (TP) concentration, expressed in milligrams of gallic acid equivalents (GAE) per liter of sample [221,222] was measured for the MF, RO, ROp, MD, and MDd fractions, with the results summarized in **Table 14**. Since olive mill wastewater (OMW) composition varies due to factors such as the extraction process, olive cultivar and ripeness, origin, and environmental conditions, the TP content was also assessed in a microfiltration fraction derived from an alternative olive oil production campaign (designated MF2). The gallic acid calibration curve utilized for quantification is depicted in **Figure 50**.

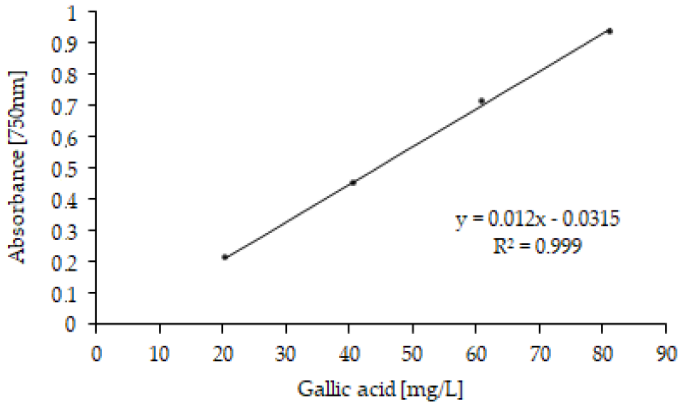

Figure 50. Calibration curve of gallic acid standard solutions over the concentration range of 20 to 80 mg/L.

Table 14. Total phenolic content in OMW samples determined by the Folin–Ciocalteu assay. Data represent mean values ± standard deviation (SD) from three independent replicates (n = 3). Absorbance values are denoted as A. Different superscript letters indicate statistically significant differences at $p < 0.001$ according to Tukey's test.

Sample Name	A (λ = 750 nm)	g GAE/L
MF1	0.188	1.304 ± 0.150^{d}
MF2	0.333	0.251 ± 0.056^{e}
ROP1	0.042	0.001 ± 0.001^{e}
ROP2	0.097	0.055 ± 0.006^{e}
RO1	0.131	8.292 ± 0.251^{b}
MD1	0.110	6.542 ± 0.227^{c}
MD2	0.216	15.375 ± 0.015^{a}
MDd1	0.180	0.012 ± 0.001^{e}
MDd2	0.150	0.010 ± 0.001^{e}

The total polyphenol (TP) content was observed to correlate with the concentration level of the respective fractions, with the MD2 sample exhibiting the greatest polyphenol concentration at 15.38 g GAE/L ($p < 0.001$). A comparable pattern was noted for antioxidant activity (AA%), as reported in **Table 15** and illustrated in **Figure 51**, where the two MD fractions derived from the final vacuum membrane distillation (VMD) purification step demonstrated the highest antioxidant activity values ($p < 0.001$).

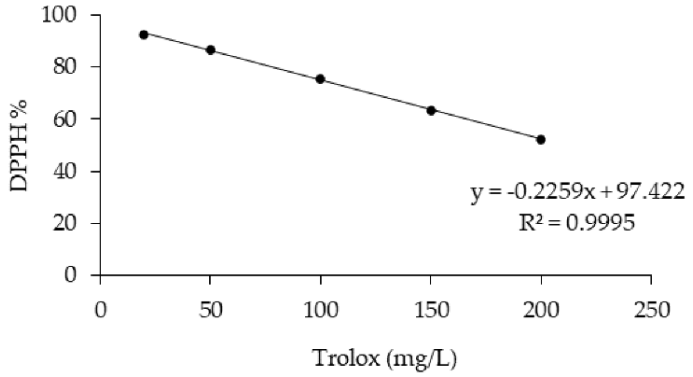

Figure 51. Calibration curve of Trolox standards in the concentration range 20 to 200 mg/L.

Table 15. Antioxidant activity percentage (AA%) measured by the DPPH assay. Values represent mean ± standard deviation (SD) from three independent experiments (n=3). Different superscript letters indicate statistically significant differences at $p < 0.001$ according to Tukey's test.

Sample Name	A (517 nm)	DPPH%	AA%
MF1	0.861	88.95 ± 0.3	11.05 ± 0.3 ^{e}
MF2	0.893	92.25 ± 0.2	7.75 ± 0.2 ^{f}
ROP1	0.898	92.77 ± 0.4	7.23 ± 0.4 ^{f}
ROP2	0.708	73.14 ± 0.1	26.86 ± 0.1 ^{d}
RO1	0.633	65.39 ± 0.2	34.61 ± 0.2 ^{c}
MD1	0.514	53.10 ± 0.2	46.90 ± 0.2 ^{b}
MD2	0.17	17.56 ± 0.3	82.44 ± 0.3 ^{a}
MDd1	0.858	88.64 ± 0.5	11.36 ± 0.5 ^{e}
MDd2	0.864	89.26 ± 0.1	10.74 ± 0.1 ^{e}

Notably, the microfiltration fractions obtained from two distinct olive oil production campaigns (MF1 and MF2) exhibited a statistically significant difference in total polyphenol content ($p < 0.001$), despite displaying comparable levels of antioxidant activity.

Minimal Inhibitory Concentrations and Minimum Bactericidal Concentration

The antibacterial properties of all purified OMW fraction, specifically MF1, RO1, ROp1, ROp2, MD1, MD2, MDd1, and MDd2 (refer to **Table 15**), were initially assessed against a panel comprising twelve bacterial strains. These strains represent a Gram-positive and Gram-negative species with clinical importance. The Gram-positive bacteria included *Staphylococcus aureus* (two strains, one methicillin-sensitive and one methicillin-resistant) and *Staphylococcus epidermidis* (two strains, similarly differentiated by methicillin sensitivity). Among the Gram-negative bacteria, *Enterococcus faecalis* and *Enterococcus faecium* were tested with strains differing in vancomycin susceptibility. Additionally, two strains of *Escherichia coli*, including one harboring New Delhi metallo-β-lactamase (NDM), and two multidrug-resistant (MDR) *Pseudomonas aeruginosa* isolates were included. The results of this initial screening indicated that the ROp1 fraction had no antibacterial activity against all bacteria tested, with minimum inhibitory concentration (MIC) values above 128 mg/mL. In contrast, all other fractions MF1, RO1, ROp2, MD1, MD2, MDd1, and MDd2 showed a good antibacterial activity on selected

strains, with MIC values ranging from 8 to 125 mg/mL (data not shown). Due to its ineffectiveness, ROp1 was excluded from further investigations. The seven active fractions were then tested against a more extensive collection of 39 Gram-positive and Gram-negative clinical isolates, including several multidrug-resistant strains. The evaluation panel was further expanded to include the phytopathogen *Pseudomonas syringae* pv. tomato (see **Tables 16** and **17**). All examined OMW fractions exhibited broad antibacterial efficacy across both antibiotic-susceptible and resistant Gram-positive and Gram-negative species. It is important to note the considerable structural disparities between Gram-negative and Gram-positive bacteria, which have a substantial impact on their divergent antibiotic resistance and susceptibility mechanisms. [223-226].

Among the fractions tested, MD2 showed the most potent antibacterial activity against Gram-positive pathogens and presented the lowest MIC values (8-16 mg/mL) against several Gram-negative strains, including colistin-resistant *Pseudomonas aeruginosa* 265, *Morganella morganii* 372, *Proteus stuartii* 374, and *Serratia marcescens* 400. These pathogens are recognised for their role in causing infections that are clinically significant. Furthermore, all OMW samples exhibited activity against *P. syringae* pv. tomato, which is an important phytopathogen that causes bacterial speck disease in tomatoes. [226]. This pathogen can also infect cruciferous plants, and some strains are pathogenic to the model plant *Arabidopsis thaliana*. Bacterial speck disease is considered one of the most devastating tomato diseases worldwide, characterized by the rapid development of fatty, dark spots on leaves, stems, and fruit, which severely reduce both the quantity and quality of the harvest [227]. Among the fractions tested, MD2 demonstrated the highest efficacy against this phytopathogen, with an MIC of 8 mg/mL and a minimum bactericidal concentration (MBC) of 31 mg/mL.

Table 16. Minimum inhibitory concentration (MIC) and minimum bactericidal concentration (MBC) values (mg/mL) of seven OMW samples against selected Gram-positive bacterial strains. All assays were performed in triplicate, with complete concordance observed (3/3). Variability among replicates was below 10%. ***** denotes a methicillin-resistant *Staphylococcus aureus* (**MRSA)**; **#** denotes a methicillin-resistant *Staphylococcus epidermidis* (**MRSE); °** denotes a vancomycin-resistant enterococci (**VRE**). na: no activity detected in the range of concentrations studied (from 125 to 4 mg/mL).

	MF1		**RO1**		**ROP2**		**MD1**		**MD2**		**MDd1**		**MDd2**	
Strain	**mic**	**mbc**	**mic**	**mbc**	**mic**	**mbc**	**mic**	**mbc**	**mic**	**mbc**	**mic**	**mbc**	**mic**	**mbc**
S. aureus														
17 *	125	na	16	31	125	na	16	31	8	16	125	na	62	na
18 *	125	na	16	31	125	na	16	16	8	16	125	na	62	na
187 *	125	na	31	31	125	na	16	31	8	16	125	na	62	na
188 *	125	na	16	31	125	na	16	16	8	16	125	na	62	na
S. epidermidis														
22#	125	na	16	31	125	na	16	16	8	16	125	na	62	125
180#	62	na	16	16	125	na	16	16	8	16	62	125	62	62
181#	62	na	16	16	125	na	16	16	8	8	125	na	62	125
222#	125	na	16	16	125	na	16	16	16	16	125	na	62	125
E. faecalis														
1°	125	na	16	62	125	na	16	62	16	31	62	na	62	na
4	125	na	16	62	125	na	16	62	16	31	62	na	31	na
50°	125	na	16	62	125	na	16	62	16	31	62	na	62	na
365°	125	na	16	125	125	na	16	125	16	31	62	na	31	na
E. faecium														
21	125	na	16	62	125	na	16	62	16	16	62	na	62	na
40	125	na	16	62	125	na	16	62	16	16	62	na	62	na
300°	125	na	16	62	125	na	16	62	16	16	62	na	62	na
362°	125	na	16	62	125	na	16	62	16	16	62	na	31	na

Table 17. Minimum inhibitory concentration (MIC) and minimum bactericidal concentration (MBC) values (mg/mL) of OMW samples against selected Gram-negative bacterial strains. Experiments were conducted in triplicate with full concordance (3/3). Variation among replicates was less than 10%. **C** indicates colistin resistance; ***** denotes a class A carbapenemase (KPC)-producing strain. na: no activity detected in the range of concentrations studied (from 125 to 4 mg/mL).

	MF1		RO1		ROP2		MD1		MD2		MDd1		MDd2	
Strain	**mic**	**mbc**	**mic**	**mbc**	**mic**	**mbc**	**mic**	**mbc**	**mic**	**mbc**	**mic**	**mbc**	**mic**	**mbc**
P. aeruginosa														
403	62	na	16	31	62	na	16	31	8	16	62	na	31	125
432	62	na	16	31	62	na	16	31	8	16	62	na	31	125
265c	125	na	16	31	125	na	16	31	16	16	62	na	31	125
1	125	na	16	31	125	na	16	31	16	16	62	na	31	125
2v	62	na	16	31	62	na	16	31	8	16	62	na	31	125
19v	125	na	16	31	125	na	16	31	8	16	62	na	31	125
16b	125	na	16	31	125	na	16	31	16	16	62	na	31	125
12b	62	na	16	31	125	na	16	31	8	16	62	na	31	125
8g	125	na	16	31	62	na	16	31	8	16	62	na	31	125
A. baumannii														
245	125	na	16	31	125	na	16	31	16	16	62	125	31	125
M. morganii														
372	125	na	16	31	125	na	16	31	16	31	62	na	31	125
P.														
374	125	na	16	31	125	na	16	31	16	16	62	na	62	125
K. pneumoniae														
375 *	125	na	31	62	125	na	31	62	16	31	62	na	62	125
376 *	62	na	16	62	62	na	16	62	8	31	62	na	62	na
377 *	125	na	31	31	125	na	31	62	16	31	62	na	62	na
S. marcescens														
400	125	na	31	31	125	na	16	31	16	31	62	na	31	125
S. maltophilia														
391	62	na	16	31	62	na	16	31	8	16	62	na	31	125
392	62	na	16	31	62	na	16	31	16	16	62	na	31	125
E. coli														
224	125	na	31	62	125	na	31	62	16	31	62	na	62	na
238 *	125	na	31	62	125	na	31	62	16	31	62	na	62	na
4	125	na	31	62	125	na	31	62	16	31	62	na	62	na
P.														
266	62	na	16	31	62	na	16	31	8	16	62	na	31	125

The difference in antibacterial activity observed among the purified OMW fractions cannot be exclusively attributed to differences in their antioxidant capacities. For instance, the MD2 fraction, which exhibited the highest antibacterial efficacy (MIC range: 8-16 mg/mL), was also characterized by the highest antioxidant activity (AA% = 82.44, **Table 15**). However, both MD1

(AA% = 46.9%) and RO1 (AA% = 34.61%) fractions demonstrated comparable antibacterial effects, with MIC values ranging from 16 to 31 mg/mL, despite their differing antioxidant profiles. Moreover, the ROP2 (AA% = 26.9%) and MDd1 (AA% = 11.36%) fractions showed similar, yet notably lower, antibacterial potency (MIC range: 62-125 mg/mL). Interestingly, the MDd2 fraction, although exhibiting reduced antioxidant activity (AA% = 10.74%), displayed greater antibacterial effectiveness than both ROP2 and MDd1.

Total polyphenol content did not show a direct correlation with antibacterial potency. For example, the RO1 and MD1 fractions, which contain differing levels of polyphenols (TP values of 8.9 and 6.5 g GAE/L, respectively), exhibited similar MIC values (16-31 mg/mL). Notably, the MDd2 sample, despite having a markedly lower total polyphenol content (TP = 0.01 g GAE/L), was comparably effective (MIC range: 31-62 mg/mL) to RO1 and MD1. Furthermore, MDd2 displayed greater antibacterial activity than the ROP2 sample (MIC range: 62-125 mg/mL), which contained a higher polyphenol concentration (TP = 0.05 g GAE/L, **Table 14**).

To exclude the potential influence of residual KCl on antibacterial activity (**Figures 48** and **49**), a 0.5 M KCl solution (equivalent to 40 g/L) was tested against all bacterial strains. The results (data not shown) confirmed that the growth of both Gram-positive and Gram-negative bacteria was not inhibited by potassium ions, even at this high concentration, thus excluding KCl as a contributing factor.

The synergistic interaction among the various components present in the OMW fractions appears to significantly enhance their antibacterial properties, as also evidenced by the minimum bactericidal concentration (MBC) values reported in **Tables 16** and **17**. Among the tested fractions, MD2 demonstrated the most pronounced bactericidal activity against both Gram-positive and Gram-negative species.

Lastly, the methodological approach adopted in this study represents an advancement in the field of OMW research. Unlike most studies, which focus on phenolic extracts or phenol-enriched fractions derived from OMW, this investigation evaluates the antimicrobial potential of the OMW fractions as directly obtained through the purification process [228-230]. Furthermore, literature often lacks quantitative assessment of antibacterial activity, generally reporting only qualitative observations. A notable exception is the work of Roila et al. [231], who quantitatively analyzed the antibacterial effects of OMW derived polyphenol extracts against 65 strains of *Pseudomonas fluorescens*, including ATCC 13525, isolated from mozzarella cheese. The MIC values they reported were consistent with those determined for the MD2 fraction in the present study.

Conclusions

An innovative purification process sequentially combining three membrane-based techniques microfiltration (MF), reverse osmosis (RO), and vacuum membrane distillation (VMD) was employed to isolate and characterize several olive mill wastewater (OMW) fractions. The eight analyzed fractions displayed distinct antioxidant activities and varying total polyphenol contents, which were associated with differences in their qualitative composition, as confirmed by infrared (IR) spectroscopic analysis. The antibacterial potential of the OMW samples considered as whole, non-fractionated mixtures were assessed through quantitative testing. With the exception for the ROp1 fraction, all analyzed samples exhibited significant antibacterial activity against clinically relevant Gram-positive and Gram-negative pathogens, with the MD2 fraction demonstrating the highest efficacy. In addition, the tested fractions proved effective in inhibiting the growth of *P. syringae* pv. tomato, a major seed-transmitted pathogen known to cause bacterial speck disease in tomato plants. Overall, the collected data suggests that OMW represents a valuable byproduct of the olive oil production chain, which can be effectively valorized through appropriate purification strategies. The antibacterial

activity of OMW extracts offers promising perspectives for therapeutic applications in human-related environments, particularly considering that phenolic compounds tend to exhibit greater bioactivity when administered as part of a complex extract than as isolated pure compounds.

Dissemination of Results

The research presented in this section was published as a scientific article in the international peer-reviewed journal Antioxidants (Basel), with the article entitled Valorization and Potential Antimicrobial Use of Olive Mill Wastewater (OMW) from Italian Olive Oil Production [232].

Multifunctional NADES-Based Extracts from *Paeonia lactiflora* Pall. Flowers for Potential Cosmetic and Pharmaceutical Applications

As highlighted in the paragraph Cosmetic valorization of botanical, agri-food waste and ethnobotanical sources, *P. lactiflora* is a perennial herbaceous plant widely renowned for its floral ornamental appeal, distinctive pleasant scent, and utilisation in folk remedies. Roots and barks are traditionally used in Chinese medicine for various properties, including anti-inflammatory, antioxidant, antibacterial, anticancer, cardiovascular, and neuroprotective effects. Considering the growing interest and demand in the pharmaceutical and cosmetic fields for sustainable, and bioactive botanical derivatives, this study aimed to apply NaDES extraction on fresh flowers of *Paeonia lactiflora* Pall. The purpose was to obtain a natural, ready-to-use cosmetic ingredient, with synergistic antioxidant activity, antimicrobial functionalities, and olfactive properties. The eutectic systems investigated in this study consisted of betaine as the hydrogen bond acceptor, combined with glycerol and/or sorbitol as hydrogen bond donors. The extraction process was performed under microwave irradiation, with optimization of key parameters. Gas chromatography-mass spectrometry (GC–MS) analysis was employed to characterize the volatile aromatic components and antimicrobial assays were carried out on the samples against different Gram-positive and Gram-negative strains. In addition, Preliminary long-term studies (up to 9 months) on these combined properties highlighted the stabilizing effect of NaDES on the active metabolites, confirmed their potential as natural and functional ingredients that can be directly incorporated into pharmaceutical and cosmetic formulations, offering enhanced efficacy and improved stability.

Experimental Section

Chemicals

Betaine, sorbitol, glycerine, DPPH (2,2-diphenyl-1-picrylhydrazyl), Trolox (6-hydroxy-2,5,7,8-tetramethylchroman-2-carboxylic acid), Folin–Ciocalteu phenol reagent and gallic acid used as a reference standard were purchased from Sigma-Aldrich (Milan, Italy). Phosphate-buffered saline (PBS, Sigma, Milan, Italy), NaDES solvents were prepared in the laboratory following the heating method of Dai et al. [128]. and by microwave activation (MW) according to the method of Souza et al. [210]. suitably modified. The Milli-Q-system (Millipore SA, Molsheim, France) was used to produce freshly prepared redistilled water. Mueller-Hinton (MH) broth (Merck, Darmstadt, Germany) was used for general bacterial culture. For solid media, Columbia Blood Agar plates, Mannitol Salt Agar, and Mueller-Hinton Agar were purchased from Biolife (Italy). Tryptic Soy Broth (TSB), glucose, phosphate-buffered saline (PBS), and ethanol were obtained from Sigma-Aldrich (Milan, Italy).

Instrumentation

- MW multimode cavity prototype, equipped with a specially designed Pyrex reactor, a magnetron operating at 2.45 GHz, two optical fiber probes for temperature measurement, and a control unit that allows managing different process parameters such as emitted power, temperature setpoint, and mechanical stirring.
- Thermo scientific UV/vis spectrophotometer (Evolution 300, Fischer Scientific, GmbH, Schwerte, Germany*)*.
- Ultrasonic Cleaner Transonic 130 C.R. (*ACAD Pharmaceutical*).
- Microplate reader (Bio-Rad Laboratories S.r.l.).

Plant Material

Fresh flowers of *Paeonia lactiflora* Pall. were collected in May 2024 in Tiglieto, Liguria (Italy; 44°30'04"N, 8°35'43"E), and stored at -20 °C to prevent compound degradation.

Bacterial Strains

The antibacterial activity of the NaDES-based extracts was evaluated against a total of 38 clinically relevant bacterial strains, including 32 Gram-positive isolates and 6 Gram-negative strains. All isolates belonged to a bacterial collection obtained from the School of Medicine and Pharmacy, University of Genoa (Italy), and were identified using either the VITEK® 2 system (BioMérieux, Florence, Italy) or matrix-assisted laser desorption/ionization time-of-flight mass spectrometry (MALDI-TOF MS) (BioMérieux, Florence, Italy). Among the Gram-positive bacteria, 11 strains of *Staphylococcus aureus* were analyzed, including 9 methicillin-resistant strains (MRSA; n°10, 11,18,187, 189, A, B, C and D), 1 reference strain (ATCC 29213), and 1 methicillin-sensitive isolate (strain N2). Additionally, 6 methicillin-resistant *Staphylococcus epidermidis* (MRSE; n°22, 180, 181, 222, 198, 216) strains were included. Nine strains belonging to other *Staphylococcus* species were tested as well, including: *S. saprophyticus* (strain 41), *S. capitis* (strain 71), *S. warneri* (strain 74), *S. simulans* (strain 94), *S. lugdunensis* (strain 115), *S. haemolyticus* (strains 137 and 193), *S. hominis* (strain 124), and *S. auricularis* (strain 136). Except for the *S. saprophyticus* isolate, all strains were methicillin resistant. Regarding the *Enterococcus* genus, three strains belonged to *Enterococcus faecalis*, all of which were vancomycin resistant. One of these strains (strain 1a) also exhibited resistance to teicoplanin. An additional three strains were identified as *Enterococcus faecium*, all of which were resistant to both vancomycin and teicoplanin. Among the Gram-negative bacteria, three *Escherichia coli* strains were included, one of which produced class A *Klebsiella pneumoniae* carbapenemase (KPC), and another producing a New Delhi Metallo-β-lactamase (NDM-type).

The remaining three strains belonged to *Pseudomonas aeruginosa*, including one isolate from a cystic fibrosis patient that was carbapenemase-producing, and one strain that was also resistant to colistin.

NaDES preparation

The natural deep eutectic solvents (NaDES) used for the extraction of peony flowers were prepared by combining betaine as the hydrogen bond acceptor (HBA) with sorbitol and/or glycerol as hydrogen bond donors (HBDs), in appropriate molar ratios. The mixtures were subjected to constant stirring at 70 °C for 5 minutes under microwave (MW) irradiation. The composition and corresponding abbreviations of the NaDES formulations are summarized in **Table 18**.

Table 18. Summarizes the NaDES employed in the extraction of *Paeonia lactiflora* flowers, including their molar ratios, as reported in the literature.

Solvent	NaDES composition	Molar Ratio
BG	Betaine/Glycerol	1:2
BGS	Betaine/Glycerol/Sorbitol	3:2:2

Extractive Conditions

NaDES extractions were performed using a multimode microwave (MW) cavity prototype, the technical specifications of which are detailed in the Instrumentation section. Briefly, 1 g of *Paeonia lactiflora* flowers was mixed with 10 mL of NaDES solvent (PFBG and PFBGS formulations). The samples first underwent ultrasound-assisted extraction (UAE) for 10 minutes, followed by microwave-assisted extraction (MAE) for 5 minutes at a temperature setpoint of 75°C. After centrifugation, the supernatant was collected and analyzed. Total phenolic content (TPC) was quantified using the Folin Ciocalteu method, and the Radical Scavenging Activity (RSA%) was evaluated by the DPPH assay.

The same supernatant was subsequently used for antimicrobial assays, including determination of minimum inhibitory concentrations (MICs), time-kill assay, and biofilm inhibition/disregation.

Total phenolic content

The total phenolic content of each sample was assessed by the Folin-Ciocalteu UV/VIS spectrophotometric method, using gallic acid as the reference standard [178]. TPCs were calculated from a calibration curve obtained from gallic acid standard solutions in concentrations ranging from 20 to 80 mg/ L (R2=0.9988). Values are expressed as mg equivalents of gallic acid per gram of fresh peony petals (mg GAE/g). The results were derived from triplicate analyses of each extract (n=3), normalized against a negative control of the corresponding eutectic solvent, and values are given ± standard deviation (SD).

Radical scavenging activity

The radical scavenging activity of each extract was measured by DPPH assay, based on the bleaching rate of the stable radical 2,2-Diphenyl-1-picrylhydrazyl (DPPH), using Trolox as the reference standard [179], and obtaining a linear calibration curve ranging from 20 to 200 mg/L (R2=0.9952). A total of 0.1 mL of sample was mixed with 3.9 mL of DPPH methanolic solution (65 μM). After mixture storage for 30 min in the dark, absorbance was measured at 516 nm. The results were calculated as Trolox equivalents in solution (mg/L) and the percentage of radical scavenging activity (RSA%) was calculated from the ratio of de-creasing absorbance of sample solution (A_0-A_S) to absorbance of blank DPPH solutions (A_0), as expressed in Equation (1) [181]. Each analysis was performed in triplicate (n = 3) and values are given ± standard deviation (SD)

$$AA\% = \frac{(A0 - As)}{A0} * 100 \qquad (1)$$

Minimal inhibitory concentrations (MICs)

For all samples (PF-BG and PF-BGS) and NaDES solvents, Minimum Inhibitory Concentrations (MICs) were assessed on 38 bacterial strains using the microdilution method, according to the guidelines of the European Committee on Antimicrobial Susceptibility Testing [184]. After overnight incubation, bacteria cultures were diluted to yield a standardized inoculum of 1.5 x 10^8 CFU/mL. Appropriate aliquots of each suspension were added to 96-well microplates containing the same volumes of serial 2-fold dilutions ranging respectively, from 231.5 mg/mL to 0.455 mg/mL for PF-BG and from 230.5 mg/mL to 0.455 mg/mL for PF-BGS to achieve a final bacterial concentration of about 5×10^5 cells/mL. The pure NaDES employed (BG, and BGS) were also assessed to evaluate the possible antibacterial activity of the solvents themselves. After 24 h incubation at 37°C, the MIC values were determined as the lowest concentration that inhibited visible bacterial growth in the wells, compared with the compound-free control, expressed in mg/mL. All tests were performed as three independent experiments, each carried out in triplicate and MICs values were expressed as median/modal values.

Time-killing curves

Time-kill assays for the most active sample (PFBG) were conducted using a selected MRSA isolate (18, B, and ATCC29213). Briefly, a mid-log-phase bacterial culture was diluted in 10 mL of Mueller Hinton broth (MH) containing 4×MIC of the sample, resulting in a final inoculum of 3.0×10^5 CFU/mL The same inoculum was added to MH broth without the sample to serve as growth control. Tubes were incubated at 37 °C with constant shaking for 24 hours. At 0, 2, 4, 6, and 24 hours, 0.20 mL aliquots were withdrawn from each tube, appropriately diluted with 0.9% sodium chloride solution to prevent carryover of the tested compounds, plated onto MH agar plates, and incubated for 24 hours at 37 °C. Growth controls were processed in parallel. The percentage of surviving bacterial cells at each time point was

determined by comparing colony counts to those of the growth control. Results are expressed as $\log_{10}$ CFU/mL of viable cells over the 24-hour period. All experiments to define the time-kill curves for each strain were performed in triplicate.

Biofilm inhibition

The ability of the PFBG sample to inhibit biofilm formation was evaluated against seven selected *S. aureus* strains (B, 10, 11, 18, 189, ATCC 29213, and N2) using a crystal violet (CV) assay, as described by Cramton et al. [187]. After overnight incubation in fresh TSB supplemented with 0.25% glucose, bacterial cell suspensions were adjusted to a turbidity equivalent to 0.5 McFarland standard and subsequently diluted to a final concentration of approximately 1×10^5 CFU/mL in TSB. Aliquots of 200 µL of the diluted suspension were transferred into the wells of flat-bottomed 96-well polystyrene microtiter plates, and various concentrations of PF-BG (corresponding to ¼ MIC, ½ MIC, and MIC) were added. Untreated bacterial cultures served as the control group. In parallel, the NaDES BG solvent was tested under the same conditions to assess its individual effect on biofilm inhibition. After 24 hours of incubation at 37°C, the culture supernatants were carefully removed, and the wells were washed three times with phosphate-buffered saline (PBS). Once dry, 60 µL of 0.1% crystal violet solution were added to each well. Following 20 minutes of incubation, the wells were washed three times with PBS to remove excess dye, leaving only the stained biofilm. The retained stain was then solubilized with 200 µL of ethanol. The UV absorbance was measured with a microtiter plate reader at 570 nm, and the blank value, corresponding to the absorbance of TSBg treated wells with CV and ethanol, was subtracted from all readings. The percentage residual (RT) of biofilm growth was calculated using the formula:

$$(At / Ac) \times 100$$

where Ac is the absorbance measured for the control wells and At is the absorbance measured in the presence of PF-BG extract. The percentage of inhibition growth is thus obtained as:

$$100 – RT$$

Biofilm Degradation

The ability of the PFBG sample to disrupt pre-formed biofilms was evaluated against three selected *S. aureus* strains (B, 18, and ATCC 29213), using a method previously described by Vollaro et al. [186]. Briefly, after overnight incubation in fresh TSB supplemented with 0.25% glucose (TSBg), bacterial cell suspensions were adjusted to a turbidity equivalent to 0.5 McFarland standard and subsequently diluted to a final concentration of approximately 1×10^5 CFU/mL in TSBg. Aliquots of 200 µL of the diluted suspension were transferred into the wells of flat-bottomed 96-well polystyrene microtiter plates. After 24 hours of incubation, the culture supernatants were gently removed, and the wells were washed with phosphate-buffered saline (PBS). The adherent bacterial cells were then exposed to 200 µL of PBS solution containing PF-BG at concentrations of 5×MIC and 10×MIC. The plates were incubated for an additional 24 hours at 37°C. Untreated bacterial cultures were used as the control group. Biofilm biomass was assessed using crystal violet staining, following the same procedure described for the biofilm formation inhibition assay. The BG solvent was tested in parallel under the same conditions applied to the PF-BG sample. The UV absorbance was measured with a microtiter plate reader at 570 nm, and the blank value, corresponding to the absorbance of TSBg treated wells with CV and ethanol, was subtracted from all readings. The percentage residual (RT) of biofilm growth was calculated using the formula:

$$(At / Ac) \times 100$$

where Ac is the absorbance measured for the control wells and At is the absorbance measured in the presence of PF-BG extract.

percentage of inhibition growth is thus obtained as:

$$100 - RT$$

GC-MS analysis

NaDES samples (1g) were diluted with 1.2 mL of ultrapure water, then extracted with n-hexane (3 x 1 mL). The organic phase was dried over anhydrous Na_2SO_4 and completely evaporated using a gentle N2 stream at room temperature. The residue was dissolved in 50 µl of n-hexane before analysis. The analyses were carried out using a GC Model 6890N, coupled to a benchtop MS Agilent 5973 Network, (Agilent, Santa Clara, CA, USA). Chromatographic separation was performed using an Elite-5MS (5% phenyl methyl polysiloxane) capillary column of (30 m × 0.32 mm i.d.) and film 0.32 µm thick (Agilent, Santa Clara, CA, USA). One µL aliquot of each sample was manually injected in splitless mode [233]. The oven temperature program included an initial isotherm at 40 °C for 5 min, followed by a temperature ramp to 260 °C at 40 °C/min, and a final isotherm at 260 °C for 10 min. Injector and detector temperatures were set at 250°C and 280°C, respectively. Mass spectra were acquired over 40-400 amu range at 1 scan/sec with an ionizing electron energy of 70 eV. The identification of the volatile compounds was performed using retention indices (RI) and mass spectra according to Adams [203] by comparison with online published data [204], and with a NIST database mass spectral library [234]. The relative amount of each component was expressed as a percentage of the total peak area from GC/MS analyses of the whole extract.

Preliminary long-term studies

To assess the ability of eutectic solvents to preserve the properties of the extract over time [235], and to evaluate the potential of the NaDES-based extract as a multifunctional ingredient, a preliminary long-term stability study was conducted on PF-BG sample. Consequently, instrumental analyses were repeated in regard to the Folin-Ciocalteu and the DPPH assay, in

accordance with the procedures previously outlined, after 90 days (t90) and up to 9 months (t180). The antibacterial activity was then re-evaluated after a period of 90 days by determining the MIC.

Statistical Analysis

Microbiological analyses were assessed in triplicate, and data were subjected to analysis of variance (ANOVA) using GraphPad Prism version 8.0.0 for Windows, GraphPad Software, San Diego, CA, USA. Wherever F values were significant, the Tukey test was used for means comparison. Significance was defined at $p < 0.001$.

Results and Discussion

MW NaDES extraction

Following a previously published MW procedure [202], two extracts (PF-BG, PF-BGS) were obtained, from the corresponding NaDES solvents (BG and BGS), within five minutes, after a simple filtration, from fresh flowers of *P. lactiflora*. Considering solvents and peony metabolites extracted as a synergic bioactive complex, the NaDES-based samples were directly analyzed and used without the need to isolate the extracted molecules.

The polarity of the NaDES components, when combined with the dielectric heating of microwave irradiation, resulted in the swift attainment and sustenance of the target process temperature setpoint (75°C). This occurrence transpired within a time frame of merely 10-15 seconds. The constant temperature was then maintained through power modulation within the range of 0-300 watts. An inherent continuous feedback mechanism within the MW prototype meticulously controlled this process, thereby preventing overheating and the subsequent thermal degradation of the botanical matrix and extracts.

Total Phenolic Content (TPC) and Radical Scavenging Activity (RSA%)

Table 19 summarizes the results related to the total phenolic content (TPC) and percentage of radical scavenging activity (RSA%) for the NaDES-based extracts obtained. Both samples (PF-BG, PF-BGS) demonstrated strong and stable antioxidant activity (around 87%), consistent with the corresponding TPC values, expressed as milligrams of gallic acid equivalents for gram (mg GAE/g) of fresh leaves (34.38 and 33.78 mg GAE/g for PF-BG and PF-BGS, respectively).

To exclude the possibility of interferences by the eutectic mixtures in the estimation of the total phenolic content, the Folin Ciocalteu method was slightly modified, using the eutectic extraction solvent in the blank preparation.

Table 19. Total phenolic content (TPC) and radical scavenging activity (RSA%) of NaDES samples (PF-BG, PF-BGS) by means of DPPH (2,2-Diphenyl-1-picrylhydrazyl) and Folin–Ciocalteu assays (mean value ± standard deviation SD) of three independent experiments (n = 3).

NaDES Sample	TPC (mg GAE/g ± SD)	RSA % (± SD)
PF-BG	34.38 ± 0.03	87.50 ± 0.06
PF-BGS	33.78 ± 0.02	86.98 ± 0.06

Minimal Inhibitory Concentrations (MICs)

The antibacterial activity of the NaDES-based extracts (PF-BG and PF-BGS) and the corresponding eutectic solvents (BG and BGS) were evaluated by calculating the Minimal Inhibitory Concentrations (MICs), against 38 bacterial isolates, according to the guidelines of the European Committee on Antimicrobial Susceptibility Testing (EUCAST) [184]. Both samples disclosed variable levels of activity against all the Gram-positive species considered, while they resulted inactive against all Gram-negative strains tested (data not shown).

Table 20 presents the MIC values of both NaDES-based samples PF-BG and PF-BGS, assessed against all the susceptible species considered. PF-BG seems to have a general, greater antibacterial potency and a broader spectrum of activity, when compared to PF-BGS. As regards

S. aureus, MIC values of PF-BG fall within a range from 7.2 to 14.4 mg/mL (PF-BGS: from 14.4 to 57.6 mg/mL) and in case of *S. epidermidis* from 3.6 to 7.2 mg/mL (PF-BGS: from 14.4 to 28.8 mg/mL). Even in the comparative study of the coagulase-negative species, sample PF-BG performs better than PF-BGS with MIC values from 0.9 to 14.4 mg/mL (PF- BGS from 7.2 to 57.6 mg/mL). The most sensitive species to this NaDES-based extract were found to be *S. saprophyticus*, *S. warneri*, *S. hominis* and *S. auricularis* (MIC 0.9 mg/mL), followed by *S. capitis* (MIC 1.8 mg/mL), *S. simulans* (MIC 7.2 mg/mL), *S. lugdunensis* and *S. haemolyticus* (MIC 14.4 mg/mL). Moreover PF-BG shows a lower but meaningful performance against the Enterococcus genus (28.8 mg/mL, against *E. faecalis*, 57.6 mg/mL against *E. faecium* isolates) while PF-BGS sample seems to be inactive. Neither NaDES solvent BG nor BGS displayed any activity across the entire range of concentrations studied.

Table 20. Minimal Inhibitory Concentrations (MICs) expressed as mg/mL of NaDES solvents (BG, BGS) and NaDES-based extracts (PF-BG PF-BGS) against Gram-positive bacterial species. Experiments were carried out in triplicate. The degree of concordance in all the experiments was 3/3. Variation among triplicate samples was less than 10%.

Bacterial species	**Strain**	**MIC (mg/mL)**			
		BG	**PF-BG**	**BGS**	**PF-BGS**
S. aureus	10*	-	7.2	-	28.8
	11*	-	7.2	-	28.8
	18 *	-	7.2	-	57.6
	187 *	-	7.2	-	14.4
	189 *	-	7.2	-	28.8
	A*	-	14.5	-	28.8
	B*	-	14.5	-	28.8
	C*	-	14.5	-	14.4
	D*	-	14.5	-	14.4
	N2	-	7.2	-	28.8
	ATTC 29213	-	7.2	-	14.4
S. epidermidis	22 *	-	7.2	-	28.8
	180 * §	-	3.6	-	28.8
	181* §	-	3.6	-	14.4
	222 * §	-	3.6	-	28.8
	198* §	-	7.2	-	14.4
	216* §	-	7.2	-	14.4
S. coagulase negative	*S. saprophyticus 41*	-	0.9	-	7.2
	*S. capitis 71**	-	1.8	-	7.2
	*S. warneri 74**	-	0.9	-	7.2
	*S. simulans 94**	-	7.2	-	28.8
	*S. lugdunensis 115**	-	14.4	-	57.6
	*S. haemolyticus 137**	-	14.4	-	57.6
	*S. haemolyticus 193**	-	14.4	-	28.8
	*S. hominis 124**	-	0.9	-	7.2
	*S. auricularis 136**	-	0.9	-	3.6
E. faecalis	1a^{vt}	-	28.8	-	-
	365^{v}	-	28.8	-	-
	431^{v}	-	28.9	-	-
E. faecium	*185*^{vt}	-	57.8	-	-
	186^{vt}	-	57.8	-	-
	300^{vt}	-	57.8	-	-

* = methicillin resistance; § = linezolid resistance, v = vancomycin resistance; t = teicoplanin resistance; V = vancomycin resistance; T = teicoplanin resistance.

In view of the results obtained, disclosing the optimum level of activity of PF-BG, this sample was selected for further investigations, to ascertain the extent of its antimicrobial efficiency.

Time-Kill test

To determine the antibacterial mechanism of action of the extract, time-kill assays were performed on S. aureus, as the most clinically relevant species. For this purpose, bactericidal curves were obtained, studying three selected strains (18, B, and ATCC 29213), at a concentration four times higher than the MIC, for 24 hours. All strains, despite displaying different resistance phenotypes, showed overlapping results, exemplified in **Figure 52** by the 18 MRSA strain. As shown, strain treatment with PF-BG revealed the extract's bacteriostatic activity at 24 hours, essentially maintaining the bacterial load of the initial inoculum, after a slight reduction in the initial bacterial concentration during the first 6 hours.

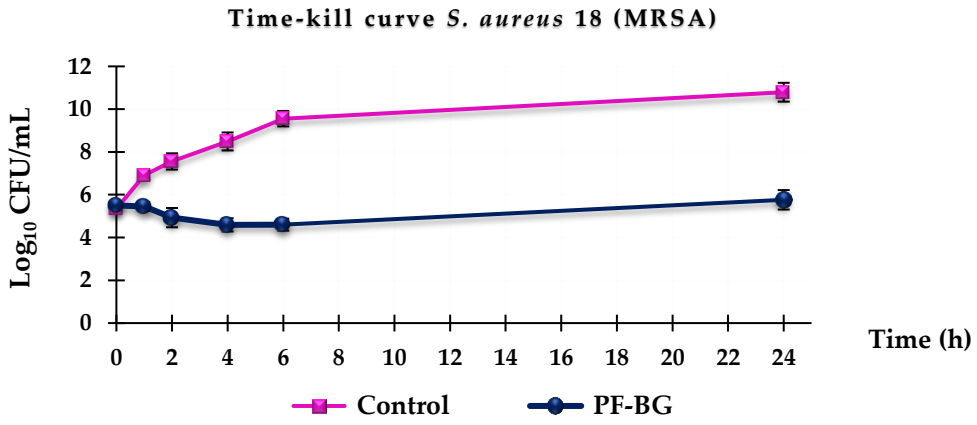

Figure 52. Time-kill curve for PF-BG performed at a concentration of 4xMIC on *S. aureus* 18 (MRSA) across 24 hours test.

Biofilm inhibition/degradation

The potential of PF-BG sample in preventing the biofilm formation by *S. aureus* was subsequently assessed, according to Cramton et al. [187], on seven selected clinical and reference strains, namely B, 10, 11,18, 189, N2, and ATCC 29213.

Assuming a potential cosmetic use of the PF-BG extract as preservant against Gram-positive strains, its inhibitory potency was compared with that of Sodium de-hydroacetate (SDA), a

broad-spectrum antimicrobial agent against bacteria, yeasts, and molds, authorized by the European Cosmetics Regulation 1223/09 as a preserving ingredient (Annex 5, reference n. 13) at a maximum concentration of 0.6% [236].

For the determination of SDA biofilm inhibition, the MIC values of SDA against the 7 selected *S. aureus* strains (required for carrying on the experiments) were previously assessed (**Table 21**).

Table 21. Minimal Inhibitory Concentrations of SDA, expressed as mg/mL, against selected S. aureus strains. Experiments were carried out in triplicate. The degree of concordance in all the experiments was 3/3. Variation among triplicate samples was less than 10%.

Species	***Strain***	**MIC (mg/mL)**
S. aureus	10*	3.8
	11*	7.6
	18*	3.8
	189*	7.6
	B*	7.6
	N2	7.6
	ATTC 29213	7.6

* = methicillin resistance

Results are reported in **Figures 54-55** and **Table 22-23**.

Figures 53 and **54** display the results related to the quantified biofilm biomass formation obtained by the Cristal violet assay [187]. Data are expressed as the optical density (OD) of each well stained with crystal violet, measured at 570 nm using a microplate reader.

The OD of each selected strain containing 3 different PF-BG and SDA concentrations (1/4 MIC, 1/2 MIC and MIC) respectively, in comparison to the control (strain without sample) are reported. In **Table 23** the corresponding inhibition percentages for each strain under the various tested conditions are reported.

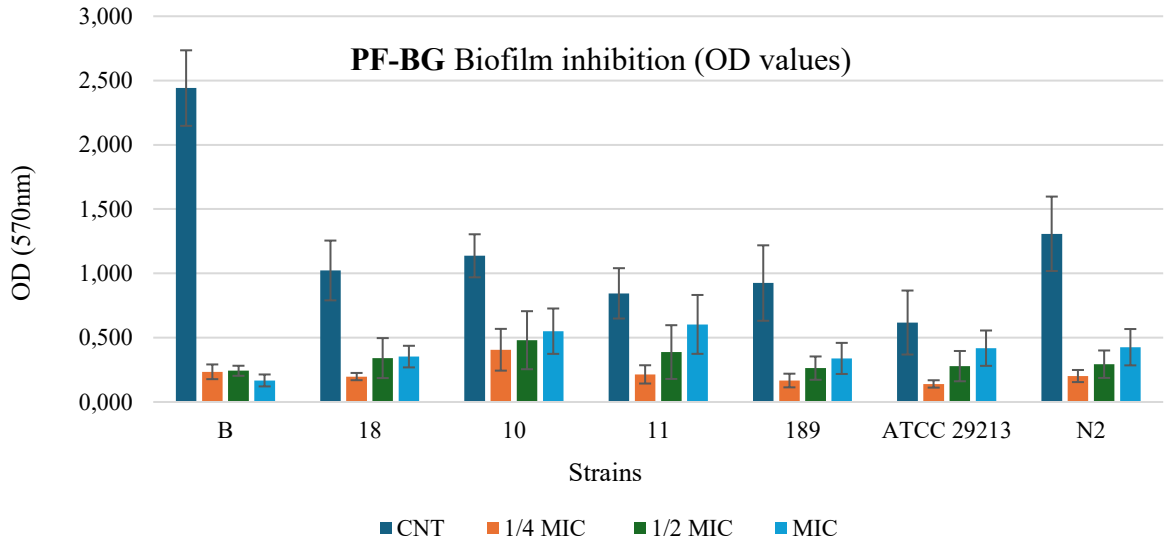

Figure 53. Inhibitory effect of **PF-BG** in the biofilm formation assay on different strains of *S. aureus* obtained by the crystal violet (CV) method. Biofilm biomass was quantified by measuring the optical density (OD) of the CV after its solubilization in ethanol at 570 nm. Treatments include an untreated control (CNT, blue), MIC (yellow), 1/4 MIC (orange), and 1/2 MIC (grey). Data are reported as mean value of four independent experiments (n = 4).

Regarding PF-BG, for all strains, the CNT sample is significantly different from 1/4 MIC 1/2 MIC and MIC ($p<0.001$). For strain 11, there is also a significant difference for 1/4 MIC vs MIC and for 1/2 MIC vs MIC. For strain AT20213, there is also a significant difference for 1/4 MIC vs MIC.

Table 22. Inhibition percentage of biofilm formation (±SD) at different concentration **(**1/4 MIC. 1/2 MIC and MIC) of **PF-BG**

***S. aureus* strain**	**% Inhibition of Biofilm Formation**			
	Control	**1/4 MIC**	**1/2 MIC**	**MIC**
B*	100	90.4 ± 2.1	90.1 ± 1.8	93.1 ± 1.8
18*	100	80.7 ± 4.2	66.6 ± 9.1	65.5 ± 5.2
10*	100	64.3 ± 13.1	57.7 ± 18.0	51.6 ± 17.3
11*	100	74.6 ± 6.4	54.1 ± 24.8	28.6 ± 27.4
189*	100	81.9 ± 4.6	71.5 ± 9.0	63.4 ± 12.0
ATCC 29213	100	77.3 ± 10.4	54.9 ±10.4	32.3 ± 21.6
N2	100	84.6 ± 3.9	77.5 ± 11.1	67.4 ± 14.6

* = methicillin resistance

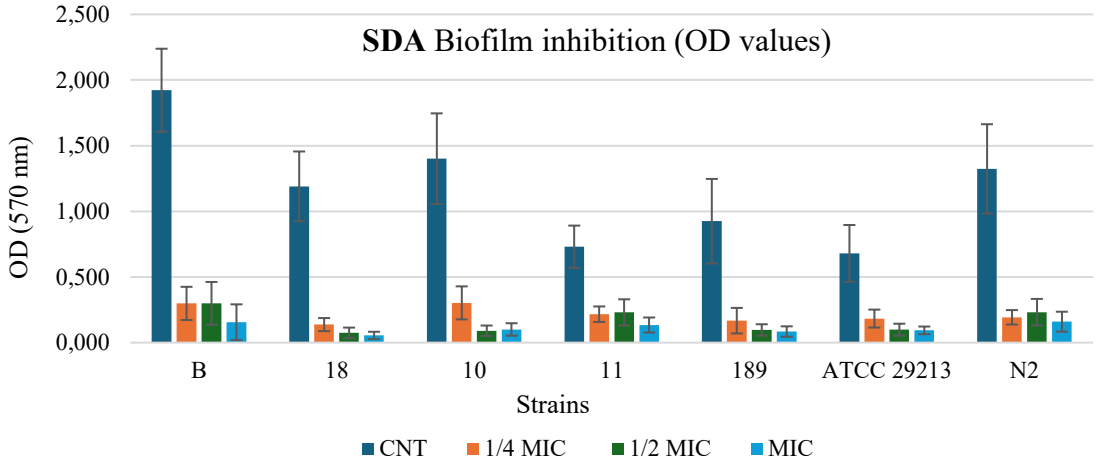

Figure 54. Inhibitory effect of **SDA** in the biofilm formation assay on different strains of *S. aureus* obtained by the crystal violet (CV) method. Biofilm biomass was quantified by measuring the optical density (OD) of the CV after its solubilization in ethanol at 570 nm. Treatments include an untreated control (CNT, blue), MIC (yellow), 1/4 MIC (orange), and 1/2 MIC (grey). Data are reported as mean value of four independent experiments (n = 4).

Regarding SDA, for all strains, the CNT sample is significantly different from 1/4 MIC 1/2 MIC and MIC ($p<0.001$); for all strains 1/4 MIC 1/2 MIC and MI are not significantly different.

Table 23. Inhibition percentage of biofilm formation at different concentration **(**1/4 MIC ½ MIC and MIC) of **SDA**.

S. aureus **strains**	**% Inhibition of Biofilm Formation**			
	Control	**1/4 MIC**	**1/2 MIC**	**MIC**
B*	100	84.5 ± 9.9	84.5 ± 10.3	92.0 ± 8.9
18*	100	88.5 ± 4.7	93.7 ± 2.5	95.4 ± 1.2
10*	100	78.5 ± 10.0	93.6 ± 2.9	92.9 ± 4.1
11*	100	70.4 ± 12.1	68.5 ± 17.5	81.7 ± 5.9
189*	100	81.9 ± 15.9	89.6 ± 7.0	90.9 ± 4.2
ATCC 29213	100	73.1 ± 12.0	85.5 ± 6.5	86.3 ± 4.3
N2	100	85.4 ± 6.9	82.5 ± 8.7	87.9 ± 4.0

* = Methicillin resistance-

PF-BG sample demonstrated the capacity to inhibit biofilm formation across all analyzed *S. aureus* strains, notably even at concentrations below the MIC. In particular, strain B, an excellent biofilm producer, showed a remarkable reduction in biofilm formation in the presence

of PF-BG, an effect that was very similar across the three tested concentrations, with an inhibition percentage ranging between 90 and 93%. This behavior differs from those observed for the remaining six strains analyzed, for which a decrease in inhibitory capacity is observed as the concentration of PF-BG increases. For these strains, inhibition at ¼ MIC ranged between 64% (strain 10) and 85% (strain N2), at ½ MIC between 54% (strain 11) and 76% (strain N2), and at MIC between 29% (strain 11) and 67% (strain N2). Therefore, along with the heterogeneous ability of the different strains to produce biofilm, susceptibility to the PF-BG extract was also found to be strain-dependent, with isolate B being very susceptible, strains 18, 189, and N2 showing intermediate susceptibility, and the remaining isolates, 10, 11, and ATCC29213, showing lower sensitivity. Identical concentrations of the solvent BG, when tested on the same strains of *S. aureus*, proved completely ineffective in inhibiting biofilm formation (data not shown).

As reported in **Figure 54** SDA compound, characterized by MIC values comparable to those of PF-BG, demonstrated a slightly better antibiofilm potency than the NaDES-based extract, and, also in this case, heterogeneous among the different strains tested. In particular, inhibition at 1/4 MIC ranged between 70 and 89%, between 69 and 94% at 1/2 MIC, and between 82 and 96% at MIC concentrations. Although at MIC values, SDA has shown greater effectiveness in reducing biofilm formation by the strains considered compared to PF-BG, it is certainly noteworthy that at sub-MIC values, particularly at 1/4 MIC, the antibiofilm potency of PF-BG and SDA is essentially comparable. The ability of PF-BG to disrupt mature biofilms was also tested at 5xMIC and 10×MIC on three different strains. No significant disruption was observed, confirming the resilience of mature biofilms.

The microbiological evaluation of the NaDES-based extracts PF-BG and PF-BGS revealed their promising antibacterial properties against various Gram-positive multi resistant strains of species belonging to the genera Staphylococcus, including MRSA and MRSE isolates, and

Enterococcus ones. Although the Total Phenolic Content (TPC) and the Radical Scavenging Activity (RSA%) of both NaDES-based extracts were comparable, the PF-BG sample showed superior efficacy compared to PF-BGS in terms of minimum inhibitory concentrations (MIC values for PF-BG were consistently lower than those of PF-BGS) and a broader spectrum of action, being active even against two enterococcal species such as *E. faecalis* and *E. faecium*. Noteworthy is the fact that both extracts, although with different potencies, showed excellent activity also against a wide number of coagulase-negative Staphylococcus species, with MICs up to 0.91 mg/mL for S. saprophyticus, S. warneri, S. hominis, and S. auricularis. Neither PF-BG nor PF-BGS showed activity against Gram-negative strains included in this study. This limitation is consistent with the intrinsic resistance mechanisms of Gram-negative bacteria, mainly due to the presence of the outer membrane, an extremely impermeable structure that can hinder the penetration or retention of NaDES-based hydrophilic compounds. For the above-mentioned reasons, and due to the lower viscosity of the PF-BG sample compared to PF-BGS, which makes it easier to handle, further microbiological studies were conducted only on the former extract. Time-kill kinetics, subsequently performed on selected MRSA strains, confirmed the bacteriostatic nature of PF-BG, capable of maintaining the initial bacterial inoculum stable for 24 hours. This suggests that PF-BG at 4×MIC may inhibit bacterial proliferation without inducing cell lysis, a property that could be advantageous in reducing inflammatory responses in potential topical applications. The NaDES based extract also inhibited biofilm formation in all tested selected S. aureus strains. This inhibition was particularly consistent (90-93%) at the various concentrations tested for strain B, an excellent biofilm producer whose MIC was higher than those of the remaining strains, for which, the biofilm inhibition tendency was different and variable. In fact, for the remaining six strains, inhibition ranged from 64% to 85% at ¼ MIC and decreased at higher MIC concentrations (inhibition between 29% and 67%). This behavior could suggest a possible hormetic effect of

the sample, a biphasic dose-response in which low amounts induce a stronger biological response compared to higher doses, which may instead reduce efficacy by triggering stress adaptation. This inverse trend in the dose response, observed in different strains, might reflect complex mechanisms of interaction between the components of PF-BG and the regulatory pathways of biofilm, potentially involving disruption of quorum sensing or interference with the synthesis of extracellular polymeric substance, which is crucial for biofilm formation. The strain-dependent variability in response further highlights the need for mechanistic studies to clarify the molecular targets of PF-BG. The comparative analysis with sodium dehydroacetate (SDA), revealed that the NaDES-based extract possesses antibiofilm activity comparable to that of the preservative at sub-MIC levels (1/4 MIC). This outcome is of pertinence when considering the comparison of a pure molecule with a natural complex consisting of a solvent (NaDES) and extracted active metabolites. Therefore, although SDA was slightly more effective at MIC concentrations, the similar performance of PF-BG at lower dosages highlights its potential as a natural alternative for cosmetic applications, especially when biofilm control is critical.

GC-MS analysis

The GC-MS of the volatile fraction of PF-BG, the most promising sample, was performed as a preliminary analysis, to verify and attribute the scented character of the NaDES-based extract. Among several volatile compounds, here not reported, three typical and characteristic terpenoids, commonly used as fragrances, were isolated and identified: a monocyclic monoterpene (d-limonene, 0.02%) and two oxygenate derivatives (2-phenylethanol, and Citronellol, 0.62% and 0.15% respectively). Analytical results and olfactive characters are reported in **Table 24**.

Table 24. retention indices, relative percentage, identification method and olfactive description of the aromatic compounds of interest.

Compound[a]	RI[b]	RI[c]	Mean % (± SD)	Identif. Method[d]	Olfactive description
Limonene	1014	1015	0.02 ± 0.08	NIST, RI	lemon, orange
2-phenylethanol	1139	1139	0.62 ± 0.12	NIST, RI	honey, spice, rose, lilac
Citronellol	1230	1229	0.15 ± 0.09	NIST, RI	rose

[a]Compounds listed in order of their elution on an Elite-5 column. [b]RI = Retention Indices according to Adams [203] and with online published data [204]. [c] RI = Retention Indices determined on an Elite-5 column using a homologous series of n-hydrocarbons [234]. [d]Method of identification: NIST = National Institute of Standards and Technology database library [205] ; RI = Retention Indices, in agreement with literature values [203,204].

Regarding GC-MS analysis, as might be expected, the number of scented volatile compounds, was very low. Only limonene, 2-phenylethanol and citronellol were detected in the NaDES extract. Nonetheless, their presence gives an interesting olfactive contribution to the sample, for a pleasant and distinctive fragrance.

Preliminary long stability studies

Long-term stability studies conducted on PF-BG (TPC, RSA, MIC) demonstrated good chemical and microbiological stability of the potential NaDES-based ingredient after 90 days (t90) and up to 9 months (t180). The antibacterial activity was then re-evaluated after a period of 90 days by determining the MIC (Minimum Inhibitory Concentration) on selected bacterial strains of S. *aureus, S. epidermidis, E. faecalis, and E. faecium*, according to the protocol described above. The results of the study are set out in **Tables 25** and **26**.

Table 25. TPC and RSA% values of **PF-BG** sample after 90 days (t_{90}) and 9 months (t_{180}). The initial value (t_0) is also reported for comparison. Mean values (n=3) ± standard deviation (SD).

PF-BG	TPC (mg GAE/g ± SD)	RSA % (± SD)
$\mathbf{t_0}$	34.38 ± 0.03	87.50 ± 0.06
$\mathbf{t_{90d}}$	34.31 ± 0.05	87.30 ± 0.03
$\mathbf{t_{180}}$	32.75 ± 0.02	85.80 ± 0.04

Table 26. MIC values for the PF-BG sample at time zero (t_0) and after 90 days (t90).

Strain	**MIC t_0**	**MIC t_{90}**
S. aureus 18*	7.2	7.2
S. epidermidis 22*	7.2	7.2
E. *faecalis* 1°	14.4	14.4
E. faecium 185°	28.8	28.8

*Resistance to methicillin, ° resistance to vancomycin and teicoplanin

The PF-BG sample evaluated after 90 days and after 9 months retained its properties, as stated by the TPC and RSA% values, comparable to the initial values. Furthermore, the extracts analyzed after 90 days showed stability, maintaining constant antibacterial activity against the strains analyzed.

Preliminary long-term stability studies have highlighted the ability of NaDES solvents to act as metabolite stabilizers; this has allowed the PF-BG sample to maintain its antibacterial capacity even after 90 days and to retain its antioxidant properties for up to 9 months.

The observed chemical and biological stability are closely aligned with the visual evaluation results. **Figure 55** provides a visual assessment of the stabilizing effect of NaDES solvents, comparing the long-term integrity of the peony matrix in the NaDES-based solvent (BG) versus water.

A significant degradation and microbial contamination (mould presence) was observed in the water sample after 5 days of storage. BG sample showed only a discrete colour change (without mould formation), after 180 days, confirming the potential of NaDES in preserving the matrix unaltered during time.

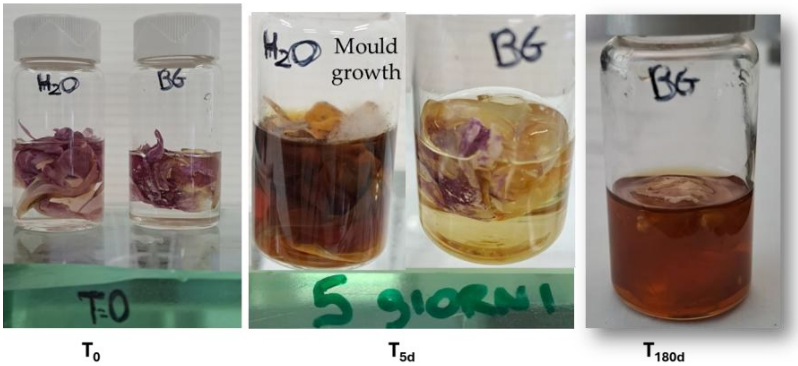

Figure 55. Visual comparison of NaDES BG and water samples after the maceration process.

These results indicate that the NaDES-based extract could be applied as a ready-to-use ingredient, with synergistic functionality, exploiting the well-known intrinsic cosmetic properties of the NaDES components together with the biological properties of the active compounds.

Conclusions

The extractive process applied can be considered sustainable, adhering to several principles of green extraction, considering the use of alternative natural solvents (NaDES), an alternative energetic source (microwave activation) and a renewable and recycled natural source (*Lactiflora pall* flowers). The HBA and HBD selected for the extractive procedure (betaine, glycerol and sorbitol) give rise to eutectic systems characterised by good stability, safety and intrinsic dermo cosmetic properties, in addition to their high extraction efficiency. The final extract complexes obtained, consisting of the active metabolites of the plant and NaDES itself, were then easily evaluated in their entirety as potential ready-to use ingredients, assessing antioxidant and antimicrobial properties. By this way, NaDES extracts could be directly enclosed in the final products, avoiding further purification steps and increasing the naturalness and performance of the formulations.

Dissemination of Results

During my PhD, the manuscript entitled Multifunctional NADES-Based Extracts from *Paeonia lactiflora* Pall. Flowers for Potential Cosmetic and Pharmaceutical Applications was under submission. At the end of the doctoral program, it was accepted and subsequently published in the international peer-reviewed journal *Molecules* [Villa, C.; Russo, E.; Schito, A.M.; Robustelli della Cuna, F.S.; Sottani, C.; Barabino, M.; Caviglia, D. Multifunctional NADES-Based Extracts from *Paeonia lactiflora* Pall. Flowers for Potential Cosmetic and Pharmaceutical Applications. *Molecules* **2026**, *31*(1), 97. https://doi.org/10.3390/molecules31010097].

Preliminary studies on Tocosh flour (*solanum tuberosum* L.) properties for potential pharmaceutical and cosmetic applications.

In Latin American tradition, food fermentation represented an efficient strategy to preserve native crops to maintain adequate stocks for survival. In particular, potato Tocosh is an ancestral fermented flour still prepared in small communities from the highlands of Central Peruvian Andes. The aim of this research was to investigate Tocosh as a new potential pharmaceutical and cosmetic multifunctional ingredient with rheological, antioxidant and preservation properties. With this purpose, the product was analysed and characterized, with regard to the volatile fraction, by GC-MS analysis, (responsible for the odor), amylose content and gelling behaviour (in comparison to potato starch), polyphenolic amount, radical scavenging activity and antimicrobial properties. Furthermore, to enhance the suitability of the product for dermocosmetic applications, a simple preliminary treatment was attempted to neutralize its stinky odor, by exploiting Fischer esterification.

Experimental Section

Gelling properties

Regarding the study of the rheological properties of Tocosh, different evaluations were carried out in comparison with commercial potato starch. Parameters such as the amylose-amylopectin ratio, water-binding capacity (WBC) and viscosity in aqueous media were taken into consideration.

Amylose/amylopectine ratio determination

UV spectroscopic analysis [237] using Lugol reagent was performed on both Tocosh and starch (S) samples. The percentage of amylose to total starch can be determined from absorbances (A)

at 620 and 550 nanometers (corresponding to amylose and amylopectin peak wavelengths respectively) as follows:

$$\text{Amylose \%} = 107{,}7 \times B - 77{,}4$$

where B = A620nm/A550nm, against the reagent blank

Water-Binding Capacity (WBC) and rheological behaviour

A suspension of 5 g of Tocosh and starch respectively, in 75 mL water, was stirred for 1 h at 60°C [238]. After centrifugation, free water was removed from the wet samples and drained for 10 min. WBC was calculated using the following formula:

$$WBC\ (\%) = (W2 - W1)/W1 \times 100\%$$

Where W1 and W2 correspond to the weight of original samples and wet gel, respectively.

Viscosity

The viscosity of the prepared gels was determined using a Brookfield rotational viscometer (Viscostar model). Samples of 50 mL were subjected to shear rates ranging from 2.5 to 100 (rpm) s-1. All measurements were carried out at room temperature.

Total Phenolic Content (TPC) and Radical Scavenging Activity (RSA)

Being Tocosh a heterogenous mixture, not completely soluble in water, before the evaluation of its antioxidant properties, an extraction in 80% ethanol was required. Three different procedures were applied and compared: maceration, (room temperature, 72 h - ME), rapid heating extraction, (75 °C, 30 min - RE), Soxhlet extraction (reflux, 3 h - SE). The total polyphenol content (TPC) was quantified using the Folin-Ciocalteu assay [239], while antioxidant activity was assessed by the DPPH assay [179].

To assess TPC and RSA, an ethanolic extraction of Tocosh samples (matrix/solvent ratio 1:5) at 75°C for 30 min. was performed, followed by centrifugation, and supernatant recovery. TPC was assessed by the Folin-Ciocalteu spectrophotometric method, considering gallic acid as the reference standard [240]. Results are expressed as gallic acid equivalents (mg GAE/g T).

The radical scavenging activity of Tocosh was measured by DPPH (2,2-Diphenyl-1-picrylhydrazyl) assay, using Trolox as the reference standard [232]. The results were expressed as percentage of antioxidant activity (RSA%).

GC-MS Analysis

Tocosh samples were analyzed using headspace solid phase microextraction coupled with GC-MS. In detail, 2 g of Tocosh were placed in a headspace vial (50 mL), subsequently heated for 40 min. at 50°C. The SPME fiber was exposed to headspace for 40 min. and finally analyzed by GC-MS [241].

Microbiological evaluation

Different microbiological tests were performed on both Tocosh flour and its extracts. Due to the heterogenous nature of the flour, its solution in Muller Hinton broth (MH) for a MIC detection, was not possible. For this reason, at first, a sowing by inclusion assay on the entire flour was applied. Identification with MALDI-TOF technique (Matrix-Assisted Laser Desorption/Ionization Time-Of-Flight) of a peculiar bacterial strain isolated after this procedure was performed. Other assays (a modified Kirby-Bauer disc diffusion test, and MIC values calculation) were carried on the different extracts previously obtained (ME, RE, SE).

MIC

To assess the antimicrobial efficacy of the samples MICs were determined according to the broth microdilution method outlined by the European Committee on Antimicrobial

Susceptibility Testing (EUCAST) [184]. Briefly, bacterial cultures were incubated overnight and subsequently diluted to obtain a standardized inoculum of approximately 1.5×10^8 CFU/mL. Aliquots of each suspension were dispensed into 96-well microtiter plates containing serial 2-fold dilutions of each sample resulting in a final bacterial concentration of ~5×10^5 CFU/mL per well. After 24 hours of incubation at 37 °C, the MIC was defined as the lowest concentration at which no visible bacterial growth was observed. All MIC determinations were performed in triplicate. The experiments yielded full concordance (3/3 replicates) and MIC values were expressed as the median or modal result.

Kirby-Bauer disk diffusion test

The Kirby-Bauer disk diffusion method, as detailed in section Sample Evaluation [188] s a widely used standardized test for assessing the antimicrobial activity of compounds against bacterial strains.

In this study, the test was modified to better assess the activity of the test sample. Instead of using impregnated paper discs, 100 µL of test sample was deposited directly on the surface of Mueller-Hinton agar plates previously inoculated with the bacterial strain. This modification allowed the assessment of antimicrobial activity without the need for disc supports, ensuring direct contact between the extract and the microbial substrate. After incubation under standard conditions, the zones of inhibition were observed.

Sowing by inclusion

An alternative antimicrobial assay was performed by incorporating Tocosh flour directly into the culture medium. Specifically, 1.25 g of Tocosh flour, 0.55 g of Mueller-Hinton powder, and 0.2 g of agar were suspended in 25 mL of distilled water. The mixture was sterilized by autoclaving at 121 °C for 30 minutes. After sterilization, the molten agar medium was poured into sterile Petri dishes and allowed to solidify at room temperature. Six plates were prepared,

each inoculated with a different bacterial strains: *S. aureus, S. epidermidis, E. faecalis, E. faecium, E. coli, and P. aeruginosa*. Bacterial inocula were prepared by culturing each strain to the logarithmic growth phase and adjusting the suspensions to the 0.5 McFarland standard (~1.5 × 10^8 CFU/mL). Standardized inocula were then distributed uniformly onto the agar surface to evaluate bacterial growth inhibition.

Results and discussion

Rheological properties

In evaluating the rheological properties of Tocosh (T), for its potential use as a gelling agent, in comparison to potato starch (PS), the spectrophotometric determination of amylose/amylopectin ratio showed a slightly lower amylose content (T: 28% against PS: 33%). Nevertheless, the study encompasses a whole flour, in comparison to a pure starch that exclusively comprises the two polysaccharides of interest. Given the unavailability of a precise composition for Tocosh, a comparative analysis is currently not feasible. However, it can be posited that the rheological performance of Tocosh is comparable to that of starch when the two substances are used in equivalent amounts, as confirmed by the WBC assay (T=85%, PS= 88%, **Table 27**) and rheological profiles (viscosity determined by a Brookfield rotational viscosimeter **Figure 56**).

Table 27. Comparison of Tocosh and Starch for amylose percentage and WBC%

	Tocosh	**Potato Starch**
Amylose (%)	28.1 ± 0.5	33.3 ± 0.4
WBC (%)	85.3 ± 0.2	88.3 ± 0.2

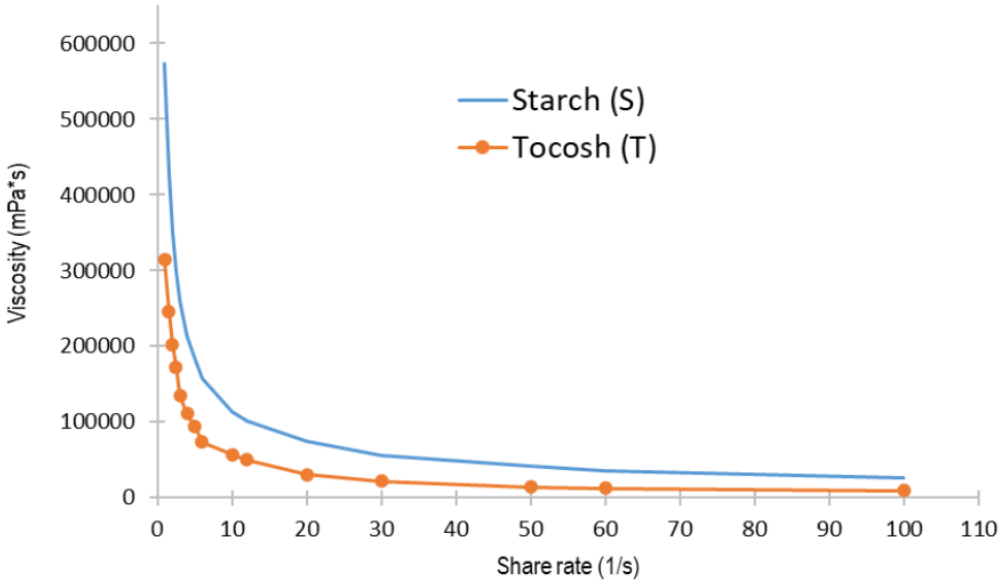

Figure 56. Rheological behaviour of Tocosh gel in comparison to starch gel.

Total Phenolic Content (TPC) and Radical Scavenging Activity (RSA)

Tocosh extraction in 80% ethanol led to different quantitative results (TPC and RSA), depending on the extraction method applied. The rapid heating extraction at 75 °C for 30 minutes (RE) provided the highest recovery of phenolic compounds and the better antioxidant activity (37.90 mg GAE/g and 42.52 RSA % respectively, **Table 28**).

Table 28. TPC and RSA% of ethanolic extracts from Tocosh flour.

Tocosh Extraction EtOH 80% - 1:20 sample/solvent w/V)	**TPC (mg GAE/g ± SD)**	**RSA % (± SD)**
ME – Maceration (72h -RT)	35.25 ± 0.02	25.93 ± 0.42
RE - Rapid Extraction (30 min – 75°C)	37.90 ± 0.03	42.52 ± 0.60
SE - Soxhlet Extraction (3hrs)	21.16 ± 0.06	35.53 ± 0.48

Microbiological evaluation

The evaluation of the antimicrobial potential of Tocosh using the scalar microdilution technique in broth has not yet led to satisfactory results. This is attributable to the difficulties in preparing the analytical sample, due to the heterogeneous composition of the flour, which is not very soluble in water and in Mueller-Hinton (MH) broth. This prevents a clear reading of the MIC and requires further investigation using alternative methods. For this reason, exploiting the gelling properties of the whole Tocosh flour, a sowing by inclusion assay has been performed, but the method requires improvements. At the moment, the most interesting result concerns a MALDI-TOF study (conducted at the Microbiology laboratories of the S. Martino Polyclinic Hospital of Genoa) of a strain isolated on several MH medium plates after plating of Tocosh samples. The identified strain is *Bacillus licheniformis*, a spore-forming species widely recognized in literature for its probiotic properties. This result may provide a microbiological rationale for the traditional use of Tocosh in supporting the human immune system. Other assays were carried out on Tocosh ethanolic extracts, after solvent evaporation and solubilization in DMSO (22 mg/mL). Preliminary results suggest a potentially interesting antimicrobial activity, as confirmed by the modified Kirby-Bauer disc diffusion test, performed on *Staphylococcus aureus* (**Figure 57**).

Figure 57. Modified Kirbi-Bauer disc diffusion of Tocosh extracts in DMSO: TS= Soxhlet, T30 = rapid extraction.

GC-MS analysis

GC-MS analysis, of the volatile fraction of Tocosh, performed at the Institute Maugeri in Pavia, disclosed the presence of butyric, acetic, and caproic acids (81.35%, 9%, and 4.78% respectively), responsible for the characteristic stinky odor. The presence of these acids was exploited converting them into the corresponding ethanolic scented esters, by the Fischer esterification. Overcoming this olfactive drawback, by a simple pre-treatment, Tocosh could be considered a promising potential multifunctional ingredient, with excellent gelling properties, good antioxidant capacity and pleasant fragrance.

Conclusion

The results of this study establish Tocosh flour as a promising multifunctional ingredient. Rheological analysis confirmed its potential as a functional agent: the water-binding capacity (WBC) of Tocosh (85.3%) was comparable to that of potato starch (PS: 88.3%), and viscosity profiles suggest its suitability as a gelling agent. Regarding bioactive potential, the highest recovery of phenolic compounds and superior antioxidant activity were achieved using the rapid extraction (RE) method (80% ethanol at 75°C for 30 minutes), yielding 37.90 mg GAE/g of TPC and 42.52% RSA. Microbiological analysis provided justification for the traditional use of Tocosh: the isolation of the spore-forming species Bacillus licheniformis, recognized for its probiotic properties, suggests a potential health benefit. Furthermore, preliminary modified Kirby-Bauer disk diffusion tests indicated potentially interesting antimicrobial activity of the ethanol extracts against Staphylococcus aureus. The characteristic odor was attributed by GC-MS analysis primarily to short-chain fatty acids, with butyric acid contributing 81.35% of the volatile fraction. This odor problem can be overcome by converting these acids into the corresponding fragrant ethanol esters via Fischer esterification. In summary, by addressing the odor issue, Tocosh presents itself as a valuable ingredient that combines functional gelling

properties, good antioxidant capacity, and significant microbiological potential. Future research will focus on refining the antimicrobial tests to fully characterize the observed activity.

Dissemination of Results

The research results were presented at 1st SITELF National Cosmetology Conference - SITCOSM held in Bari providing an opportunity to share findings with the scientific community.

BIBLIOGRAPHY

1. European Commission, Joint Research Centre, Institute for Environment and Sustainability. *International reference life cycle data system (ILCD) handbook :General guide for life cycle assessment-Detailed guidance*; Publications Office of the European Union: Luxembourg, **2010**.
2. Jawahir, I.S.; Bradley, R. Technological Elements of Circular Economy and the Principles of 6R-Based Closed-Loop Material Flow in Sustainable Manufacturing. *Procedia CIRP* **2016**, *40*, 103–108, doi:10.1016/j.procir.2016.01.067.
3. McGregor, M.J. Economics of natural resources and the environment: D. W. Pearce and R. K. Turner. *Agric. Syst.* **1991**, *37*, 100–101, doi:10.1016/0308-521X(91)90051-B.
4. Pearce, D.; Turner, R. Economics of natural resources and the environment. *Am. J. Agric. Econ.* **1991**, *73*, 1264–1265, doi:10.2307/1242904.
5. European Commission. A new circular economy action plan for a cleaner and more competitive Europe. Available online: https://eur-lex.europa.eu/legal-content/EN/TXT/?uri=CELEX:52020DC0067
6. Joshi, K.; Venkatachalam, A.; Jawahir, I.S. A new methodology for transforming 3R concept into 6R concept for improved product sustainability. *In Proceedings of the IV Global Conference on Sustainable Product Development and Life Cycle Engineering*; São Carlos, Brazil, 3-6 October **2006**.
7. Reimagine Co. *The 6 R's: Reuse, reduce, repair, refuse, recycle, reimagine*. Available online: https://reimagineco.ca/blogs/news/the-6-rs
8. Anastas, P.T.; Warner, J.C. *Green Chemistry: Theory and Practice*; Oxford University Press, **2000**; ISBN 978-0-19-850698-0.
9. Chemat, F.; Vian, M.A.; Cravotto, G. Green Extraction of Natural Products: Concept and Principles. *Int. J. Mol. Sci.* **2012**, *13*, 8615–8627, doi:10.3390/ijms13078615.
10. Jin, Q.; Yang, L.; Poe, N.; Huang, H. Integrated Processing of Plant-Derived Waste to Produce Value-Added Products Based on the Biorefinery Concept. *Trends Food Sci. Technol.* **2018**, *74*, 119–131, doi:10.1016/j.tifs.2018.02.014.
11. Pathania, S.; Kaur, N. Utilization of fruits and vegetable by-products for isolation of dietary fibres and its potential application as functional ingredients. *Bioact. Carbohydr. Diet. Fibre* **2022**, *27*, 100295, doi:10.1016/j.bcdf.2021.100295.
12. Nabi, B.G.; Mukhtar, K.; Ansar, S.; Hassan, S.A.; Hafeez, M.A.; Bhat, Z.F.; Mousavi Khaneghah, A.; Haq, A.U.; Aadil, R.M. Application of ultrasound technology for the effective management of waste from fruit and vegetable. *Ultrason. Sonochem.* **2023**, *102*, 106744, doi:10.1016/j.ultsonch.2023.106744.
13. Fărcaș, A.C.; Socaci, S.A.; Nemeș, S.A.; Pop, O.L.; Coldea, T.E.; Fogarasi, M.; Biriș-Dorhoi, E.S. An update regarding the bioactive compound of cereal by-products: health benefits and potential applications. *Nutrients* **2022**, *14*, 3470, doi:10.3390/nu14173470.
14. Sá, A.G.A.; Silva, D.C. da; Pacheco, M.T.B.; Moreno, Y.M.F.; Carciofi, B.A.M. Oilseed by-products as plant-based protein sources: amino acid profile and digestibility. *Future Foods* **2021**, *3*, 100023, doi:10.1016/j.fufo.2021.100023.
15. Ali, M.Y.; Sina, A.A.I.; Khandker, S.S.; Neesa, L.; Tanvir, E.M.; Kabir, A.; Khalil, M.I.; Gan, S.H. Nutritional composition and bioactive compounds in tomatoes and their impact on human health and disease: a review. *Foods* **2021**, *10*, 45, doi:10.3390/foods10010045.
16. Hadidi, M.; Aghababaei, F.; Gonzalez-Serrano, D.J.; Goksen, G.; Trif, M.; McClements, D.J.; Moreno, A. Plant-based proteins from agro-industrial waste and by-products: Towards a more

circular economy. *Int. J. Biol. Macromol.* **2024**, *261*, 129576, doi:10.1016/j.ijbiomac.2024.129576.

17. Joshi, N.; Pransu, G.; Adam Conte-Junior, C. Critical review and recent advances of 2d materials-based gas sensors for food spoilage detection. *Crit. Rev. Food Sci. Nutr.* **2023**, *63*, 10536-10559, doi:10.1080/10408398.2022.2078950.

18. Nirmal, N.P.; Khanashyam, A.C.; Mundanat, A.S.; Shah, K.; Babu, K.S.; Thorakkattu, P.; Al-Asmari, F.; Pandiselvam, R. Valorization of fruit waste for bioactive compounds and their applications in the food industry. *Foods* **2023**, *12*, 556, doi:10.3390/foods12030556.

19. Perra, M.; Bacchetta, G.; Muntoni, A.; De Gioannis, G.; Castangia, I.; Rajha, H.N.; Manca, M.L.; Manconi, M. An outlook on modern and sustainable approaches to the management of grape pomace by integrating green processes, biotechnologies and advanced biomedical approaches. *J. Funct. Foods* **2022**, *98*, 105276, doi:10.1016/j.jff.2022.105276.

20. Szabo, K.; Mitrea, L.; Călinoiu, L.F.; Teleky, B.-E.; Martău, G.A.; Plamada, D.; Pascuta, M.S.; Nemeş, S.-A.; Varvara, R.-A.; Vodnar, D.C. Natural polyphenol recovery from apple-, cereal-, and tomato-processing by-products and related health-promoting properties. *Molecules, Int. J. Mol. Scis* **2022**, *27*, 7977, doi:10.3390/molecules27227977.

21. Wedamulla, N.E.; Fan, M.; Choi, Y.-J.; Kim, E.-K. Citrus peel as a renewable bioresource: Transforming waste to food additives. *J. Funct. Foods* **2022**, *95*, 105163, doi:10.1016/j.jff.2022.105163.

22. Jin, Z.; Lan, Y.; Ohm, J.-B.; Gillespie, J.; Schwarz, P.; Chen, B. Physicochemical composition, fermentable sugars, free amino acids, phenolics, and minerals in brewers' spent grains obtained from craft brewing operations. *J. Cereal Sci.* **2022,** *104*, 103413, doi:10.1016/j.jcs.2022.103413.

23. Verni, M.; Rizzello, C.G.; Coda, R. Fermentation biotechnology applied to cereal industry by-products: Nutritional and functional insights. *Front. Nutr.* **2019**, *6*, 42, doi:10.3389/fnut.2019.00042.

24. Khwaldia, K.; Attour, N.; Matthes, J.; Beck, L.; Schmid, M. Olive byproducts and their bioactive compounds as a valuable source for food packaging applications. *Compr. Rev. Food Sci. Food Saf.* **2022**, *21*, 1218-1253, doi:10.1111/1541–4337.12882.

25. Otero, P.; Garcia-Oliveira, P.; Carpena, M.; Barral-Martinez, M.; Chamorro, F.; Echave, J.; Garcia-Perez, P.; Cao, H.; Xiao, J.; Simal-Gandara, J.; Prieto, M.A. Applications of by-products from the olive oil processing: Revalorization strategies based on target molecules and green extraction technologies. *Trends Food Sci. Technol.* **2021**, *116*, 1084–1104, doi:10.1016/j.tifs.2021.09.007.

26. Difonzo, G.; de Gennaro, G.; Pasqualone, A.; Caponio, F. Potential use of plant-based by-products and waste to improve the quality of gluten-free foods. *J. Sci. Food Agric.* **2022**, *102*, 2199–2211, doi:10.1002/jsfa.11702.

27. Caputo, L.; Nazzaro, F.; Souza, L.F.; Aliberti, L.; De Martino, L.; Fratianni, F.; Coppola, R.; De Feo, V. *Laurus nobilis*: composition of essential oil and its biological activities. *Molecules*, *Int. J. Mol. Sci* **2017**, *22*, 930, doi:10.3390/molecules22060930.

28. Patrakar, R.; Mansuriya, M.; Patil, P. Phytochemical and pharmacological review on *Laurus nobilis*. *Int. J. Pharm. Chem. Sci.* **2012**, *1*, 595–602

29. Dobroslavić, E.; Repajić, M.; Dragović-Uzelac, V.; Elez Garofulić, I. Isolation of *Laurus Nobilis* leaf polyphenols: a review on current techniques and future perspectives. *Foods* **2022**, *11*, 235, doi:10.3390/foods11020235.

30. Fidan, H.; Stefanova, G.; Kostova, I.; Stankov, S.; Damyanova, S.; Stoyanova, A.; Zheljazkov, V.D. Chemical composition and antimicrobial activity of *Laurus nobilis L*. Essential oils from Bulgaria. *Molecules*, *Int. J. Mol. Sci* **2019**, *24*, 804, doi:10.3390/molecules24040804.

31. Sharma, S. (2012). Bay leaves. In *Handbook of Herbs and Spices*; Woodhead Publishing: Cambridge, UK, **2012**; pp. 73–85, ISBN 978-0-85709-567-1.

32. Li, G.; Zeng, X.; Xie, Y.; Cai, Z.; Moore, J.C.; Yuan, X.; Cheng, Z.; Ji, G. Pharmacokinetic properties of isorhamnetin, kaempferol and quercetin after oral gavage of total flavones of *Hippophae rhamnoides* L. in rats using a UPLC-MS method. *Fitoterapia* **2012**, *83*, 182–191, doi: 10.1016/j.fitote.2011.10.012.

33. Konovalov, D.A.; Alieva, N.M. Phenolic compounds of *Laurus nobilis* (Review). *Pharm. Pharmacol.* **2019**, *7*, 244–259, doi:10.19163/2307-9266-2019-7-5-244-259.

34. Muñiz-Márquez, D.B.; Martínez-Ávila, G.C.; Wong-Paz, J.E.; Belmares-Cerda, R.; Rodríguez-Herrera, R.; Aguilar, C.N. Ultrasound-assisted extraction of phenolic compounds from *Laurus Nobilis L*. and their antioxidant activity. *Ultrason. Sonochem.* **2013**, *20*, 1149–1154, doi: 10.1016/j.ultsonch.2013.02.008.

35. Rossetti, I.; Rabitti, D; Preda, S; Robustelli Della Cuna, F. S. Genus *Paeonia*: Phytochemical study, pharmacological activities, clinical application and toxicology. *Natural1* **2022**, 52–61.

36. Ma, W.; Ren, H.; Meng, X.; Liu, S.; Du, K.; Fang, S.; Chang, Y. A review of the ethnopharmacology, phytochemistry, pharmacology, pharmacokinetics and quality control of *Paeonia lactiflora* Pall. *J. Ethnopharmacol.* **2024**, *335*, 118616, doi:10.1016/j.jep.2024.118616.

37. European Commission. *CosIng-Cosmetics database*. Available online: https://ec.europa.eu/growth/tools-databases/cosing/

38. Li, P.; Shen, J.; Wang, Z.; Liu, S.; Liu, Q.; Li, Y.; He, C.; Xiao, P. Genus *Paeonia*: A comprehensive review on traditional uses, phytochemistry, pharmacological activities, clinical application, and toxicology. *J. Ethnopharmacol.* **2021**, *269*, 113708, doi:10.1016/j.jep.2020.113708.

39. Xu, S.-Y.; Cao, H.-Y.; Yang, R.-H.; Xu, R.-X.; Zhu, X.-Y.; Ma, W.; Liu, X.-B.; Yan, X.-Y.; Fu, P. Genus Paeonia monoterpene glycosides: A systematic review on their pharmacological activities and molecular mechanisms. *Phytomedicine* **2024**, *127*, 155483, doi:10.1016/j.phymed.2024.155483.

40. Tan, Y.-Q.; Chen, H.-W.; Li, J.; Wu, Q.-J. Efficacy, chemical constituents, and pharmacological actions of Radix Paeoniae Rubra and Radix Paeoniae Alba. *Front. Pharmacol.* **2020**, *11*, 1054, doi:10.3389/fphar.2020.01054.

41. He, D.-Y.; Dai, S.-M. Anti-inflammatory and immunomodulatory effects of *Paeonia lactiflora* Pall., a traditional Chinese herbal medicine. *Front. Pharmacol.* **2011**, *2*, 10, doi:10.3389/fphar.2011.00010.

42. Peng, L.; Ma, Z.; Chu, W.; Jiang, P.; Fu, Y.; Wang, P. identification and hepatoprotective activity of total glycosides of paeony with high content of paeoniflorin extracted from *Paeonia lactiflora* Pall. Food Chem. Toxicol. **2023**, *173*, 113624, doi: 10.1016/j.fct.2023.113624.

43. Wang, H.; Yu, W.; Wang, T.; Fang, D.; Wang, Z.; Wang, Y. Therapeutic potential and pharmacological insights of total glucosides of paeony in dermatologic diseases: A comprehensive review. *Front. Pharmacol.* **2025**, *15*, 1423717.

44. Jiang, H.; Li, J.; Wang, L.; Wang, S.; Nie, X.; Chen, Y.; Fu, Q.; Jiang, M.; Fu, C.; He, Y. Total glucosides of paeony: a review of its phytochemistry, role in autoimmune diseases, and mechanisms of action. *J. Ethnopharmacol*. **2020**, *258*, 112913.

45. Zhang, Z.; Ren, A.; Liu, Y.; Yin, M.; Feng, Y.; Liu, Y.; Peng, H.; Chu, S. Comprehensive chemical profiling and comparison of different medicinal cultivars of *Paeonia lactiflora* Pall. *Microchem. J.* **2025**, *213*, 113674, doi:10.1016/j.microc.2025.113674.

46. Kumar, S.; Ratha, K.K.; Rao, M.M.; Acharya, R. A comprehensive review on the phytochemistry, pharmacological, ethnobotany, and traditional uses of *Paeonia* species. *J. Herbmed Pharmacol.* **2022**, *12*, 13–24, doi:10.34172/jhp.2023.02.

47. Wang, Q.-S.; Gao, T.; Cui, Y.-L.; Gao, L.-N.; Jiang, H.-L. Comparative studies of paeoniflorin and albiflorin from *Paeonia lactiflora* on anti-inflammatory activities. *Pharm. Biol.* **2014**, *52*, 1189–1195, doi:10.3109/13880209.2014.880490.

48. Tong, N.-N.; Zhou, X.-Y.; Peng, L.-P.; Liu, Z.-A.; Shu, Q.-Y. A comprehensive study of three species of *paeonia* stem and leaf phytochemicals, and their antioxidant activities. *J. Ethnopharmacol.* **2021**, *273*, 113985, doi:10.1016/j.jep.2021.113985.

49. Liu, L.; Yuan, Y.; Zuo, J.; Tao, J. Composition and antioxidant activity of *Paeonia lactiflora* petal flavonoid extract and underlying mechanisms of the protective effect on H_2O_2-induced oxidative damage in BRL3A cells. *Hortic. Plant J.* **2023**, *9*, 335–344, doi:10.1016/j.hpj.2022.06.001.

50. Wu, Y.; Jiang, Y.; Zhang, L.; Zhou, J.; Yu, Y.; Zhou, Y.; Kang, T. Chemical profiling and antioxidant evaluation of *Paeonia lactiflora* Pall. "Zhongjiang" by HPLC-ESI-MS combined with DPPH assay. *J. Chromatogr. Sci.* **2021**, *59*, 795–805, doi:10.1093/chromsci/bmab005.

51. Lim, J.-W.; Kang, M.-K.; Kim, H.-E. Antibacterial effects of *Paeonia lactiflora* extract on oral microcosm biofilms. *Appl. Sci.* **2024**, *14*, 11290, doi:10.3390/app142311290.

52. Jin, Y.; Lin, J.; Shi, H.; Jin, Y.; Cao, Q.; Chen, Y.; Zou, Y.; Tang, Y.; Li, Q. The active ingredients in Chinese peony pods synergize with antibiotics to inhibit MRSA growth and biofilm formation. *Microbiol. Res.* **2024**, *281*, 127625, doi:10.1016/j.micres.2024.127625.

53. Sang, H.; Jin, H.; Song, P.; Xu, W.; Wang, F. Gallic acid exerts antibiofilm activity by inhibiting methicillin-resistant *Staphylococcus aureus* adhesion. *Sci. Rep.* **2024**, *14*, 17220, doi:10.1038/s41598-024-68279-w.

54. Ho, J.-Y.; Chang, H.-W.; Lin, C.-F.; Liu, C.-J.; Hsieh, C.-F.; Horng, J.-T. Characterization of the anti-influenza activity of the Chinese herbal plant *Paeonia lactiflora*. *Viruses* **2014**, *6,* 1861–1875, doi:10.3390/v6041861.

55. Zhou, X.; Alimu, A.; Zhao, J.; Xu, X.; Li, X.; Lin, H.; Lin, Z. Paeonia genus: A systematic review of active ingredients, pharmacological effects and mechanisms, and clinical applications for the treatment of cancer. *Arch. Pharm.* Res. **2024**, *47*, 677–695, doi:10.1007/s12272-024-01512-2.

56. Schicchi, R.; Camarda, L.; Spadaro, V.; Pitonzo, R. Caratterizzazione chimica della manna estratta nelle Madonie (Sicilia) da cultivar di *Fraxinus angustifolia* e di *Fraxinus ornus* (Oleaceae). *Quad Bot Amb Appl* **2006**, *17*, 139–162.

57. Oieni, S. Il frassino da manna in Sicilia. *Monti e Boschi* 1953, 4, 113–123.

58. Cornara, L.; Sanclemente, G.; Robustelli della Cuna, F.S.; Preda, S.; Raimondo, F. La manna, il dono delle Madonie. *Erbor. Domani* **2017**, 74–85.

59. Lubrano, C.; Touzeau, B.; Laperdrix, C.; Robin, J. Development of a cosmetic plant active ingredient: Sustainable and scientific considerations. The example of an ash manna tree extract (*Fraxinus ornus* L.). *Planta Med.* **2013**, *79*, SL13, doi:10.1055/s-0033-1351839.

60. Caligiani, A.; Tonelli, L.; Palla, G.; Marseglia, A.; Rossi, D.; Bruni, R. Looking beyond sugars: Phytochemical profiling and standardization of manna exudates from Sicilian *Fraxinus excelsior* L. *Fitoterapia* **2013**, *90*, 65–72, doi:10.1016/j.fitote.2013.07.002.

61. Spadaro, V.; Raimondo, F.M. La manna delle Madonie (Sicilia): dai frassini ai prodotti farmaceutici e alimentari. In *Atti del Convegno Alimed* 2011; Palermo, Italy, **2011**; pp. 36–36.

62. Attanzio, A.; D'Anneo, A.; Pappalardo, F.; Bonina, F.P.; Livrea, M.A.; Allegra, M.; Tesoriere, L. Phenolic composition of hydrophilic extract of manna from Sicilian *Fraxinus angustifolia* Vahl and its reducing, antioxidant and anti-inflammatory activity *in vitro*. *Antioxidants* **2019**, *8,* 494, doi:10.3390/antiox8100494.

63. Lazzarini, E.; Lonardoni, A.R. La manna: salute della natura; Edizioni Mediterranee: Rome, Italy, **1984**.

64. Trease, G.E.; Evans, W.C. *Farmacognosia*. Piccin: Padova, Italy, **1995**; pp. 315–316

65. Kinghora, A.D.; Soejarto, D.D.; Inglett, G.E. Sweetening agents of plant origin. *Crit. Rev. Plant Sci.* **1986**, *4*, 79–120, doi:10.1080/07352688609382220.

66. Velásquez-Milla, D.; Casas, A.; Torres-Guevara, J.; Cruz-Soriano, A. Ecological and socio-cultural factors influencing *in situ* conservation of crop diversity by traditional Andean households in Peru. *J. Ethnobiol. Ethnomedicine* **2011**, *7*, 40, doi:10.1186/1746-4269-7-40.

67. Valle Santos, A. O. Perspectivas de comercializacion de una bebida instatanea preparada a base de tocosh, kiwicha y cacao. s.l.:s.n., **2013**.

68. LLontop, L.F.G.; Ruiz, J.C.; Calvo, M. del R.C. Efecto citoprotector del extracto mixto de *Solanum tuberosum* L. "papa", *Minthostachys mollis* L. "muña" y *Uncaria tomentosa* L. "uña de gato" en las lesiones ulcerosas de ratas inducidas por etanol. *REBIOL* **2020**, *40*, 177–187.

69. Jiménez Guerrero, C.F.; Bernardi Espinoza, D. Tipificación y determinación de los cambios en la composición de la microbiota presente en los distintos procesos de elaboración del tocosh de papa (*Solanum tuberosum*). *Univ. Peru. Cienc. Apl. UPC* **2019**.

70. Sandoval Vegas, M.H.; Tenorio Mucha, J.; Tinco Jayo, A.; Loli Ponce, R.A.; Calderón Pinillos, S. Efecto antioxidante y citoprotector del tocosh de Solanum tuberosum 'papa' en la mucosa gástrica de animales de experimentación. *An. Fac. Med.* **2015**, *76*, 15, doi:10.15381/anales.v76i1.11070.

71. Oyola-Coral, M.A.; Padilla-Fabian, R.A.; Jamanca-Gonzales, N.C. Optimización por diseño de mezcla D-optimal de la aceptabilidad general de una galletaenriquecida con harina de tocosh (*Solanum tuberosum* L.) y harina de kiwicha (*Amaranthus caudatus*). *QuantUNAB* **2023**, *2*, e71–e71, doi:10.52807/qunab.v2i1.71.

72. Cochachi Yauri, A.C.; Pajuelo Inga, A.G. *Análisis y descripción de pruebas de flotación para un mineral polimetálico (Cu, Pb y Zn) en Palca-Huancavelica 2024*. Bachelor's Thesis, Universidad Nacional del Centro del Perú, Huancayo, Perù, **2024**.

73. Zimmerer, K.; Jones, A.D.; Haan, S. de; García, G.C.; Creed-Kanashiro, H.; Carrasco, M.; Mesa, K.; Tello, M.; Tubbeh, R. Climate change and food: Challenges and opportunities in tropical mountains and agrobiodiversity hotspots. *ReVista: Harvard Review of Latin America* **2018**, 53–57.

74. Velasco-Chong, J.R.; Herrera-Calderón, O.; Rojas-Armas, J.P.; Hañari-Quispe, R.D.; Figueroa-Salvador, L.; Peña-Rojas, G.; Andía-Ayme, V.; Yuli-Posadas, R.Á.; Yepes-Perez, A.F.; Aguilar, C. Tocosh flour (*Solanum tuberosum* L.): A Toxicological assessment of traditional Peruvian Fermented potatoes. *Foods* **2020**, *9*, 719, doi:10.3390/foods9060719.

75. Dhiman, A.; Suhag, R.; Chauhan, D.S.; Thakur, D.; Chhikara, S.; Prabhakar, P.K. Status of beetroot processing and processed products: Thermal and emerging technologies intervention. *Trends Food Sci. Technol.* **2021**, *114*, 443–458, doi:10.1016/j.tifs.2021.05.042.

76. Chhikara, N.; Kushwaha, K.; Sharma, P.; Gat, Y.; Panghal, A. Bioactive compounds of beetroot and utilization in food processing industry: A critical review. *Food Chem*. **2019**, *272*, 192–200, doi:10.1016/j.foodchem.2018.08.022.

77. Mirmiran, P.; Houshialsadat, Z.; Gaeini, Z.; Bahadoran, Z.; Azizi, F. Functional properties of beetroot (*Beta vulgaris*) in management of cardio-metabolic diseases. *Nutr. Metab*. **2020**, *17*, 3, doi:10.1186/s12986-019-0421-0.

78. Clifford, T.; Howatson, G.; West, D.J.; Stevenson, E.J. The potential benefits of red beetroot supplementation in health and disease. *Nutrients* **2015**, *7*, 2801–2822, doi:10.3390/nu7042801.

79. Abdo, E.M.; Mansour, H.M.M.; Darwish, A.M.G.; El-Sohaimy, S.A.; Gomaa, M.A.E.; Shaltout, O.E.; Allam, M.G. Beetroot stalk extract as a functional colorant for stirred yogurt beverages: effect on nutritional value and stability during storage. *Fermentation* **2023**, *9*, 878, doi:10.3390/fermentation9100878.

80. Sadowska-Bartosz, I.; Bartosz, G. Biological properties and applications of betalains. *Molecules, Int. J. Mol. Sci* **2021**, *26*, 2520, doi:10.3390/molecules26092520.

81. Kumar, S.; Brooks, M.S.-L. Use of red beet (*Beta vulgaris* L.) for antimicrobial applications-a critical review. *Food Bioprocess Technol.* **2018**, *11*, 1–42, doi:10.1007/s11947-017-1942-z.

82. Stoica, F.; Râpeanu, G.; Rațu, R.N.; Stănciuc, N.; Croitoru, C.; Țopa, D.; Jităreanu, G. Red beetroot and its by-products: a comprehensive review of phytochemicals, extraction methods, health benefits, and applications. *Agriculture* **2025**, *15*, 270, doi:10.3390/agriculture15030270.

83. Eilat-Adar, S.; Sinai, T.; Yosefy, C.; Henkin, Y. Nutritional recommendations for cardiovascular disease prevention. *Nutrients* **2013**, *5*, 3646–3683, doi:10.3390/nu5093646.

84. Giuffrè, A.M. Influence of cultivar and harvest year on triglyceride composition of olive oils produced in Calabria (Southern Italy). *Eur. J. Lipid Sci. Technol.* **2013**, *115*, 928–934, doi:10.1002/ejlt.201200390.

85. Inglese, P.; Famiani, F.; Galvano, F.; Servili, M.; Esposto, S.; Urbani, S. Factors affecting extra-virgin olive oil composition. In *Horticultural Reviews*; John Wiley & Sons, Ltd, **2010**; pp. 83–147 ISBN 978-0-470-87237-6.

86. Rodríguez-Gutiérrez, G.; Lama-Muñoz, A.; Ruiz-Méndez, M.V.; Rubio-Senent, F.; Fernández-Bolaños, J.; Rodríguez-Gutiérrez, G.; Lama-Muñoz, A.; Ruiz-Méndez, M.V.; Rubio-Senent, F.; Fernández-Bolaños, J. New olive-pomace oil improved by hydrothermal pre-treatments. In *Olive Oil - Constituents, Quality, Health Properties and Bioconversions*; IntechOpen, **2012** ISBN 978-953-307-921-9.

87. Lee, Z.S.; Chin, S.Y.; Lim, J.W.; Witoon, T.; Cheng, C.K. Treatment technologies of palm oil mill effluent (POME) and olive mill wastewater (OMW): A brief review. *Environ. Technol. Innov.* **2019**, *15*, 100377, doi:10.1016/j.eti.2019.100377.

88. Fiorentino, A.; Gentili, A.; Isidori, M.; Monaco, P.; Nardelli, A.; Parrella, A.; Temussi, F. Environmental effects caused by olive mill wastewaters: toxicity comparison of low-molecular-weight phenol components. *J. Agric. Food Chem.* **2003**, *51*, 1005–1009, doi:10.1021/jf020887d.

89. Rupani, P.F.; Singh, R.P.; Ibrahim, M.H.; Esa, N. Review of current palm oil mill effluent (POME) treatment methods: Vermicomposting as a sustainable practice. **2010**. *World Appl. Sci. J.* 2010, 10, 1190–1201.

90. El-Abbassi, A.; Kiai, H.; Hafidi, A.; García-Payo, M.C.; Khayet, M. Treatment of olive mill wastewater by membrane distillation using polytetrafluoroethylene membranes. *Sep. Purif. Technol.* **2012**, *98*, 55–61, doi:10.1016/j.seppur.2012.06.026.

91. Carnevale, M.C.; Gnisci, E.; Hilal, J.; Criscuoli, A. Direct contact and vacuum membrane distillation application for the olive mill wastewater treatment. *Sep. Purif. Technol.* **2016**, *169*, 121–127, doi:10.1016/j.seppur.2016.06.002.

92. Bottino, A.; Capannelli, G.; Comite, A.; Costa, C.; Firpo, R.; Jezowska, A.; Pagliero, M. Treatment of olive mill wastewater through integrated pressure-driven membrane processes. *Membranes* **2020**, *10*, 334, doi:10.3390/membranes10110334.

93. Tapia-Quirós, P.; Montenegro-Landívar, M.F.; Reig, M.; Vecino, X.; Cortina, J.L.; Saurina, J.; Granados, M. Recovery of polyphenols from agri-food by-products: The olive oil and winery industries cases. *Foods* **2022**, *11*, 362, doi:10.3390/foods11030362.

94. Alfano, A.; Corsuto, L.; Finamore, R.; Savarese, M.; Ferrara, F.; Falco, S.; Santabarbara, G.; De Rosa, M.; Schiraldi, C. Valorization of olive mill wastewater by membrane processes to recover natural antioxidant compounds for cosmeceutical and nutraceutical applications or functional foods. *Antioxidants* **2018**, *7*, 72, doi:10.3390/antiox7060072.

95. Bender, C.; Straßmann, S.; Heidrich, P. Cellular antioxidant effects and bioavailability of food supplements rich in hydroxytyrosol. *Appl. Sci.* **2021**, *11*, 4763, doi:10.3390/app11114763.

96. Obied, H.K.; Allen, M.S.; Bedgood, D.R.; Prenzler, P.D.; Robards, K.; Stockmann, R. Bioactivity and analysis of biophenols recovered from olive mill waste. *J. Agric. Food Chem.* **2005**, *53*, 823–837, doi:10.1021/jf048569x.

97. Covas, M.-I.; Nyyssönen, K.; Poulsen, H.E.; Kaikkonen, J.; Zunft, H.-J.F.; Kiesewetter, H.; Gaddi, A.; De la Torre, R.; Mursu, J.; Bäumler, H.; Nascetti, S.; Salonen, J.T.; Fitó, M.; Virtanen, J.;

Marrugat, J. The effect of polyphenols in olive oil on heart disease risk factors: A randomized trial. *Ann. Intern. Med.* **2006**, *145*, 333–341, doi:10.7326/0003-4819-145-5-200609050-00006.

98. Montedoro, G.; Servili, M.; Baldioli, M.; Miniati, E. Simple and hydrolyzable phenolic compounds in virgin olive oil. 1. Their extraction, separation, and quantitative and semiquantitative evaluation by HPLC. *J. Agric. Food Chem.* **1992**, *40*, 1571–1576, doi:10.1021/jf00021a019.

99. Nakayama, H.; Nishi, N.; Matsuo, Y.; Tanaka, T.; Kotoda, N.; Ishimaru, K. A new secoiridoid glucoside from *Olea europaea*. *J. Asian Nat. Prod. Res.* **2022**, *24*, 1093–1100, doi:10.1080/10286020.2021.2017898.

100. Brenes, M.; García, A.; García, P.; Rios, J.J.; Garrido, A. Phenolic compounds in Spanish olive oils. *J. Agric. Food Chem.* **1999**, *47*, 3535–3540, doi:10.1021/jf990009o

101. Angerosa, F.; d'Alessandro, N.; Corana, F.; Mellerio, G. Characterization of phenolic and secoiridoid aglycons present in virgin olive oil by gas chromatography-chemical ionization mass spectrometry. *J. Chromatogr. A* **1996**, *736*, 195–203, doi:10.1016/0021-9673(95)01375-X.

102. Andreasen, M.F.; Christensen, L.P.; Meyer, A.S.; Hansen, Å. Content of phenolic acids and ferulic acid dehydrodimers in 17 rye (*Secale cereale* L.) varieties. *J. Agric. Food Chem.* **2000**, *48*, 2837–2842, doi:10.1021/jf991266w.

103. Prim, N.; Pastor, F.I.J.; Diaz, P. biochemical studies on cloned *Bacillus* sp. BP-7 phenolic acid decarboxylase PadA. *Appl. Microbiol. Biotechnol.* **2003**, *63*, 51–56, doi:10.1007/s00253-003-1371-y.

104. Nergiz, C.; Ünal, K. Determination of phenolic acids in virgin olive oil. *Food Chem.* **1991**, *39*, 237–240, doi:10.1016/0308-8146(91)90164-J.

105. Maga, J.A.; Katz, I. Simple phenol and phenolic compounds in food flavor. *Crit. Rev. Food Sci. Nutr.* **1978**, *10*, 323–372, doi:10.1080/10408397809527255.

106. Allen, D.B.; Maguire, J.J.; Mahdavian, M.; Wicke, C.; Marcocci, L.; Scheuenstuhl, H.; Chang, M.; Le, A.X.; Hopf, H.W.; Hunt, T.K. Wound hypoxia and acidosis limit neutrophil bacterial killing mechanisms. *Arch. Surg.* **1997**, *132*, 991–996, doi:10.1001/archsurg.1997.01430330057009.

107. Dissemond, J.; Goos, M.; Wagner, S.N. The role of oxidative stress in the pathogenesis and therapy of chronic wounds. *Hautarzt* **2002**, *53*, 718–723, doi:10.1007/s00105-001-0325-5.

108. Dai, T.; Tanaka, M.; Huang, Y.-Y.; Hamblin, M.R. Chitosan preparations for wounds and burns: antimicrobial and wound-healing effects. *Expert Rev. Anti Infect. Ther.* **2011**, *9*, 857–879, doi:10.1586/eri.11.59.

109. Abd El-Alim, S.H.; Salama, A.; Darwish, A.B. Provesicular elastic carriers of simvastatin for enhanced wound healing activity: An in-vitro/in-vivo Study. *Int. J. Pharm.* **2020**, *585*, 119470, doi:10.1016/j.ijpharm.2020.119470.

110. Gu, Y.; Jérôme, F. Bio-based solvents: An emerging generation of fluids for the design of eco-efficient processes in catalysis and organic chemistry. *Chem. Soc. Rev.* **2013**, *42*, 9550–9570, doi:10.1039/C3CS60241A.

111. Häckl, K.; Kunz, W. Some aspects of green solvents. *Comptes Rendus Chim.* **2018**, *21*, 572–580, doi:10.1016/j.crci.2018.03.010.

112. Villa, C.; Caviglia, D.; Robustelli della Cuna, F.S.; Zuccari, G.; Russo, E. NADES application in cosmetic and pharmaceutical fields: an overview. *Gels* **2024**, *10*, 107, doi:10.3390/gels10020107.

113. Dai, Y. *Natural deep eutectic solvents and their application in natural product research and development*. PhD Thesis, Leiden University, Leiden, The Netherlands, **2013**.

114. Teles, A.R.R.; Capela, E.V.; Carmo, R.S.; Coutinho, J.A.P.; Silvestre, A.J.D.; Freire, M.G. Solvatochromic parameters of deep eutectic solvents formed by ammonium-based salts and carboxylic acids. *Fluid Phase Equilibria* **2017**, *448*, 15–21, doi:10.1016/j.fluid.2017.04.020.

115. Osch, D.J.G.P. van; Kollau, L.J.B.M.; Bruinhorst, A. van den; Asikainen, S.; Rocha, M.A.A.; Kroon, M.C. Ionic liquids and deep eutectic solvents for lignocellulosic biomass fractionation. *Phys. Chem. Chem. Phys.* **2017**, *19*, 2636–2665, doi:10.1039/C6CP07499E.

116. Mero, A.; Koutsoumpos, S.; Giannios, P.; Stavrakas, I.; Moutzouris, K.; Mezzetta, A.; Guazzelli, L. Comparison of physicochemical and thermal properties of choline chloride and betaine-based deep eutectic solvents: The influence of hydrogen bond acceptor and hydrogen bond donor nature and their molar ratios. *J. Mol. Liq.* **2023**, *377*, 121563, doi:10.1016/j.molliq.2023.121563.

117. Florindo, C.; Oliveira, F.S.; Rebelo, L.P.N.; Fernandes, A.M.; Marrucho, I.M. Insights into the synthesis and properties of deep eutectic solvents based on cholinium chloride and carboxylic acids. *ACS Sustain. Chem. Eng.* **2014**, *2*, 2416–2425, doi:10.1021/sc500439w.

118. Zhang, Q.; Vigier, K.D.O.; Royer, S.; Jérôme, F. Deep eutectic solvents: Syntheses, properties and applications. *Chem. Soc. Rev.* **2012**, *41*, 7108–7146, doi:10.1039/C2CS35178A.

119. Welton, T. Room-temperature ionic liquids. Solvents for synthesis and catalysis. *Chem. Rev.* **1999**, *99*, 2071–2084, doi:10.1021/cr980032t.

120. Visser, A.E.; Swatloski, R.P.; Rogers, R.D. pH-Dependent partitioning in room temperature ionic liquids provides a link to traditional solvent extraction behavior. *Green Chem.* **2000**, *2*, 1–4, doi:10.1039/A908888A.

121. Zainal-Abidin, M.H.; Hayyan, M.; Hayyan, A.; Jayakumar, N.S. New horizons in the extraction of bioactive compounds using deep eutectic solvents: a review. *Anal. Chim. Acta* **2017**, *979*, 1–23, doi:10.1016/j.aca.2017.05.012.

122. Zein El Abedin, S.; Endres, F. Ionic liquids: The link to high-temperature molten salts? *Acc. Chem. Res.* **2007**, *40*, 1106–1113, doi:10.1021/ar700049w.

123. Abbott, A.P.; Capper, G.; Davies, D.L.; Rasheed, R.K.; Tambyrajah, V. Novel solvent properties of choline chloride/urea mixtures. *Chem. Commun.* **2003**, 70–71, doi:10.1039/B210714G.

123. Kudłak, B.; Owczarek, K.; Namieśnik, J. Selected issues related to the toxicity of ionic liquids and deep eutectic solvents: a review. *Environ. Sci. Pollut. Res.* **2015**, *22*, 11975–11992, doi:10.1007/s11356-015-4794-y.

125. Ijardar, S.P.; Singh, V.; Gardas, R.L. Revisiting the physicochemical properties and applications of deep eutectic solvents. *Molecules*, *Int. J. Mol. Sci* **2022**, *27*, 1368, doi:10.3390/molecules27041368.

126. Abbott, A.P.; Boothby, D.; Capper, G.; Davies, D.L.; Rasheed, R.K. Deep eutectic solvents formed between choline chloride and carboxylic acids: versatile alternatives to ionic liquids. *J. Am. Chem. Soc.* **2004**, *126*, 9142–9147, doi:10.1021/ja048266j.

127. Wagle, D.V.; Deakyne, C.A.; Baker, G.A. Quantum chemical insight into the interactions and thermodynamics present in choline chloride based deep eutectic solvents. *J. Phys. Chem. B* **2016**, *120*, 6739–6746, doi:10.1021/acs.jpcb.6b04750.

128. Dai, Y.; van Spronsen, J.; Witkamp, G.-J.; Verpoorte, R.; Choi, Y.H. Natural deep eutectic solvents as new potential media for green technology. *Anal. Chim. Acta* **2013**, *766*, 61–68, doi:10.1016/j.aca.2012.12.019.

129. Choi, Y.H.; van Spronsen, J.; Dai, Y.; Verberne, M.; Hollmann, F.; Arends, I.W.C.E.; Witkamp, G.-J.; Verpoorte, R. Are natural deep eutectic solvents the missing link in understanding cellular metabolism and physiology? *Plant Physiol.* **2011**, *156*, 1701–1705, doi:10.1104/pp.111.178426.

130. Liu, Y.; Friesen, J.B.; McAlpine, J.B.; Lankin, D.C.; Chen, S.-N.; Pauli, G.F. Natural deep eutectic solvents: Properties, applications, and perspectives. *J. Nat. Prod.* **2018**, *81*, 679–690, doi:10.1021/acs.jnatprod.7b00945.

131. Obluchinskaya, E.D.; Daurtseva, A.V.; Pozharitskaya, O.N.; Flisyuk, E.V.; Shikov, A.N. Natural deep eutectic solvents as alternatives for extracting phlorotannins from brown algae. *Pharm. Chem. J.* **2019**, *53*, 243–247, doi:10.1007/s11094-019-01987-0.

132. Obluchinskaya, E.D.; Pozharitskaya, O.N.; Shevyrin, V.A.; Kovaleva, E.G.; Flisyuk, E.V.; Shikov, A.N. Optimization of extraction of phlorotannins from the arctic *Fucus vesiculosus* using natural deep eutectic solvents and their HPLC profiling with tandem high-resolution mass spectrometry. *Mar. Drugs* **2023**, *21*, 263, doi:10.3390/md21050263.

133. Dai, Y.; Verpoorte, R.; Choi, Y.H. Natural deep eutectic solvents providing enhanced stability of natural colorants from safflower (*Carthamus tinctorius*). *Food Chem.* **2014**, *159*, 116–121, doi:10.1016/j.foodchem.2014.02.155.

134. Xin, R.; Qi, S.; Zeng, C.; Khan, F.I.; Yang, B.; Wang, Y. A functional natural deep eutectic solvent based on trehalose: Structural and physicochemical properties. *Food Chem.* **2017**, *217*, 560–567, doi:10.1016/j.foodchem.2016.09.012.

135. Faggian, M.; Sut, S.; Perissutti, B.; Baldan, V.; Grabnar, I.; Dall'Acqua, S. Natural deep eutectic solvents (NADES) as a tool for bioavailability improvement: Pharmacokinetics of rutin dissolved in proline/glycine after oral administration in rats: Possible application in nutraceuticals. *Molecules*, *Int. J. Mol. Sci* **2016**, *21*, 1531, doi:10.3390/molecules21111531.

136. Sut, S.; Faggian, M.; Baldan, V.; Poloniato, G.; Castagliuolo, I.; Grabnar, I.; Perissutti, B.; Brun, P.; Maggi, F.; Voinovich, D.; Peron, G.; Dall'Acqua, S. Natural deep eutectic solvents (NADES) to enhance berberine absorption: An in vivo pharmacokinetic study. *Molecules*, *Int. J. Mol. Sci* **2017**, *22*, 1921, doi:10.3390/molecules22111921.

137. Mano, F.; Aroso, I.M.; Barreiros, S.; Borges, J.P.; Reis, R.L.; Duarte, A.R.C.; Paiva, A. Production of poly(vinyl alcohol) (pva) fibers with encapsulated natural deep eutectic solvent (NADES) using electrospinning. *ACS Sustain. Chem. Eng.* **2015**, *3*, 2504–2509, doi:10.1021/acssuschemeng.5b00613.

138. Vieira Sanches, M.; Freitas, R.; Oliva, M.; Mero, A.; De Marchi, L.; Cuccaro, A.; Fumagalli, G.; Mezzetta, A.; Colombo Dugoni, G.; Ferro, M.; Mele, A.; Guazzelli, L.; Pretti, C. Are natural deep eutectic solvents always a sustainable option? A bioassay-based study. *Environ. Sci. Pollut. Res.* **2023**, *30*, 17268–17279, doi:10.1007/s11356-022-23362-5.

139. Fernández, M. de los Á.; Boiteux, J.; Espino, M.; Gomez, F.J.V.; Silva, M.F. Natural deep eutectic solvents-mediated extractions: The way forward for sustainable analytical developments. *Anal. Chim. Acta* **2018**, *1038*, 1–10, doi:10.1016/j.aca.2018.07.059.

140. Jeong, K.M.; Ko, J.; Zhao, J.; Jin, Y.; Yoo, D.E.; Han, S.Y.; Lee, J. Multi-functioning deep eutectic solvents as extraction and storage media for bioactive natural products that are readily applicable to cosmetic products. *J. Clean. Prod.* **2017**, *151*, 87–95, doi:10.1016/j.jclepro.2017.03.038.

141. Liu, W.; Zhang, K.; Qin, Y.; Yu, J. A simple and green ultrasonic-assisted liquid–liquid microextraction technique based on deep eutectic solvents for the HPLC analysis of sesamol in sesame oils. *Anal. Methods* **2017**, *9*, 4184–4189, doi:10.1039/C7AY01033H.

142. Milano, F.; Giotta, L.; Guascito, M.R.; Agostiano, A.; Sblendorio, S.; Valli, L.; Perna, F.M.; Cicco, L.; Trotta, M.; Capriati, V. Functional enzymes in nonaqueous environment: The case of photosynthetic reaction centers in deep eutectic solvents. *ACS Sustain. Chem. Eng.* **2017**, *5*, 7768–7776, doi:10.1021/acssuschemeng.7b01270.

143. Zahrina, I.; Nasikin, M.; Krisanti, E.; Mulia, K. Deacidification of palm oil using betaine monohydrate-based natural deep eutectic solvents. *Food Chem.* **2018**, *240*, 490–495, doi:10.1016/j.foodchem.2017.07.132.

144. Paiva, A.; Craveiro, R.; Aroso, I.; Martins, M.; Reis, R.L.; Duarte, A.R.C. Natural deep eutectic solvents - Solvents for the 21st Century. *ACS Sustain. Chem. Eng.* **2014**, *2*, 1063–1071, doi:10.1021/sc500096j.

145. Radošević, K.; Ćurko, N.; Gaurina Srček, V.; Cvjetko Bubalo, M.; Tomašević, M.; Kovačević Ganić, K.; Radojčić Redovniković, I. Natural deep eutectic solvents as beneficial extractants for enhancement of plant extracts bioactivity. *LWT* **2016**, *73*, 45–51, doi:10.1016/j.lwt.2016.05.037.

146. Wen, Q.; Chen, J.-X.; Tang, Y.-L.; Wang, J.; Yang, Z. Assessing the toxicity and biodegradability of deep eutectic solvents. *Chemosphere* **2015**, *132*, 63–69, doi:10.1016/j.chemosphere.2015.02.061.

147. Pena-Pereira, F.; Kloskowski, A.; Namieśnik, J. Perspectives on the replacement of harmful organic solvents in analytical methodologies: A framework toward the implementation of a generation of eco-friendly alternatives. *Green Chem.* **2015**, *17*, 3687–3705, doi:10.1039/C5GC00611B.

148. Anastas, P.; Eghbali, N. Green chemistry: Principles and practice. *Chem. Soc. Rev.* **2009**, *39*, 301–312, doi:10.1039/B918763B.

149. Dai, Y.; Witkamp, G.-J.; Verpoorte, R.; Choi, Y.H. Tailoring properties of natural deep eutectic solvents with water to facilitate their applications. *Food Chem.* **2015**, *187*, 14–19, doi:10.1016/j.foodchem.2015.03.123.

150. Martins, M.; Aroso, I.M.; Reis, R.L.; Duarte, A.R.C.; Craveiro, R.; Paiva, A. Enhanced performance of supercritical fluid foaming of natural-based polymers by deep eutectic solvents. *AIChE J.* **2014**, *60*, 3701–3706, doi:10.1002/aic.14607.

151. Wei, Z.; Qi, X.; Li, T.; Luo, M.; Wang, W.; Zu, Y.; Fu, Y. Application of natural deep eutectic solvents for extraction and determination of phenolics in *Cajanus cajan* leaves by ultra performance liquid chromatography. *Sep. Purif. Technol.* **2015**, *149*, 237–244, doi:10.1016/j.seppur.2015.05.015

152. Wei, Z.-F.; Wang, X.-Q.; Peng, X.; Wang, W.; Zhao, C.-J.; Zu, Y.-G.; Fu, Y.-J. Fast and green extraction and separation of main bioactive flavonoids from Radix Scutellariae. *Ind. Crops Prod.* **2015**, *63*, 175–181, doi:10.1016/j.indcrop.2014.10.013.

153. Gutiérrez, M.C.; Ferrer, M.L.; Yuste, L.; Rojo, F.; del Monte, F. Bacteria incorporation in deep-eutectic solvents through freeze-drying. *Angew. Chem. Int. Ed.* **2010**, *49*, 2158–2162, doi:10.1002/anie.200905212.

154. Florindo, C.; Romero, L.; Rintoul, I.; Branco, L.C.; Marrucho, I.M. From phase change materials to green solvents: Hydrophobic low viscous fatty acid–based deep eutectic solvents. *ACS Sustain. Chem. Eng.* **2018**, *6*, 3888–3895, doi:10.1021/acssuschemeng.7b04235.

155. Bajkacz, S.; Adamek, J. Development of a method based on natural deep eutectic solvents for extraction of flavonoids from food samples. *Food Anal. Methods* **2018**, *11*, 1330–1344, doi:10.1007/s12161-017-1118-5.

156. Gomez, F.J.V.; Espino, M.; Fernández, M.A.; Silva, M.F. A greener approach to prepare natural deep eutectic solvents. *ChemistrySelect* **2018**, *3*, 6122–6125, doi:10.1002/slct.201800713.

157. Chemat, F.; Cravotto, G. *Microwave-assisted extraction for bioactive compounds*; Food Engineering Series; Springer: Berlin/Heidelberg, Germany, **2013**.

158. Zhao, B.-Y.; Xu, P.; Yang, F.-X.; Wu, H.; Zong, M.-H.; Lou, W.-Y. Biocompatible deep eutectic solvents based on choline chloride: Characterization and application to the extraction of rutin from *Sophora japonica*. *ACS Sustain. Chem. Eng.* **2015**, *3*, 2746–2755, doi:10.1021/acssuschemeng.5b00619.

159. Gutiérrez, M.C.; Ferrer, M.L.; Mateo, C.R.; Del Monte, F. Freeze-drying of aqueous solutions of deep eutectic solvents: A suitable approach to deep eutectic suspensions of self-assembled structures. *Langmuir* **2009**, *25*, 5509–5515, doi:10.1021/la900552b.

160. Francisco, M.; van den Bruinhorst, A.; Kroon, M.C. Low-transition-temperature mixtures (LTTMs): A new generation of designer solvents. *Angew. Chem. Int. Ed.* **2013**, *52*, 3074–3085, doi:10.1002/anie.201207548.

161. Mišan, A.; Nađpal, J.; Stupar, A.; Pojić, M.; Mandić, A.; Verpoorte, R.; Choi, Y.H. The perspectives of natural deep eutectic solvents in agri-food sector. *Crit. Rev. Food Sci. Nutr.* **2020**, *60*, 2564–2592, doi:10.1080/10408398.2019.1650717.

162. Craveiro, R.; Aroso, I.; Flammia, V.; Carvalho, T.; Viciosa, M.T.; Dionísio, M.; Barreiros, S.; Reis, R.L.; Duarte, A.R.C.; Paiva, A. Properties and thermal behavior of natural deep eutectic solvents. *J. Mol. Liq.* **2016**, *215*, 534–540, doi:10.1016/j.molliq.2016.01.038.

163. Benoit, C.; Charton, V.; Vogelgesang, B. The use of NADES to support innovation in the cosmetic industry. In *Eutectic Solvents and Stress in Plants*; Verpoorte, R.; Witkamp, G.-J.; Choi, Y.H., Eds.; *Advances in Botanical Research*; Academic Press: Cambridge, MA, USA, **2020**; Volume *97*, pp. 309–332, doi:10.1016/bs.abr.2020.09.009.

164. Rente, D.; Cvjetko Bubalo, M.; Panić, M.; Paiva, A.; Caprin, B.; Radojčić Redovniković, I.; Duarte, A.R.C. Review of deep eutectic systems from laboratory to industry, taking the application in the cosmetics industry as an example. *J. Clean. Prod.* **2022**, *380*, 135147, doi:10.1016/j.jclepro.2022.135147.

165. Sanchez-Prado, L.; Garcia-Jares, C.; Llompart, M. Microwave-assisted extraction: application to the determination of emerging pollutants in solid samples. *J. Chromatogr. A* **2010**, *1217*, 2390–2414, doi:10.1016/j.chroma.2009.11.080.

166. X-Rite Blog. UV spectrophotometer. Available online: https://www.xrite.com/it-it/blog/uv-spectrophotometer.

167. Loupy, A. Solvent-free reactions. In *Modern Solvents in Organic Synthesis*; Knochel, P., Ed.; Topics in Current Chemistry; Springer Berlin Heidelberg: Berlin, Heidelberg, 1999; Volume *206*, pp. 153–207.

168. Hu, Q.; He, Y.; Wang, F.; Wu, J.; Ci, Z.; Chen, L.; Xu, R.; Yang, M.; Lin, J.; Han, L.; Zhang, D. Microwave technology: A novel approach to the transformation of natural metabolites. *Chin. Med.* **2021**, *16*, 87, doi:10.1186/s13020-021-00500-8.

169. Cripps, S. Microwave power sources for industrial, scientific and medical applications. *Philos. Trans. R. Soc. Math. Phys. Eng. Sci.* **2025**, *383*, 20240069, doi:10.1098/rsta.2024.0069.

170. Microwave chemistry: How it all works. Available online: http://cem.com/e107/page130.html

171. Chegg.Com. The image below depicts how a microwave oven sets up a standing wave inside the cavity. Available online: https://www.chegg.com/homework-help/questions-and-answers/image-depicts-microwave-oven-sets-standing-wave-inside-cavity-turntable-moves-food-nodes-l-q48095161.

172. Stefanidis, G.; Navarrete Muñoz, A.; Strum, G.; Stankiewcz, A. A helicopter view of microwave application to chemical processes: Reactions, separations, and equipment concepts. *Rev. Chem. Eng.* **2014**, *30*, 233–259, doi:10.1515/revce-2013-0033.

173. Virot, M.; Tomao, V.; Ginies, C.; Visinoni, F.; Chemat, F. Microwave-integrated extraction of total fats and oils. *J. Chromatogr. A* **2008**, *1196–1197*, 57–64, doi:10.1016/j.chroma.2008.05.023.

174. Sparr Eskilsson, C.; Björklund, E. Analytical-scale microwave-assisted extraction. *J. Chromatogr. A* **2000**, *902*, 227–250, doi:10.1016/S0021-9673(00)00921-3.

175. Gomes, S.M.; Campos, F.; Martins, M.C.L.; Monteiro, C.; Santos, L. Exploring the bioactive potential and biocompatibility of extracts from agro-industrial residues for cosmetic applications. *Int. J. Mol. Sci.* **2025**, *26*, 9169, doi:10.3390/ijms26189169.

176. Gălbău, C.-Ş.; Irimie, M.; Neculau, A.E.; Dima, L.; Pogačnik da Silva, L.; Vârciu, M.; Badea, M. The potential of plant extracts used in cosmetic product applications-antioxidants delivery and mechanism of actions. *Antioxidants* **2024**, *13*, 1425, doi:10.3390/antiox13111425.

177. Knez, E.; Kadac-Czapska, K.; Grembecka, M. Evaluation of spectrophotometric methods for assessing antioxidant potential in plant food samples-A critical approach. *Appl. Sci.* **2025**, *15*, 5925, doi:10.3390/app15115925.

178. Pérez, M.; Dominguez-López, I.; Lamuela-Raventós, R. M. The chemistry behind the folin-ciocalteu method for the estimation of (poly)phenol content in food: Total phenolic intake in a mediterranean dietary pattern. *J. Agric. Food Chem.* **2023**, *71*, 17543–17553.

179. Brand-Williams, W.; Cuvelier, M. E.; Berset, C. use of a free radical method to evaluate antioxidant activity. *LWT - Food Sci. Technol.* **1995**, *28*, 25–30.

180. Behrendorff, J.B.; Vickers, C.E.; Chrysanthopoulos, P.; Nielsen, L.K. 2,2-Diphenyl-1-picrylhydrazyl as a screening tool for recombinant monoterpene biosynthesis. *Microb. Cell Factories* **2013**, *12*, 76, doi:10.1186/1475-2859-12-76.

181. Aree, T.; Jongrungruangchok, S. Structure-antioxidant activity relationship of β-cyclodextrin inclusion complexes with olive tyrosol, hydroxytyrosol and oleuropein: Deep insights from X-ray analysis, DFT calculation and DPPH assay. *Carbohydr. Polym.* **2018**, *199*, 661–669, doi:10.1016/j.carbpol.2018.07.019.

182. Halla, N.; Fernandes, I.P.; Heleno, S.A.; Costa, P.; Boucherit-Otmani, Z.; Boucherit, K.; Rodrigues, A.E.; Ferreira, I.C.F.R.; Barreiro, M.F. Cosmetics preservation: a review on present strategies. *Molecules*, *Int. J. Mol. Sci* **2018**, *23*, 1571, doi:10.3390/molecules23071571.

183. Pendleton, J.N.; Gorman, S.P.; Gilmore, B.F. Clinical relevance of the ESKAPE pathogens. *Expert Rev. Anti Infect. Ther.* **2013**, *11*, 297–308, doi:10.1586/eri.13.12.

184. EUCAST - Available online: https://www.eucast.org/.

185. Watts, J.L.; Shryock, T.R.; Apley, M.; Bade, D.J.; Brown, S.D.; Gray, J.T.; Heine, H.; Papich, M.G.; Silley, P.; Zurenko, G.E. Performance Standards for Antimicrobial Disk and Dilution Susceptibility Tests for Bacteria Isolated from Animals; Approved Standard-Third Edition; CLSI Document VET01-A3; Clinical and Laboratory Standards Institute: Wayne, PA, USA, **2008**.

186. Vollaro, A.; Catania, M.R.; Iesce, M.R.; Sferruzza, R.; D'Abrosca, B.; Donnarumma, G.; De Filippis, A.; Cermola, F.; DellaGreca, M.; Buommino, E. Antimicrobial and anti-biofilm properties of novel synthetic lignan-like compounds. *New Microbiol.* **2019**, *42*, 21–28.

187. Cramton, S. E.; Gerke, C.; Götz, F. *In vitro* methods to study staphylococcal biofilm formation. In *Microbial Growth in Biofilms - Part A*: *Developmental and Molecular Biological Aspects*; Doyle, R. J., Ed.; *Methods in Enzymology*; Academic Press: San Diego, CA, USA, **2001**; Volume *336*, pp. 239–255.

188. ASM. *Kirby-Bauer Disk Diffusion Susceptibility Test Protocol*. Available online: https://asm.org/getattachment/2594ce26-bd44-47f6-8287-0657aa9185ad/kirby-bauer-disk-diffusion-susceptibility-test-protocol-pdf.pdf

189. Balouiri, M.; Sadiki, M.; Ibnsouda, S.K. Methods for *in vitro* evaluating antimicrobial activity: a review. *J. Pharm. Anal.* **2016**, *6*, 71–79, doi:10.1016/j.jpha.2015.11.005.

190. Singhal, N.; Kumar, M.; Kanaujia, P.K.; Virdi, J.S. MALDI-TOF mass spectrometry: An emerging technology for microbial identification and diagnosis. *Front. Microbiol*. **2015**, *6*, 791, doi:10.3389/fmicb.2015.00791.

191. Seng, P.; Rolain, J.-M.; Fournier, P.E.; La Scola, B.; Drancourt, M.; Raoult, D. MALDI-TOF-mass spectrometry applications in clinical microbiology. *Future Microbiol.* **2010**, *5*, 1733–1754, doi:10.2217/fmb.10.127.

192. La Placa M. *Principi di microbiologia medica*; Esculapio: Bologna, Italy, **2012**; XIII edizione.

193. Tong, S.Y.C.; Davis, J.S.; Eichenberger, E.; Holland, T.L.; Fowler, V.G., Jr. *Staphylococcus aureus* infections: Epidemiology, pathophysiology, clinical manifestations, and management. *Clin. Microbiol. Rev.* **2015**, *28*, 603–661.

194. Lakhundi, S.; Zhang, K. Methicillin-resistant *Staphylococcus aureus*: Molecular characterization, evolution, and epidemiology. *Clin Microbiol Rev*, **2018**, *31*, e00020-18.

195. Ehlers, S.; Merrill, S.A. *Staphylococcus saprophyticus infection.* In *StatPearls*; StatPearls Publishing: Treasure Island, FL, USA, **2025**.

196. Kloos, W.E.; Schleifer, K.H. Isolation and characterization of staphylococci from human skin II. Descriptions of four new species: *Staphylococcus warneri, Staphylococcus capitis, Staphylococcus hominis*, and *Staphylococcus simulans*. *Int. J. Syst. Evol. Microbiol.* **1975**, *25*, 62–79, doi:10.1099/00207713-25-1-62.

197. Schleifer, K.H.; Kloos, W.E. Isolation and characterization of staphylococci from human skin I. Amended descriptions of *staphylococcus epidermidis* and *staphylococcus saprophyticus* and descriptions of three new species: *Staphylococcus cohnii, Staphylococcus haemolyticus, and Staphylococcus xylosus*. *Int. J. Syst. Evol. Microbiol.* **1975**, *25*, 50–61, doi:10.1099/00207713-25-1-50.

198. Hurvitz, N.; Cahan, L.O.S.; Gross, I.; Grupel, D.; Megged, O.; Pasternak, Y.; Temper, V.; Levy, R.; Weiser, G.; Hashavya, S. The role of *Staphylococcus lugdunensis* as a pathogen in children: A multicentre retrospective study. *J. Med. Microbiol.* **2021**, *70*, 001357, doi:10.1099/jmm.0.001357.

199. Greco-Stewart, V.S.; Ali, H.; Kumaran, D.; Kalab, M.; Rood, I.G.H.; de Korte, D.; Ramírez-Arcos, S. Biofilm formation by *Staphylococcus capitis* strains isolated from contaminated platelet concentrates. *J. Med. Microbiol*. **2013**, *62*, 1051–1059, doi:10.1099/jmm.0.050500-0.

200. Allocati, N.; Masulli, M.; Alexeyev, M.F.; Di Ilio, C. *Escherichia coli* in Europe: An overview. *Int. J. Environ. Res. Public. Health* **2013**, *10*, 6235–6254, doi:10.3390/ijerph10126235.

201. Wilson, M.G.; Pandey, S. *Pseudomonas aeruginosa*. In *StatPearls*; StatPearls Publishing: Treasure Island (FL), USA, 2025.

202. Caviglia, D.; Russo, E.; Preda, S.; Robustelli della Cuna, F.S.; Villa, C. *In situ* NADES microwave-mediated extraction of bioactive compounds from *Beta Vulgaris* L. Var. Rubra waste. *Int. J. Food Sci. Technol.* **2024**, *59*, 3271–3282, doi:10.1111/ijfs.17073

203. Adams, R.P. *Identification of Essential Oil Components by Gas Chromatography Mass Spectroscopy*; Allured Publishing Corporation: Carol Stream, IL, USA, **2007**.

204. Flavornet. Available online: https://www.flavornet.org/

205. *NIST/EPA/NIH Mass Spectral Library 2023*; Wiley Science Solutions: Hoboken, NJ, USA, **2023**.

206. Caputo, L.; Nazzaro, F.; Souza, L.F.; Aliberti, L.; De Martino, L.; Fratianni, F.; Coppola, R.; De Feo, V. *Laurus nobilis*: Composition of essential oil and its biological activities. *Molecules*, *Int. J. Mol. Sci* **2017**, *22*, 930, doi:10.3390/molecules22060930.

207. Caviglia, D.; Russo, E.; Schito, A.M.; Robustelli della Cuna, F.S.; Grignani, E.; Lionetti, N.; Villa, C. NaDES-based extracts by microwave activation from *Laurus Nobilis* L. leaves: Sustainable multifunctional ingredients for potential cosmetic and pharmaceutical applications. *Molecules, Int. J. Mol. Sci* **2025**, *30*, 3006, doi:10.3390/molecules30143006.

208. Oddo, E.; Saiano, F.; Alonzo, G.; Bellini, E. An investigation of the seasonal pattern of mannitol content in deciduous and evergreen species of the Oleaceae growing in northern Sicily. *Ann. Bot.* **2002**, *90*, 239–243, doi:10.1093/aob/mcf177.

209. Villa, C.; Cuna, F.S.R. della; Grignani, E.; Perteghella, S.; Panzeri, D.; Caviglia, D.; Russo, E. Evaluation of the biological activity of manna exudate, from *Fraxinus Ornus* L., and its potential use as hydrogel formulation in dermatology and cosmetology. *Gels* **2024**, *10*, 351, doi:10.3390/gels10060351.

210. Souza, O.A.; Ramalhão, V.G. da S.; Trentin, L. de M.; Funari, C.S.; Carneiro, R.L.; Bolzani, V. da S.; Rinaldo, D. Combining natural deep eutectic solvent and microwave irradiation towards the

eco-friendly and optimized extraction of bioactive phenolics from *Eugenia uniflora* L. *Sustain. Chem. Pharm.* **2022**, *26*, 100618, doi:10.1016/j.scp.2022.100618.

211. Nkhili, E.; Tomao, V.; El Hajji, H.; El Boustani, E.-S.; Chemat, F.; Dangles, O. Microwave-assisted water extraction of green tea polyphenols. *Phytochem. Anal.* **2009**, *20*, 408–415, doi:10.1002/pca.1141.

212. Zghari, B.; Doumenq, P.; Romane, A.; Boukir, A. GC-MS, FTIR and 1H, 13C NMR structural analysis and identification of phenolic compounds in olive mill wastewater extracted from Oued Oussefrou Effluent (Beni Mellal-Morocco). *J. Mater. Environ. Sci.* **2017**, *8*, 4496–4509, doi:10.26872/jmes.2017.8.12.475.

213. Susi H., Byler D.M. Resolution-enhanced Fourier transform infrared spectroscopy of enzymes. *Method Enzymol*. **1986**; *130*, 290–311. doi: 10.1016/0076-6879(86)30015-6.

214. Sienkiewicz-Gromiuk, J.; Tarasiuk, B.; Mazur, L. New organic single crystal of (benzylthio)acetic acid: Synthesis, crystal structure, spectroscopic (ATR-FTIR, 1H and 13C NMR) and thermal characterization. *J. Mol. Struct.* **2016**, *1110*, 65–71, doi:10.1016/j.molstruc.2016.01.016.

215. Rodríguez, F.J; Schlenger, P; García-Valverde M. Monitoring changes in the structure and properties of humic substances following ozonation using UV-Vis, FTIR and 1 H NMR techniques. *Sci. Total Environ*. **2016**, *541*, 623–637. doi: 10.1016/j.scitotenv.2015.09.127.

216. El Hajjouji, H.; Fakharedine, N.; Ait Baddi, G.; Winterton, P.; Bailly, J.R.; Revel, J.C.; Hafidi, M. Treatment of olive mill wastewater by aerobic biodegradation: an analytical study using gel permeation chromatography, ultraviolet–visible and Fourier transform infrared spectroscopy. *Bioresour. Technol.* **2007**, *98*, 3513–3520, doi:10.1016/j.biortech.2006.11.033.

217. Boukir, A.; Guiliano, M.; Asia, L.; Hallaoui, A.E.; Mille, G. A fraction to fraction study of photo-oxidation of BAL 150 crude oil asphaltenes. *Analusis* **1998**, *26*, 358–364, doi:10.1051/analusis:1998185.

218. Ayers, S.; Zink, D.L.; Mohn, K.; Powell, J.S.; Brown, C.M.; Murphy, T.; Brand, R.; Pretorius, S.; Stevenson, D.; Thompson, D.; et al. Flavones from *Struthiola argentea* with anthelmintic activity *in vitro*. *Phytochemistry* **2008**, *69*, 541–545, doi:10.1016/j.phytochem.2007.08.003.

219. Hajji, L.; Boukir, A.; Assouik, J.; Pessanha, S.; Figueirinhas, J.L.; Carvalho, M.L. Artificial aging paper to assess long-term effects of conservative treatment: Monitoring by infrared spectroscopy (ATR-FTIR), X-Ray diffraction (XRD), and energy dispersive X-Ray fluorescence (EDXRF). *Microchem. J.* **2016**, *124*, 646–656, doi:10.1016/j.microc.2015.10.015.

220**.** Francioso, O.; Ferrari, E.; Saladini, M.; Montecchio, D.; Gioacchini, P.; Ciavatta, C. TG–DTA, DRIFT and NMR characterisation of humic-like fractions from olive wastes and amended soil. *J. Hazard. Mater.* **2007**, *149*, 408–417, doi:10.1016/j.jhazmat.2007.04.002.

221. Klimczak, I.; Małecka, M.; Szlachta, M.; Gliszczyńska-Świgło, A. Effect of storage on the content of polyphenols, vitamin C and the antioxidant activity of orange juices. *J. Food Compos. Anal.* **2007**, *20*, 313–322, doi:10.1016/j.jfca.2006.02.012.

222. López-Froilán, R.; Hernández-Ledesma, B.; Cámara, M.; Pérez-Rodríguez, M.L. Evaluation of the antioxidant potential of mixed fruit-based beverages: A new insight on the Folin-Ciocalteu Method. *Food Anal. Methods* **2018**, *11*, 2897–2906, doi:10.1007/s12161-018-1259-1.

223. Kakoullis, L.; Papachristodoulou, E.; Chra, P.; Panos, G. Mechanisms of antibiotic resistance in important Gram-positive and Gram-negative pathogens and novel antibiotic solutions. *Antibiotics* **2021**, *10*, 415, doi:10.3390/antibiotics10040415.

224. Band, V.I.; Weiss, D.S. Mechanisms of antimicrobial peptide resistance in Gram-negative bacteria. *Antibiotics* **2015**, *4*, 18–41, doi:10.3390/antibiotics4010018.

225. Bialvaei, A.Z.; Samadi Kafil, H. Colistin: Mechanisms and prevalence of resistance. *Curr. Med. Res. Opin.* **2015**, *31*, 707–721, doi:10.1185/03007995.2015.1018989.

226. Preston, G.M. *Pseudomonas syringae* pv. tomato: The right pathogen, of the right plant, at the right time. *Mol. Plant Pathol.* **2000**, *1*, 263–275, doi:10.1046/j.1364-3703.2000.00036.x.

227. Schneider R.W., Grogan R.G. Bacterial speck of tomato: Sources of inoculum and establishment of a resident population. *Phytopathology*. **1977**, *67*, 388–394. doi: 10.1094/Phyto-67-388.

228. Belaqziz, M.; Tan, S.P.; El-Abbassi, A.; Kiai, H.; Hafidi, A.; O'Donovan, O.; McLoughlin, P. Assessment of the antioxidant and antibacterial activities of different olive processing wastewaters. *PLoS ONE* **2017**, *12*, e0182622, doi:10.1371/journal.pone.0182622.

229. Leouifoudi, I.; Harnafi, H.; Zyad, A. Olive mill waste extracts: Polyphenols content, antioxidant, and antimicrobial activities. *Adv. Pharmacol. Sci.* **2015**, *2015*, 714138, doi:10.1155/2015/714138.

230. Schlupp, P.; Schmidts, T.M.; Pössl, A.; Wildenhain, S.; Lo Franco, G.; Lo Franco, A.; Lo Franco, B. Effects of a phenol-enriched purified extract from olive mill wastewater on skin cells. *Cosmetics* **2019**, *6*, 30, doi:10.3390/cosmetics6020030.

231. Roila, R.; Branciari, R.; Ranucci, D.; Ortenzi, R.; Urbani, S.; Servili, M.; Valiani, A. Antimicrobial activity of olive mill wastewater extract against *Pseudomonas fluorescens* isolated from mozzarella cheese. *Ital. J. Food Saf.* **2016**, *5*, 5760, doi:10.4081/ijfs.2016.5760.

232. Russo, E.; Spallarossa, A.; Comite, A.; Pagliero, M.; Guida, P.; Belotti, V.; Caviglia, D.; Schito, A.M. Valorization and potential antimicrobial use of olive mill wastewater (OMW) from Italian olive oil production. *Antioxidants* **2022**, *11*, 903, doi:10.3390/antiox11050903.

233. Kilic, A.; Hafizoglu, H.; Kollmannsberger, H.; Nitz, S. Volatile constituents and key odorants in leaves, buds, flowers, and fruits of *Laurus nobilis* L. *J. Agric. Food Chem*. **2004**, *52*, 1601–1606.

234. Cavalloro, V.; Robustelli della Cuna, F.S.; Malovini, A.; Villa, C.; Sottani, C.; Balestra, M.; Bracco, F.; Martino, E.; Collina, S. Essential oils from *Papaver rhoeas* and their metabolomic profiling. *Metabolites* **2024**, *14*, 664, doi:10.3390/metabo14120664.

235. Bencresciuto, G.F.; Carnevale, M.; Paris, E.; Gallucci, F.; Santangelo, E.; Migliori, C.A. A sustainable alternative for cosmetic applications: NADES extraction of bioactive compounds from hazelnut by-products. *Sustainability* **2025**, *17*, 1516, doi:10.3390/su17041516.

236. European Commission. Regulation (EC) No. 1223/2009 of the European Parliament and of the Council of 30 November 2009 on cosmetic products. *Off. J. Eur. Union* **2009**, *L342*, 59–209.

237. Fajardo, D.; Jayanty, S.S.; Jansky, S.H. Rapid high throughput amylose determination in freeze dried potato tuber samples. *J. Vis. Exp.* **2013**, *78*, e50407, doi:10.3791/50407..

238. Xu, F.; Zhang, L.; Liu, W.; Liu, Q.; Wang, F.; Zhang, H.; Hu, H.; Blecker, C. Physicochemical and structural characterization of potato starch with different degrees of gelatinization. *Foods* **2021**, *10*, 1104, doi:10.3390/foods10051104.

239. Singleton, V.L.; Orthofer, R.; Lamuela-Raventós, R.M. Analysis of total phenols and other oxidation substrates and antioxidants by means of Folin-Ciocalteu reagent. In *Methods in Enzymology*; Packer, L., Ed.; Academic Press: London, UK, **1999**; Volume *299*, pp. 152–178.

240. Herbello-Hermelo, P.; Lamas, J.P.; Lores, M.; Domínguez-González, R.; Bermejo-Barrera, P.; Moreda-Piñeiro, A. Polyphenol bioavailability in nuts and seeds by an *in vitro* dialyzability approach. *Food Chem.* **2018**, *254*, 20–25, doi:10.1016/j.foodchem.2018.01.183.

241. Rincón, A.A.; Pino, V.; Ayala, J.H.; Afonso, A.M. Multiple headspace solid-phase microextraction for quantifying volatile free fatty acids in cheeses. *Talanta* **2014**, *129*, 183–190, doi:10.1016/j.talanta.2014.05.032.

Ringraziamenti

Desidero rivolgere un sincero ringraziamento alla Professoressa Carla Villa per avermi guidata con dedizione e professionalità passo dopo passo in questo progetto, e alla Professoressa Anna Maria Schito per il supporto e i consigli ricevuti durante lo svolgimento del lavoro.

Un pensiero e un grazie particolare vanno anche alla Professoressa Eleonora Russo, per essere stata un costante e importante punto di riferimento e per la sua disponibilità. È grazie alla loro guida se oggi riesco a raggiungere questo traguardo per me così significativo; ognuna di loro ha contribuito a rendere unica questa esperienza, che porterò per sempre nel mio cuore. Grazie anche ai Professori Chiara Brullo, Andrea Spallarossa e Bruno Tasso per il supporto ricevuto nel corso della mia ricerca.

Il mio ringraziamento più profondo è rivolto alla mia famiglia. A mio marito Stefano, che mi è stato accanto con amore in ogni momento, condividendo con me gioie e difficoltà. A mio fratello Fabio, presenza fondamentale e costante, con il quale ho condiviso ogni traguardo e ogni sfida della mia vita.

Il grazie più sentito, infine, lo devo ai miei genitori, il mio porto sicuro. Grazie per avermi sostenuta in ogni mia decisione e per aver vissuto insieme a me ogni istante di questo cammino unico. Siete stati la mia forza nei momenti di stanchezza e la mia gioia in quelli di successo; questo traguardo è tanto mio quanto vostro.